# PROPERTIES OF REACTIVE MAGNESIA-INCORPORATED CEMENTS

A THESIS SUBMITTED TO
THE GRADUATE SCHOOL OF NATURAL AND APPLIED SCIENCES
OF
MIDDLE EAST TECHNICAL UNIVERSITY

BY

MEHMET KEMAL ARDOĞA

IN PARTIAL FULFILLMENT OF THE REQUIREMENTS
FOR
THE DEGREE OF DOCTOR OF PHILOSOPHY
IN
CIVIL ENGINEERING

FEBRUARY 2022

Approval of the thesis:

**PROPERTIES OF REACTIVE MAGNESIA-INCORPORATED CEMENTS**

submitted by **MEHMET KEMAL ARDOĞA** in partial fulfillment of the requirements for the degree of **Doctor of Philosophy in Civil Engineering Department, Middle East Technical University** by,

Prof. Dr. Halil Kalıpçılar
Dean, Graduate School of **Natural and Applied Sciences** _____

Prof. Dr. Erdem Canbay
Head of the Department, **Civil Engineering** _____

Prof. Dr. İsmail Özgür Yaman
Supervisor, **Civil Engineering, METU** _____

**Examining Committee Members:**

Prof. Dr. Mustafa Şahmaran
Civil Engineering, Hacettepe University _____

Prof. Dr. İsmail Özgür Yaman
Civil Engineering, METU _____

Assoc. Prof. Dr. Tahir Kemal Erdem
Civil Engineering, Marmara University _____

Asst. Prof. Dr. Çağla Meral Akgül
Civil Engineering, METU _____

Asst. Prof. Dr. Hande Işık Öztürk
Civil Engineering, METU _____

Date: 11.02.2022

**I hereby declare that all information in this document has been obtained and presented in accordance with academic rules and ethical conduct. I also declare that, as required by these rules and conduct, I have fully cited and referenced all material and results that are not original to this work.**

Name, Last name : Mehmet Kemal Ardoğa

Signature :

# ABSTRACT

## PROPERTIES OF REACTIVE MAGNESIA-INCORPORATED CEMENTS

Ardoğa, Mehmet Kemal
Doctor of Philosophy, Civil Engineering
Supervisor: Prof. Dr. İsmail Özgür Yaman

February 2022, 121 pages

Magnesium oxide (MgO) has limited use in civil engineering applications. The presence of MgO (especially in free form) in portland cements is limited by the standards due to the risk involved in the gradual hydration of MgO that may lead to disruptive expansions after the cementitious system hardens. However, it is possible to overcome this detrimental effect by calcining magnesite at lower temperatures than that is encountered in the cement kilns and use thus obtained reactive MgO as an additive in cement. In this case, MgO will react with water to form magnesium hydroxide (brucite) while the cementitious system is still plastic. Later, brucite will carbonate to reform magnesium carbonates. In this study, firstly the synthesis of reactive magnesia from naturally – obtained magnesite was carried out at different calcination temperatures. Then the magnesia obtained was blended with CEM I and CEM II cements in varying amounts (15-50%, by mass). The cements thus obtained were studied comparatively with the control cements without reactive MgO from hydration reactions, strength, and durability characteristics points of view. It was found that the most reactive magnesia was obtained with the curing regime including 600 °C of burning temperature and 120 minutes of exposure time. It was also determined that the reactive magnesia caused a reduction in compressive strength

when cured in ambient conditions. However, generally, when cured in a carbon dioxide environment, the compressive strengths increased with increasing carbon dioxide concentration.

Keywords: Cement, Magnesium oxide, Hydration, Carbonation

# ÖZ

## REAKTİF MAGNEZYA İÇEREN ÇİMENTOLARIN ÖZELLİKLERİ

Ardoğa, Mehmet Kemal
Doktora, İnşaat Mühendisliği
Tez Yöneticisi: Prof. Dr. İsmail Özgür Yaman

Şubat 2022, 121 sayfa

Magnezyum oksit (MgO), inşaat mühendisliği uygulamalarında sınırlı kullanıma sahiptir. Portland çimentolarında MgO nun (özellikle serbest formda) varlığı, MgO nun kademeli hidratasyonunda yer alan ve çimentolu sistem sertleştikten sonra yıkıcı genleşmelere yol açabilecek risk nedeniyle standartlarla sınırlıdır. Ancak manyezitin çimento fırınlarında karşılaşılandan daha düşük sıcaklıklarda kalsine edilmesi ve bu şekilde elde edilen reaktif MgO nun çimentoda katkı maddesi olarak kullanılmasıyla bu zararlı etkinin üstesinden gelmek mümkündür. Bu durumda MgO, çimentolu sistem hala plastikken magnezyum hidroksit (brüsit) oluşturmak üzere su ile reaksiyona girecektir. Daha sonra brusit, magnezyum karbonatları yeniden oluşturmak için karbonatlaşacaktır. Bu çalışmada, öncelikle farklı kalsinasyon sıcaklıklarında doğal olarak elde edilen manyezitten reaktif magnezya sentezi gerçekleştirilmiştir. Daha sonra elde edilen magnezya, CEM I ve CEM II çimentoları ile değişen oranlarda (%15-50, kütlece) karıştırılmıştır. Bu şekilde elde edilen çimentolar, hidratasyon reaksiyonları, mukavemet ve dayanıklılık özellikleri açısından reaktif MgO içermeyen kontrol çimentoları ile karşılaştırmalı olarak incelenmiştir. En reaktif magnezyanın 600 °C yanma sıcaklığı ve 120 dakikalık maruz kalma süresi içeren kürleme rejimi ile elde edildiği bulunmuştur. Ayrıca

reaktif magnezyanın ortam koşullarında kürlendiğinde basınç dayanımında azalmaya neden olduğu tespit edilmiştir. Ancak, genel olarak, bir karbondioksit ortamında kürlendiğinde, artan karbondioksit konsantrasyonu ile basınç dayanımları artmıştır.

Anahtar Kelimeler: Çimento, Magnezyum oksit, hidratasyon, karbonatlaşma

*To my hero, my dad,*
*may your soul rest in peace…*

## ACKNOWLEDGMENTS

I would like to express my deepest appreciation to my supervisors Prof. Dr. Mustafa Tokyay and Prof. Dr. İsmail Özgür Yaman for their support, criticism, guidance and supervision during the preparation of this thesis.

I would like to thank to my parents, Nedim Ardoğa and Safiye Neşe Ardoğa, and my brother Armağan Ardoğa for their great support and patience despite our difficult times. Special thanks also go to my fiancé Bahar N. Can for her wonderful support and motivation during the preparation of my thesis.

For their great support, I should express my great appreciation to Prof. Dr. Sinan Turhan Erdoğan, Assoc. Prof. Dr. Serdar Göktepe and Assist. Prof. Dr. Çağla Meral Akgül.

Prof. Dr. Turhan Y. Erdoğan, whom I am always honored of assisting in for his courses, had great contributions to my academic career and even in my personal life. My condolences to him. May he rest in peace!

For their support and help, I would like to thank to Dr. Burhan Aleessa Alam, Meltem Tangüler Bayramtan, Dr. Utku Albostan, Dr. Feyza Soysal Albostan, Sepehr Seyedian, Dr. Mehran Ghasabeh, Özgür Paşaoğlu, Dr. Murat Şahin, Muhammet Atasever, Aykut Bilginer, Sinan Fırat Dal, Sadık Karakaş, Gülşah Bilici and Cuma Yıldırım.

Last but not least, this study or other similar studies would not have been possible without the heroism of our ancestors. I would like to express my gratitude to Mustafa Kemal Atatürk, İsmet İnönü and their fellow fighters.

This work is partially funded by METU Scientific Research Projects under grant number BAP-07-02-2014-007-400.

## TABLE OF CONTENTS

## LIST OF TABLES

TABLES

## LIST OF FIGURES

FIGURES

# CHAPTER 1

# INTRODUCTION

## 1.1. General

Concrete is the most widely used construction material all over the world and its main material, binding other constituents together and providing higher strength and durability against most of chemical agents is the portland cement. With the appropriate mix design, the portland cement concrete can remain for years. Despite the benefits, there is a huge drawback for using this type of cement: the great quantity of carbon dioxide emissions during its production. This emission includes the carbon dioxide produced from both the calcination of the raw materials and the consumption of the carbon – based fuels for the burning process.

To cut down the high amount of carbon dioxide emissions of the portland cement, several solutions are proposed. One of the popular solutions is the addition of reactive magnesia to portland cement fraction. Since the burning temperature of reactive magnesia is very lower than the production temperature of portland cement, the required amount of fuel, and correspondingly the carbon dioxide emission will be lower. The other important reason for suggesting this material is its carbon dioxide holding capacity. The cements containing reactive magnesia have the ability to absorb carbon dioxide because of its strength gain mechanism. It is put forward that it is possible to develop a carbon – negative cement, using reactive magnesia.

The reactive magnesia has the potential to produce different types of magnesium carbonates mainly depending on the carbon dioxide concentration in air and the pH of the pore solution. These products not only decrease the environmental impact of

the concrete but also leads to an increase in the mechanical and reduction in permeability properties.

## 1.2. Objective and Scope

This study has four main objectives. Firstly, it is aimed to produce reactive magnesia, by calcining the naturally-obtained magnesite. The second one is to study the effect of different carbon dioxide concentration of the curing on reactive magnesia cements having mineral admixtures. Thirdly, the determination of mechanical properties and durability characteristics of these reactive magnesia cements is targeted. The final one is the microstructural characterization of the hydration and carbonation products. For these objectives, firstly, the optimum burning regime leading to the production of the most reactive magnesia was found by adjusting the burning temperature and the exposure time. Then, the reactive magnesia was mixed in different proportions with portland cement including fly ash and ground granulated blast furnace slag. The cement pastes and mortars were subjected to the curing regimes having ambient, 20 % and 50 % carbon dioxide levels. The long- and short-term mechanical and durability of the samples were determined and the hydration and carbonation products were analyzed by XRD and SEM.

Within this framework, Chapter 1 contains general information about the study. It also describes the objective and scope of the thesis. Chapter 2 presents a review of the literature on reactive magnesia cement and carbonation. The experimental procedure followed, the chemical and physical properties of raw materials and cements, and an explanation of the experiments carried out form Chapter 3. Chapter 4 presents the results of experiments. A discussion of results is also given in this chapter. Finally, in Chapter 5, the study, discussion of results and conclusions are summarized. The recommendations for further studies are also given.

# CHAPTER 2

# LITERATURE REVIEW

## 2.1. Use of Reactive Magnesia in Cements

### 2.1.1. Introduction

The reactive magnesia (magnesium oxide) cements are defined as the cements containing reactive magnesia as the main binding agent. Magnesia-based cements has been in use for more than 150 years (Walling & Provis, 2016). However, their use is limited due to two main reasons:

- Magnesia (MgO) is basically obtained from magnesite ($MgCO_3$). When compared with limestone ($CaCO_3$) which is the basic raw material for Portland cement production, magnesite deposits are scarce and only locally available throughout the world.
- Portland cements attain their binding value by the hydration of several phases ($C_3S$, $C_2S$, and $C_3A$) with cementitious properties. These phases are formed by the calcination of a suitable combination of limestone and clay. The former is the source of CaO and the latter is the source of $SiO_2$ and $Al_2O_3$. These oxides react with each other at calcination temperatures around 1500 ºC to form the three major compounds mentioned above. However, the replacement of $CaCO_3$ by $MgCO_3$ does not result in similar reaction products as seen in the comparative ternary diagrams given in Figure 2.1.

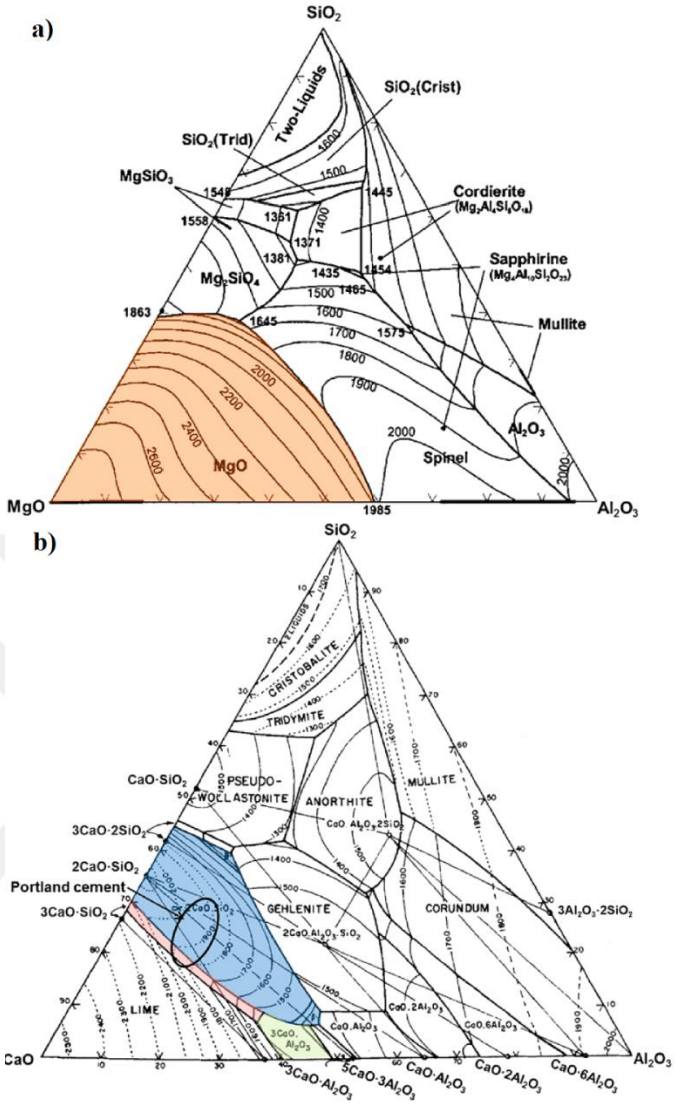


Figure 2.1. Ternary diagrams of (a) $MgO$-$SiO_2$-$Al_2O_3$ and (b) $CaO$-$SiO_2$-$Al_2O_3$ systems (Walling & Provis, 2016).

The presence of magnesia (MgO), especially in free form, in portland cements may have detrimental effects on the volume stability of cementitious systems. This effect depends on the maximum temperature at which the magnesia is exposed to. For the production of the portland cement, the calcareous and siliceous materials are mixed and burned at about 1400 ºC in the rotary kilns of cement factories. In the temperatures of about 600 ºC, the magnesium carbonate, as one of the main

impurities of the calcareous sources, starts to decompose, loses its carbon dioxide and forms magnesia, in other words, the magnesium carbonate calcines as shown in Eqn. 2.1.

$$MgCO_3 \xrightarrow{600^0C} MgO + CO_2 \uparrow \quad \text{Eqn. 2.1}$$

Normally, the hydration of MgO, as given by Eqn. 2.2 is quite rapid if the calcination temperature is below 1000 ºC.

$$MgO + H_2O \rightarrow Mg(OH)_2 \quad \text{Eqn. 2.2}$$

The MgO in the portland cement clinker, however, is subjected to very high temperatures (up to 1400 – 1600 ºC) in the rotary kiln. Thus, it is termed as deadly burned magnesia and becomes much less reactive and the hydration takes place long after hardening. The delayed hydration of free MgO in portland cement concrete results in volume expansion and eventually causes disruptive cracking sometime after hardening.

The carbonation of brucite ($Mg(OH)_2$) given by Eqn. 2.3 can result in the formation of nesquehonite ($MgCO_3.3H_2O$) which causes further expansion.

$$Mg(OH)_2 + CO_2 + 2H_2O \rightarrow MgCO_3 \cdot 3H_2O \quad \text{Eqn. 2.3}$$

While the hydration reaction given in Eqn. 2.2 causes 117 % volume expansion, the the total expansion from magnesia to nesquehonite is about 568 % (Chatterji, 1995; Qureshi & Al-Tabbaa, 2014).

Therefore, magnesia content in the portland cements should be limited in the standards in order to prevent the risk of unsoundness and durability problems. However, all those undesirable effects are due to the presence of deadly-burned, low reactivity magnesia in the portland cements.

### 2.1.2. Production and Reactivity of Magnesia

Two percent of the Earth crust, by weight, is formed by magnesium, in addition, the concentration of the magnesium in seawater is about 1300 ppm. In nature, it is found in the forms of the compounds like magnesium carbonates (magnesite, dolomite, nesquehonite, lansfordite etc.) and chlorites (Shand, 2006). 8 % of the sediments by weight on Earth consists of the carbonate rocks and just the dolomite forms 30 % of the carbonates by weight (Shand, 2006). The total global reserve for the magnesite is estimated as 13 billion tonnes, and the production is about 14 million tonnes per year (Al-Tabbaa, 2013). For Turkey, the magnesite production is generally made in Eskişehir-Kütahya, Erzincan and Konya regions and the total amount of magnesite is about 145 million tonnes (MTA, 1981; Shand, 2006). Only for the Eskişehir-Kütahya region, the annual rate of the magnesite production is about 900 thousand tonnes (Shand, 2006).

The magnesia (magnesia oxide) can be obtained by either a dry process which involves the calcination of magnesite, as given by Eqn. 2.1 or by a wet process from magnesium-bearing brines or sea water (Al-Tabbaa, 2013; Shand, 2006; Walling & Provis, 2016).

The magnesium is the most abundant element in seawater solution after sodium and chlorine (Shand, 2006). The precipitation process is based on the addition of $CaCl_2$ to the seawater and decrease the sulfate ion concentration to form $MgCl_2$. $Ca(OH)_2$ is added to the brine containing $MgCl_2$ and then, $Mg(OH)_2$ precipitated is heated to remove its water, as given in Eqns 2.4 and 2.5 (Walling & Provis, 2016).

$$MgCl_2 + Ca(OH)_2 \rightarrow CaCl_2 + Mg(OH)_2 \quad \text{Eqn. 2.4}$$

$$MgCl_2 + CaMg(OH)_4 \rightarrow CaCl_2 + 2Mg(OH)_2 \quad \text{Eqn. 2.5}$$

The magnesia can also be obtained directly from the pyrohydrolysis on the magnesium chloride-rich brine using superheated steam up to 1000 °C, as given by Eqn. 2.6 (Walling & Provis, 2016).

$$MgCl_2 \cdot 6H_2O \xrightarrow{\sim 1000\,^{\circ}C} MgO + 2HCl + 5H_2O \quad \text{Eqn. 2.6}$$

In the dry process, the magnesite is heated to remove its carbon dioxide. Although the calcination temperature depends on the amount of the impurities, crystallographic structure, and microstructure of the raw materials, it was reported to be generally between 402 and 750 °C (Shand, 2006).

Magnesia is typically classified according to the calcination temperature of magnesite. Increased temperature and time of calcination result in reduced fineness and crystallinity which in turn reduce the reactivity of magnesia. In most technical literature, three classes of magnesia reactivity are stated as follows (Al-Tabbaa, 2013; Shand, 2006):

- **High reactivity magnesia:** The magnesia is light burned. That is, the burning temperature is below 1000 ºC. It is also called caustic or reactive magnesia. It has the lowest crystallinity, highest surface area and the highest reactivity with water.
- **Medium reactivity magnesia:** The burning temperature of magnesium carbonate is between 1000 and 1400 ºC. It is called as hard-burned magnesia.
- **Low reactivity magnesia:** The burning temperature of magnesium carbonate is over 1400 ºC. The magnesia obtained is crystalline. It has the lowest specific surface are and the lowest reactivity with water. It is called as dead-burned magnesia or periclase.

The European Commission, on the other hand, grades the types of the magnesia as (a) caustic-calcined, (b) dead-burned and (c) fused magnesia. The calcination temperature ranges for them are stated as 600 – 1300 °C, 1600 – 2200 °C, and > 2200 ºC, respectively (Joint Research Centre, 2013; Walling & Provis, 2016).

In nature, the periclase, the crystalline magnesia, is found rarely in its pure form. Its color is white but, it can also be yellow, black or brown depending on its impurities. Its crystal form has a face-centered cubic (FCC) structure and its density is reported to be 3.58 g/cm$^3$ (Shand, 2006).

The properties of the magnesia change with respect to the highest calcination temperature experienced by the raw materials. In the studies, the reactivities of the magnesias produced at different burning temperatures are investigated and it is stated that the temperature increase leads to the decrease in the magnesia reactivity (Birchal et al., 2000; Demir et al., 2003; Mo et al., 2009, 2010; Zhu et al., 2013).

The comparison of magnesia obtained from the same magnesite at burning temperatures of 600, 650, 700, 750, and 1100 ºC and different burning periods indicated that reactivity as described by a term $X_{corrected}$, which is defined as the decomposition ratio of magnesia from magnesite ore decreases with increasing burning temperature and time, as illustrated in Figure 2.2.

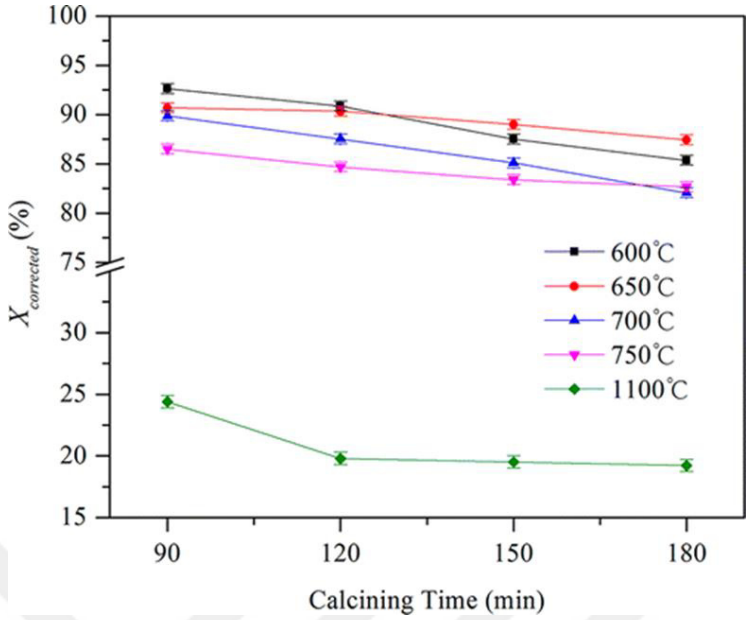


Figure 2.2. The MgO conversion ratio ($X_{corrected}$) at different burning temperatures and time (Zhu et al., 2013).

Maryška and Blâha (1997) investigated the hydration rates of MgO obtained at different burning temperatures and stated that as the burning temperature increases the reactivity decreases, even at high temperatures of hydration, as illustrated in Figure 2.3.

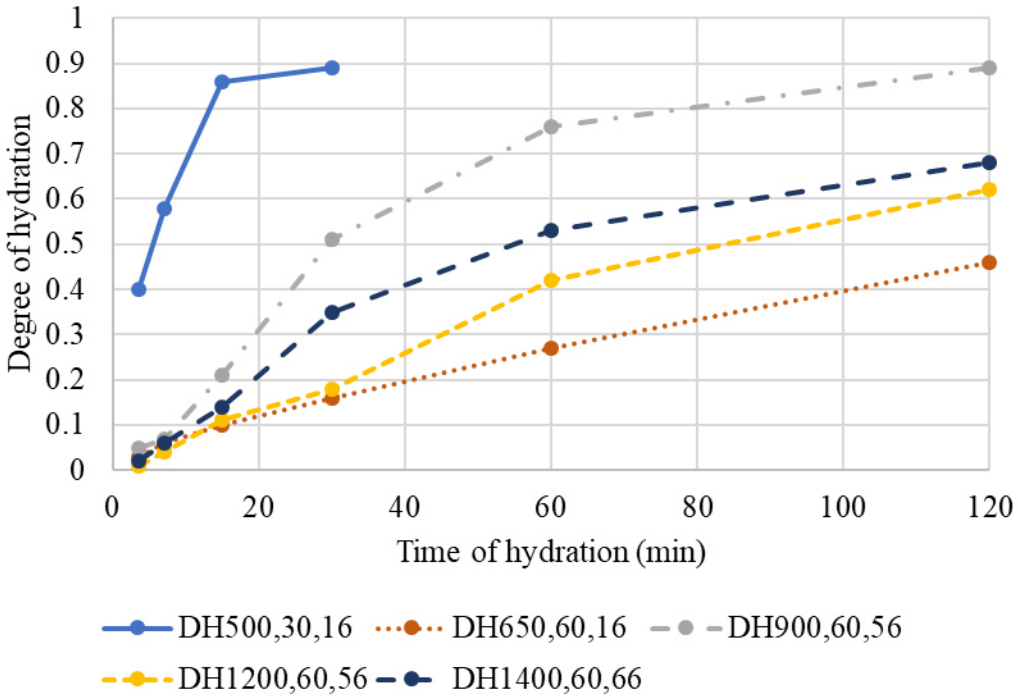


Figure 2.3. Degree of hydration of MgO obtained at different burning temperatures and times for different hydration temperatures (Maryška & Bláha, 1997) (DHX,Y,Z in the legend indicates degree of hydration of MgO obtained by burning magnesite at temperature X in ºC, for Y minutes, and at temperature of hydration of Z in ºC, respectively).

When the XRD patterns of the starting material (magnesite ore) and different magnesia samples obtained for the different burning temperatures are compared, it is observed that the increase in the temperature caused increased crystallinity, implying a decrease in the reactivity of the magnesia obtained (Walling & Provis, 2016; Zhu et al., 2013).

Besides the increase in crystallinity, the effect of higher temperatures on the magnesia reactivity is claimed to be due to the reduction in the defects and porosity, and correspondingly, the specific surface area of the magnesia (Kabir & Hooton, 2020; Mo et al., 2009, 2010, 2014; Cise Unluer, 2018; Walling & Provis, 2016).

Other than the temperature to which the magnesium carbonate is exposed, the exposure time and type and amount of impurities present in magnesite are reported to affect the reactivity of magnesia, significantly (Mo et al., 2010; Zhu et al., 2013).

### 2.1.3. Hydration and Carbonation Reactions of Magnesia

The hydration reaction occurs at the magnesia surface with water to form magnesium hydroxide (brucite) under ambient carbon dioxide concentration. The hydration processes given by Eqns 2.7 – 2.10 consist of the dissolution of the magnesia and the precipitation of the magnesium hydroxide (brucite) at supersaturation (pH ~10.5) (Al-Tabbaa, 2013; Dung & Unluer, 2016). Therefore, the hydration rate of magnesia is reported to depend on the diffusion rate of the reaction ions (Mo et al., 2014). The brucite can be formed near the site of the magnesia and they can fill its interior pores since the transformation leads to an increase of 128.7 % in volume (Mo et al., 2010; Mo & Panesar, 2012). In addition to the hydration kinetics, it is affected by the foreign compounds which can form a barrier preventing the water penetration (Mo et al., 2014; Cise Unluer, 2018). The morphology of the brucite formed is reported to be depending on the formation conditions (Al-Tabbaa, 2013).

$$MgO_{(solid)} + H_2O \rightarrow Mg(OH)^{+}_{(surface)} + OH^{-}_{(aq)} \quad \text{Eqn. 2.7}$$

$$Mg(OH)^{+}_{(surface)} + OH^{-}_{(aq)} \rightarrow MgOH^{+} \cdot OH^{-}_{(surface)} \quad \text{Eqn. 2.8}$$

$$MgOH^{+} \cdot OH^{-}_{(surface)} \rightarrow Mg^{2+}_{(aq)} + 2OH^{-}_{(aq)} \quad \text{Eqn. 2.9}$$

$$Mg^{2+}_{(aq)} + 2OH^{-}_{(aq)} \rightarrow Mg(OH)_{2(solid)} \quad \text{Eqn. 2.10}$$

The system of $H_2O$ – $CO_2$ – MgO is not completely understood, however, it can be generally stated that in the presence of water and at sufficient concentration of the carbon dioxide, the magnesium hydroxide reacts to form metastable hydrated magnesium carbonates as shown in Eqns 2.11-2.13 (Al-Tabbaa, 2013; Tanaka et al., 2019). It is reported that the direct carbonation of brucite to magnesite can only occur

at high temperatures and pressures (Fricker & Park, 2013; Rausis et al., 2020). This reaction can be followed from Eqn. 2.14.

$$Mg(OH)_2 + CO_2 + 2H_2O \rightarrow \underbrace{MgCO_3 \cdot 3H_2O}_{\text{Nesquehonite}} \quad \text{Eqn. 2.11}$$

$$5Mg(OH)_2 + 4CO_2 + H_2O \rightarrow \underbrace{Mg_5(CO_3)_4(OH)_2 \cdot 5H_2O}_{\text{Dypingite}} \quad \text{Eqn. 2.12}$$

$$5Mg(OH)_2 + 4CO_2 \rightarrow \underbrace{Mg_5(CO_3)_4(OH)_2 \cdot 4H_2O}_{\text{Hydromagnesite}} \quad \text{Eqn. 2.13}$$

$$Mg(OH)_2 + CO_2 \rightarrow \underbrace{MgCO_3}_{\text{Magnesite}} + H_2O \quad \text{Eqn. 2.14}$$

These carbonation products tend to transform and the transformation generally follows the sequence given in Eqn. 2.15 (Canterford et al., 1984; Ferrini et al., 2009; A. L. Harrison et al., 2019; Hopkinson et al., 2008; Martin Liska & Al-Tabbaa, 2012; C. Unluer & Al-Tabbaa, 2013; Cise Unluer, 2018). It is suggested that the transformation could be depending on the temperature, degree of reactivity, presence of impurity, pH, and curing conditions (A. L. Harrison et al., 2019; M. Liska & Al-Tabbaa, 2009; Martin Liska & Al-Tabbaa, 2012; Rheinheimer et al., 2017; Smithson & Bakhshi, 1973).

$$\underbrace{MgCO_3 \cdot 3H_2O}_{\text{Nesquehonite}} \rightarrow \underbrace{Mg_5(CO_3)_4(OH)_2 \cdot 5H_2O}_{\text{Dypingite}} \rightarrow \underbrace{Mg_5(CO_3)_4(OH)_2 \cdot 4H_2O}_{\text{Hydromagnesite}} \rightarrow \underbrace{MgCO_3}_{\text{Magnesite}} \quad \text{Eqn. 2.15}$$

The thermodynamic stability of the carbonates formed is a debatable issue (Cise Unluer, 2018). Some of the researchers claim that for temperatures lower than ~100 ºC, the most stable carbonation product is nesquehonite (Walling & Provis, 2016). The relation between the stability of the compounds, temperature and partial pressure

of carbon dioxide (carbon dioxide concentration) can be seen in Figure 2.4 (Langmuir, 1965). Accordingly, for ambient conditions, the most stable product is nesquehonite. However, some other researchers assert that nesquehonite is metastable at room temperature and release some of its carbon dioxide and water, and they state that hydromagnesite is the most stable carbonate at room temperature (Walling & Provis, 2016).

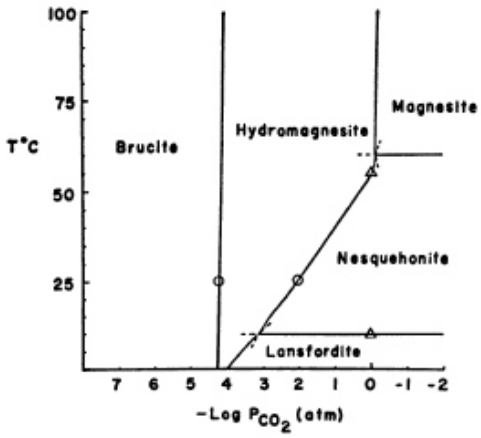


Figure 2.4. Stability relations in the system of MgO – $CO_2$ (for the RH = 100 %) (The points marked with triangles and circles represent the results obtained from the experimental studies and calculations, respectively) (Langmuir, 1965).

Similarly, the most stable phases in Mg-bearing systems are indicated to be the magnesite and brucite by other researchers (Rheinheimer et al., 2017; Tanaka et al., 2019). On the other hand, at temperatures below 60°C and for laboratory timescales, magnesite formation is inhibited (A. L. Harrison et al., 2019; Tanaka et al., 2019).

According to Walling and Provis, among the hydration/carbonation products, the product having higher stability with respect to the temperature can be seen in Figure 2.5. It can finally be stated that the possible transformation which may cause changes

in the crystal composition, volume, and morphology that would lead to dimensional instability.

The other compounds which can be identified from magnesia carbonation are hydrotalcite ($Mg_6Al_2CO_3(OH)_{16}.4H_2O$), artinite ($Mg_2CO_3(OH)_2.3H_2O$ and huntite ($Mg_3Ca(CO_3)_4$ (Walling & Provis, 2016).

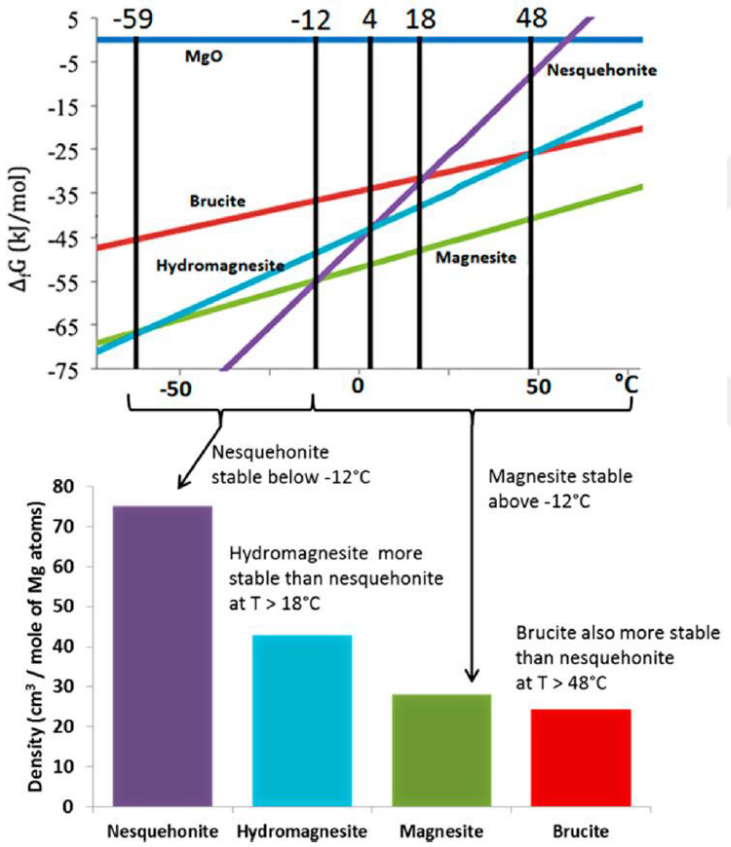


Figure 2.5. Free energy diagram for the magnesium bearing compounds (Walling & Provis, 2016).

### 2.1.4. Magnesia in Cements

The raw materials for the portland cement production are clayey and calcareous sources. These are burned at the temperatures higher than 1400 ºC at rotary kilns in cement factories. The magnesia in portland cements can be due to the presence of magnesium carbonates as the impurity in calcareous materials. The calcium carbonate calcines at about 900 ºC and during clinkering process, the magnesia, already formed by the calcination of the magnesium carbonate is also exposed to the burning temperatures of the portland cement clinker and the dead burned magnesia or periclase with a very low reactivity due to its high crystallinity and low porosity unintentionally is produced (Walling & Provis, 2016). The hydration and carbonation of the dead burned magnesia is so slow that the products are formed after the setting of the portland cement-based matrix. Since the volume of the products is higher than the magnesia and these reactions are highly exothermic, they create the tensile forces resulting cracks in hardened cement matrix (Erdoğan, 2010; Mo et al., 2010; Mo & Panesar, 2012). Therefore, the content of magnesia which may present in portland cements is limited by the standards. While according to the European standard, EN 197-1, the maximum content of the magnesia present in portland cement clinker is 5 % (TS EN 197-1, 2011), the ASTM standards limit the magnesia content in the portland cement as 6 % (ASTM C 150, 2020).

In history, the first known problem encountered about the high crystalline magnesia content in cements is the failure of bridges and viaducts in France in 1884, two years after they had been constructed. The magnesia content in the first cements produced in Germany and France is claimed to be higher than 20 % (Mehta & Monteiro, 2006). On the other hand, it is also reported that the thermal shrinkage of a concrete dam built in China in 1970s could have been compensated effectively by the delayed expansion of magnesia in cements (Mo et al., 2014).

The free lime, which is not within the structure of cement compounds, creates expansion due to the presence of water as well as the periclase, MgO. When considering only the molar increase for the periclase and free lime to form the

magnesium hydroxide and calcium hydroxide, the increase resulted from the hydration is found to be 117 % and 90 %, respectively (Chatterji, 1995). Even though the molar increase of the periclase is much higher than that of the free lime, a lower content of free lime causes excessive expansion compared to the required amount of magnesia for the same effect. This can be due to the different solubilities of the hydrated oxides in cements. When the pore solution is supersaturated with respect to a hydroxide, this hydroxide leads to the crystal growth which is the main reason for the expansion. The calcium hydroxide, having higher solubility than the magnesium hydroxide reaches its super saturation point and starts the precipitation, and correspondingly, an expansion earlier than magnesium hydrate, $Mg(OH)_2$ (Chatterji, 1995; Mo et al., 2014). By standards, to detect the expansion due to the presence of the free lime and dead burned magnesia, Autoclave or Le Chatelier expansion tests are recommended (ASTM C 150, 2020; ASTM C 151, 2018; TS EN 196-3, 2002; TS EN 197-1, 2011).

Although the most preferred test to determine the soundness performance of the cement mortars containing dead burned magnesia is the autoclave test, there can be several drawbacks to perform the experiment on the cements containing reactive magnesia (Kabir & Hooton, 2020). Firstly, the test conditions are so extreme that the hydration and carbonation products of the cements containing the reactive magnesia can be affected. The high test temperature leads to accelerate the reactions and to modify the hydration and carbonation products formed in the cement mortar (Mo et al., 2014; Walling & Provis, 2016). Secondly, the correlation between the field performance of the concrete containing reactive magnesia and the results of the laboratory tests conducted on cement pastes is not well established. In addition, the expansion limit for the cements containing reactive magnesia is not stated in the related standards (Kabir & Hooton, 2020; Mo et al., 2014; Nokken, 2010).

The effects of the magnesia in cements can be controlled by the quantity, fineness and calcination temperatures of magnesia. The storage conditions, properties of the portland cement fraction (type and strength) and mineral admixtures are important for the cement performance as well (Chatterji, 1995; Liu et al., 1998).

### 2.1.5. Reactive Magnesia Cements

The reactive magnesia cements were developed and patented by John Harrison (Al-Tabbaa, 2013). According to that patent, the reactive magnesia cement is defined as (A. J. W. Harrison, 2008);

> *"A hydraulic cement composition consisting essentially of: a hydraulic cement component; a magnesium oxide component; and a pozzolan component, wherein the magnesium oxide component consists essentially of reactive magnesium oxide hydratable to brucite and prepared by low temperature calcination at a temperature of less than 750 °C from materials excluding dolomite, and substantially ground to a particle size with greater than 95 % of the particles less than 120 μm in size, the magnesium oxide component making up at least 5 % by weight of a combination of the hydraulic cement component and the magnesium oxide component, said composition excluding components which form magnesium oxychlorides and magnesium oxysulfates with the reactive magnesium oxide."*

Generally, the reactive magnesia cements are produced by adding the reactive magnesia to the portland cement (Walling & Provis, 2016). Depending on the weight percentage of the reactive magnesia with respect to the total powder content, three different classes are proposed by Harrison (Al-Tabbaa, 2013; A. J. W. Harrison, 2003).

- **Tec-cements;** have higher amount of the portland cement than that of reactive magnesia. They are mainly used in order to enhance the durability, strength and volume stability, to reduce the permeability.
- **Enviro-cements;** are used for enhanced waste immobilization capacity. It has nearly equal amount of the reactive magnesia and portland cement.
- **Eco-cements;** with higher content of the reactive magnesia are used for porous block applications.

The reactivity of the magnesia should be known for the cement application where the magnesia is intended to be used (Al-Tabbaa, 2013). Since the volume of the hydration and carbonation products of the magnesia in cements is higher than the total volume of the reactants, these reactions create volume expansion, and correspondingly, the cracks in matrix due to the typical lower tensile strength. The use of the magnesia having lower reactivity like the dead burned magnesia, instead of the reactive magnesia, in cements, can have detrimental effects, as its reactivity is lower than the other main component of the reactive magnesia cement, the portland cement fraction. After its setting, the products of the magnesia can create tensile stresses in cement matrix (like in the case of presence of the free lime). To overcome this problem, the reactivity of the magnesia used should be similar with that of the portland cement. As among all types of magnesia, the most reactive one is the light burned magnesia, which is produced at lower temperatures, this should be preferred to be used in reactive magnesia cements, so that the reaction products of the magnesia are formed before or during the setting of the portland cement portion (Al-Tabbaa, 2013; C. Unluer & Al-Tabbaa, 2014; Walling & Provis, 2016).

The structures of the cements containing the reactive magnesia were investigated by many researchers and it is found that the high level of carbon dioxide in the environment leads to carbonation and correspondingly, a great change in micro- and meso-scale of the systems (Dung & Unluer, 2016; Walling & Provis, 2016). As well as the reactivity of magnesia, the mix design and especially the curing conditions (relative humidity, temperature and carbon dioxide levels) are important to control the carbonation of the magnesia (C. Unluer & Al-Tabbaa, 2013).

The hydration of the magnesia results in the formation of brucite, mainly (Dung & Unluer, 2016). In the studies conducted on the reactive magnesia cements, it is claimed that the hydration of the portland cement and reactive magnesia fractions occurred independently, and in the case of ambient carbon dioxide curing, the main hydration products are the hydrotalcite and brucite, whose binding properties are very poor due to their higher water demand and higher porosity (M. Liska et al., 2008; M. Liska & Al-Tabbaa, 2009; Cise Unluer, 2018; Vandeperre et al., 2008;

Walling & Provis, 2016). On the contrary, for this curing regime, the M-S-H (magnesium silicate hydrate) gels are also recognized especially in the presence of fly ash and the slight change in XRD peak of the brucite is reported to be resulted from the incorporation of $Ca^{2+}$ ions to the crystal structure of the brucite (Jin et al., 2013; Martin Liska & Al-Tabbaa, 2012; Ruan & Unluer, 2017; Vandeperre et al., 2008). Furthermore, it is suggested that the dissolution of the nesquehonite, which is considered to be a thermally unstable magnesium carbonate, tends to increase the calcium carbonate precipitation. Also, the incorporation of $Mg^{2+}$ ions is indicated to change the possible crystal structure of the calcium carbonate (Hopkinson et al., 2008).

The presence of high concentration of carbon dioxide causes the carbonation of the reactive magnesia in cements to form different types of magnesium carbonates. According to studies, the observable phases are determined to be the nesquehonite, dypingite, hydromagnesite and artinite (M. Liska & Al-Tabbaa, 2009; C. Unluer & Al-Tabbaa, 2013). Among the phases, while the nesquehonite is reported to form star-like crystal, the hydromagnesite and dypingite formed rounded rosette-like crystals (Dung & Unluer, 2016). But, the stability of these phases, especially nesquehonite, is a controversial issue (Walling & Provis, 2016). Not only the pH and temperature of the system, but also the carbon dioxide concentration causes different type of carbonates as a result of carbonation (C. Unluer & Al-Tabbaa, 2013). The carbonation rate does not depend on only the carbon dioxide level, but also the available amount of the brucite in the solution (Dung & Unluer, 2016). In addition, the carbonation degree of the unreacted magnesia is inhibited by the products collecting on its surface (Dung & Unluer, 2016). The studies approve that, to overcome these problems, the hydration, dispersion agents and hydrated magnesium carbonates serving as the nucleation sites for the new products could be added to the reactive magnesia cement systems (Dung & Unluer, 2016, 2017b, 2018; C. Unluer & Al-Tabbaa, 2013). While the hydration agent increases the reaction between magnesia and water, the dispersion agent decreases the water requirement resulting a denser microstructure. Moreover, these agents are claimed to enlarge the crystal

size of the hydrated magnesium carbonates (Dung & Unluer, 2016, 2017a). The nucleation effect enhanced by adding hydrated magnesium carbonates is found to be effective for the mechanical performance and the microstructure of the porous blocks containing reactive magnesia (C. Unluer & Al-Tabbaa, 2013). Also, the pre-curing process applied with higher levels of temperatures and carbon dioxide concentration before the main curing, is stated to have a positive impact on the mechanical properties (Dung & Unluer, 2017a).

The water requirement of the cement having reactive magnesia is stated to be higher (Walling & Provis, 2016). The reasons for this are thought to be the agglomeration of the magnesia particles when mixed with water and the porous structure of magnesia (Vandeperre et al., 2008; Walling & Provis, 2016).

Generally, the strength of the mortars prepared with the reactive magnesia cements in ambient conditions is lower when compared with that of portland cements (De Silva et al., 2009; Martin Liska & Al-Tabbaa, 2012; Cise Unluer, 2018; Walling & Provis, 2016). In addition, the binding abilities of the hydration products are reported to be lower (Martin Liska & Al-Tabbaa, 2012; Cise Unluer, 2018; Walling & Provis, 2016). However, the usage of the reactive magnesia is also suggested to compensate the strength reduction due to the interfacial transition zone. According to the study, the reactive magnesia particles have a tendency of moving towards the zone and react with excess water to form the brucite filling the zone (Chen et al., 2013). Furthermore, besides the portland cement, the reactive magnesia can be utilized with ground granulated blast furnace slag to create alkaline environment. The pastes consisting of the slag are activated producing the M-S-H gels and hydrotalcite-like phases. It is stated that the strength development of these pastes is affected by the properties and impurities of magnesia (Jin et al., 2013; Ruan & Unluer, 2017). On the other hand, modifying the curing environment with high level of carbon dioxide provides very different outcomes (Walling & Provis, 2016). In the study done by Liska, Vandeperre and Al-Tabbaa with reactive magnesia cement-based pressed masonary units, it is found that the strength of the specimens prepared pressing the mixture into small cylindrical molds with a press and cured in higher level of carbon

dioxide environment is determined as about 18 MPa for a month which is around six times that of their corresponding specimens cured in ambient conditions. For the specimens stored at ambient carbon dioxide levels, the only carbonation phase is hydrotalcite, the influence of which on the mechanical behavior is low. However, the carbonation product for the specimens cured in high level of carbon dioxide is determined to be the nesquehonite (M. Liska et al., 2008). It was stated that the strength development of the reactive magnesia cements is depending on the filling the pores and the binding strength of carbonate crystals (Dung & Unluer, 2017a, 2018; M. Liska et al., 2008; Mo & Panesar, 2012; Vandeperre et al., 2008). Instead of dypingite and/or hydromagnesite, the nesquehonite, formed as the main carbonation product in reactive magnesia cement-based systems, is determined to be the main cause of higher strength (Dung & Unluer, 2017a; C. Unluer & Al-Tabbaa, 2013). It is also reported that the strength of the carbonated phase of magnesia is higher than that of lime, so it is suggested that the accelerated carbon dioxide curing conditions leads to the higher strength contribution of the reactive magnesia than that of portland cement (De Silva et al., 2009; M. Liska & Al-Tabbaa, 2009; Walling & Provis, 2016). Moreover, it is concluded that it is possible to increase the strength gain using the dispersion and hydration agents (Dung & Unluer, 2016). Instead of the amount, the morphology of the carbonate binders is also reported to be the main factor for the performance of carbonate binders. The well-developed crystals provide higher mechanical performance to the binders (Mo & Panesar, 2012).

The calcination conditions of the reactive magnesia used have significance in the expansion properties of cement mortars having reactive magnesia. It is found that the higher calcination temperature and residence time mitigate the specific surface, correspondingly, the reactivity of the magnesia (Mo et al., 2010). The studies reveal that the reactive magnesia had a porous structure and the hydration products (ie. brucite) formed at the pores of the magnesia create a tensile stress on the magnesia grains thus the grains broken apart forming new hydration sites. While the magnesia with higher reactivity reached its ultimate expansion in a short time, the cements containing lower reactive magnesia, like the dead-burned magnesia, showed a higher

ultimate expansion in a longer time duration, causing an undesirable situation (Kabir & Hooton, 2020; Mo et al., 2009, 2010, 2014). Besides the calcination conditions, the pH of the environment was claimed to have an importance for the expansion of magnesia. In the high pH environment, more $Mg^{+2}$ ions were collected near the surface of magnesia, thus causing a higher supersaturation degree and a higher expansion. Therefore, the pozzolan additions, such as fly ash, decreasing the pH of the environment had great influence on the expansions. Moreover, it was stated that the volume stability could be affected by the mineral admixture addition due to the products of pozzolanic reaction and change in the viscoelastic properties of the cement matrix (Gaze & Smith, 1978; Mo et al., 2014). While the length change of the reactive magnesia cement mortars is generally higher than the portland cement-based systems, the performance is also depending on the average particle size of reactive magnesia (Chatterji, 1995; Mo et al., 2010, 2014). It was reported that the finer magnesia particles showed a lower expansion than the coarser ones did. The finer reactive magnesia particles were suggested to disperse easily in the pore solution during the setting of cement so that their probability to hydrate locally not causing a significant expansion was higher. But, the coarser particles were forced to hydrate in their embedded site (Chatterji, 1995).

From the durability point of view, it was believed that the expansion of the specimens having reactive magnesia could be beneficial. The carbonation products modified the pore system, causing a reduction in the total pore volume and the permeability. On the other hand, if cracks were formed in the matrix due to the excessive expansion, not only the durability but also the strength could be diminished (Jin et al., 2013; Mo et al., 2014). It was also reported that the durability of the hydrated magnesium carbonates showed the same performance as that of portland cement (Al-Tabbaa, 2013; Martin Liska & Al-Tabbaa, 2012; Cise Unluer, 2018). One of the advantages of the use of reactive magnesia over the other novel cementitious materials was considered to produce a more stable hydration product, the brucite. The solubility of $Mg(OH)_2$ (0.009 g / 100 mL water) was much lower than $Ca(OH)_2$ (0.185 g / 100 mL water) (De Silva et al., 2009; Mo et al., 2014). Secondly, it was

reported that the pH of the brucite-rich environment (10.5) was lower than that of lime-rich (12.5) and the stability of brucite, against acidic environments was better (Al-Tabbaa, 2013; Jin et al., 2013; Martin Liska & Al-Tabbaa, 2012). In addition, it was found that the stability of the magnesium carbonate was higher than the calcium carbonate (Teir et al., 2006). However, these advantages can be the drawbacks when considered the corrosion risk of the steel rebars used in concrete, due to the decrease in alkali ions creating a low alkaline environment (Ashraf, 2016; Cise Unluer, 2018).

The environmental impact of the reactive magnesia cement production is a debatable issue mainly because of its possibility to capture carbon dioxide gas from the atmosphere during its carbonation reactions, reducing its carbon dioxide emissions. Due to the complex calculation with the specific heat capacities of the raw materials, production temperatures, and mix proportions, Ruan and Unluer compared the ordinary portland cement and reactive magnesia utilizing the life cycle assessment methodology. This showed the portland cement was a more sustainable option over the reactive magnesia with respect to the carbon dioxide emission, but when the whole carbonation capacity of the reactive magnesia was considered, the reactive magnesia became the preferred option (Ruan & Unluer, 2016). The further reduction in environmental impact was also claimed to be achieved using supplementary cementitious materials (Ruan & Unluer, 2017). On the other hand, other study conducted by Shen et al., claimed that the reactive magnesia had higher carbon footprint than the portland cement since the reactive magnesia could not act as a carbon dioxide sink in ambient environment as expected (Shen et al., 2016). From the recyclability point of view, another study proved that it was possible to recycle the reactive magnesia cements completely, produced from the specimens which had been carbonated before, implying that reactive magnesia cements can be promising alternative to the portland cement (Sonat et al., 2017; Cise Unluer, 2018).

## 2.2. Carbonation

### 2.2.1. Introduction

Although the carbon dioxide concentration of the ambient environment is lower than 1 %, it can react with the materials in other words cause carbonation. The carbonation (or carbonatation) is referred to the reaction between a substance and the carbon dioxide to form a type of carbonate (Erdoğan, 2010; Tokyay, 2016).

The carbonation in cement-based materials is seemed to be an effective technique to capture carbon dioxide in atmosphere, suggesting a solution to reduce carbon dioxide emissions. The possible theoretical maximum amount of carbon dioxide mainly depends on the chemical composition of cement (Ashraf, 2016).

The ordinary portland cement paste matrix in hardened form can be composed of the hydration products of the cement compounds (C-S-H gel, calcium hydroxide, ettringite, etc.), unreacted cement particles and water (Mehta & Monteiro, 2006). Besides them, depending on the cement type and the concrete where the cement is used, aggregates, mineral and chemical admixtures can be present in the matrix.

The atmospheric carbon dioxide concentration is about 400 ppm (Ashraf, 2016). This carbon dioxide can dissolve in the cement pore solution. It was reported that the hydration products or the unreacted cement particles could react with the carbon dioxide chemically, and modify their structure and the environment where the reactions took place. The main factors affecting the carbonation were stated to be the environmental conditions (relative humidity, carbon dioxide concentration, temperature, pressure), cement properties, mix design and mineral admixtures as well as the physical properties of specimen (Ashraf, 2016; De Silva et al., 2006; Šavija & Luković, 2016; Cise Unluer, 2018). The optimum relative humidity was found to be between 50 and 70 % for the maximum carbonation (Šavija & Luković, 2016). Moreover, the cyclic carbon dioxide curing was found to be more efficient than the continuous carbon dioxide exposure. It was suggested that this process

prevented the water saturation and established the carbon dioxide pathways (Šavija & Luković, 2016).

### 2.2.2. Carbonation of Cement Matrix

The main carbonation reaction in cement matrix was reported to take place for the calcium hydroxide (portlandite) to form the calcium carbonate as the carbonation product. This process was stated to be consisting of several main steps, the dissolution of the calcium hydroxide, absorption of the carbon dioxide, formation of the carbonate ions and precipitation. Due to the formation of a thin layer on the calcium hydroxide surface, the new carbonated products were inhibited the further reactions, which meant the rate of carbonation decreased. For the carbonation, the moisture was also reported to be essential, even though the diffusivity of carbon dioxide in air is higher than that in water (M. Liska et al., 2008; Šavija & Luković, 2016). The carbonation reaction of the portlandite is basically shown in Eqn. 2.16.

$$Ca(OH)_2 + CO_2 \rightarrow CaCO_3 + H_2O \qquad \text{Eqn. 2.16}$$

It was reported that for the carbonation of C-S-H gel, the calcium ions from the gel were removed from the structure and an amorphous silica gel (in other words, calcium modified silica gel, low lime C-S-H gel or polymerized silica gel) was formed as well as various polymorphs of calcium carbonate, depending on Ca/Si ratio of the gel as shown in Eqn. 2.17. The C-S-H gels with higher Ca/Si tended to form calcite instead of the aragonite and vaterite (Ashraf, 2016; Fernández Bertos et al., 2004; Šavija & Luković, 2016). Moreover, when the ratio became lower, the rate of C-S-H gel decomposition increased, in spite of the decrease in the total possible amount of the calcium carbonate which could be formed due to the carbonation. It was realized that the carbonation rate of the C-S-H gel with former Ca/Si ratio was lower than that of the C-S-H gel having lower ratio, possibly due to the calcium

carbonate layer covering the surface of the former C-S-H gel and inhibiting the further reactions (Ashraf, 2016; Šavija & Luković, 2016). The other factors for the C-S-H carbonation are listed as the carbon dioxide concentration and environmental conditions (Fernández Bertos et al., 2004; Šavija & Luković, 2016).

$$(CaO)_x(SiO_2)(H_2O) + xCO_2 \rightarrow xCaCO_3 + SiO_2(H_2O)t + (z - t)H_2O \qquad \text{Eqn. 2.17}$$

According to the studies, the carbon dioxide dissolved in the pore solution of the cement matrix can cause to the carbonation of the ettringite resulting the formation of the calcium carbonate, gypsum and alumina gel. It was shown that the rate of the reaction was depending on the temperature. At the end of the reaction, the carbonate crystals were vaterite and the total amount of carbonates was reported to exceed that from the dissolution of calcium hydroxide (Šavija & Luković, 2016; Zhou & Glasser, 2000). The reaction is shown in Eqn. 2.18.

$$\begin{aligned} 3CaO \cdot Al_2O_3 \cdot 3CaSO_4 \cdot 32H_2O + 3CO_2 \\ \rightarrow 3CaCO_3 + 3(CaSO_4 \cdot 2H_2O) + Al_2O_3 \cdot xH_2O \\ + (26 - x)H_2O \end{aligned} \qquad \text{Eqn. 2.18}$$

The portland cement clinkers are produced in such a way that their main compounds will be the dicalcium silicate and tricalcium silicate to gain strength and durability to the concrete (Erdoğan, 2010). According to the studies, even before their use in concrete, they could react with the carbon dioxide in air (Šavija & Luković, 2016). It was found that while the polymorph of the calcium carbonate due to the reaction of $C_3S$ and γ-$C_2S$ was calcite, that for β-$C_2S$ was aragonite. In addition to these, the amorphous calcium carbonate was also recognized during the carbonation (Ashraf, 2016). The carbonation reactions of these phases are shown in Eqn. 2.19 and 2.20.

$$3CaO \cdot SiO_2 + 3CO_2 + nH_2O \rightarrow SiO_2 + nH_2O + 3CaCO_3 \quad \text{Eqn. 2.19}$$

$$2CaO \cdot SiO_2 + 2CO_2 + nH_2O \rightarrow SiO_2 + nH_2O + 3CaCO_3 \quad \text{Eqn. 2.20}$$

### 2.2.3. Consequences of Carbonation

The carbonation reactions consume some substances/compounds to produce new ones, so it should be expected that the micro- and macro-structure of the cement matrix and correspondingly, mortar and concrete were modified.

According to the studies, the rate of natural carbonation and correspondingly the strength gain due to the carbonation were low (Fernández Bertos et al., 2004). To understand the effects of carbonation, accelerated tests are performed using higher carbon dioxide concentrations or higher carbon dioxide pressures in a controlled environment during the curing regime of the test samples (Ashraf, 2016).

During carbonation, the calcium hydroxide, which is responsible for the high pH of the pore solution, is consumed by the carbon dioxide dissolved there. This leads to a decrease in the pH of the matrix, so the carbonation can be detected using a phenolphthalein indicator whose color turns into red (or pink) in a high alkaline environment. The most preferred method in cement-based systems is to use phenolphthalein for the detection of the carbonation depth (Ashraf, 2016).

The pore size distribution of the cement matrix changes due to the volume change during the carbonation. According to the studies, since the volume of the end products is higher than the reactants, a reduction in total porosity takes place and, correspondingly the permeability decreases (Ashraf, 2016; Šavija & Luković, 2016). It was suggested that the precipitation of calcium carbonate took place in smaller pores instead of larger ones due to better water condensation (Ashraf, 2016; Šavija & Luković, 2016). The further possible carbonation reactions were stated to be inhibited because the reduction in permeability resulted from the carbonation of cement matrix also decreased the carbon dioxide diffusion to the matrix (De Silva et

al., 2006). But, it was stated that this reduction could become low by the possible micro cracks formed due to the carbonation (Šavija & Luković, 2016).

Although the expansion depends on the polymorph formed at the end of the reaction, the volume of the carbonation products is generally higher than the reactants, so during the carbonation process, the net increase in volume and densification of the matrix is observed. In addition, unlike calcium hydroxide, the calcium carbonate which is the main carbonation product, has a scarce solubility in water (Ashraf, 2016; Šavija & Luković, 2016; Teir et al., 2006). Furthermore, it was suggested that the increase in volume was resulted from the heat generated due to the accelerated carbonation (Fernández Bertos et al., 2004). One of the carbonation consequences observed can be the shrinkage of cement paste, the reason of which is a debatable issue. According to one study, the carbonate layer produced on the surface of calcium hydroxide held the moisture inside its structure. But, when the moisture outside was removed due to the environmental conditions, the moisture gradient formed within this impermeable layer causing cracks. Other study suggested that the carbonation shrinkage was due to the carbonation of the C-S-H gel, where the decrease occurred in the calcium content within its structure and silica gel formation. The hydroxyl group in C-S-H gel reacted with silica gel and produced polymer chains, which were considered to be the main cause of the carbonation shrinkage (Šavija & Luković, 2016).

It was found that the carbonation generally caused the increase in the strength and elastic modulus due to the decrease in porosity and the change of the structure of C-S-H gel. But, in the cements containing blast furnace slag, a reduction in elastic modulus was also reported. At the same time, the prolonged carbon dioxide curing was claimed to have a detrimental effect on the mechanical properties. In early times, the carbonation caused the structure to be denser, resulting higher mechanical properties. But, for late ages, due to the carbonation of inner C-S-H gels, a reduction in strength was observed (Šavija & Luković, 2016; Cise Unluer, 2018). This effect could also be associated with the different polymorphs resulted from the carbonation rate. The slower the reaction was, the well-developed structures the crystals had (De

Silva et al., 2006). In addition, to obtain a significant increase in the mechanical properties, it was stated that the fresh state-system should be exposed to the carbon dioxide (Ashraf, 2016).

One of the main problems about carbonation is an increase in the possibility of the occurrence of reinforcement corrosion. In the high alkaline environment of a portland cement-based system, the reinforcements used in concrete are protected by passive protective film. During the carbonation, possibly due to the consumption of calcium hydroxide, which provides high pH-environment, this film is destroyed leaving the reinforcements vulnerable to the corrosion risk (Ashraf, 2016; Fernández Bertos et al., 2004).

# CHAPTER 3

# EXPERIMENTAL STUDY

## 3.1. General

Within the scope of this study, it was necessary to determine the effective one among the different regimes involving various burning temperatures and exposure times to obtain the most possible reactive magnesia by calcination of naturally obtained magnesite. The reactive magnesia cements produced by combining portland cement and reactive magnesia with various ratios (about 0, 15, 30, 50 and 100 %), by mass were investigated in terms of mechanical and chemical performances. In addition, to search the effect of carbon dioxide, the mortar and paste samples were cured in several curing environments having similar relative humidity (90 %) and temperature (25 ºC), but different carbon dioxide concentrations (0.04, 20 and 50 %).

All the processes and experiments were performed in the Materials of Construction Laboratory, Department of Civil Engineering, Middle East Technical University, except for the chemical and thermogravimetric analyses which were done in the Central Laboratory of METU.

## 3.2. Raw Materials

As the raw material for reactive magnesia, the magnesite, the chemical analysis of which is shown in Table 3.1, was obtained from the company "KÜMAŞ" (Kütahya Manyezit İşletmeleri A.Ş.). Its chemical analysis shows that it has a high amount of magnesium oxide and carbon dioxide. Assuming that all oxides and carbon dioxide

belong to a carbonate, it is determined that the amount of magnesium carbonate in magnesite is higher than 90 %. The amount of calcium carbonate is found to be lower than 2 %.

The magnesite, obtained from KÜMAŞ, was ground using a laboratory ball mill to reach a fineness of about 4000 $cm^2/g$ according to ASTM C 204 (ASTM C 204, 2018). That part of the material, which passed through a 1-mm sieve, was heated as described in Section 4.1.1., to produce reactive magnesia.

CEM I 42.5 R portland cement produced according to TS EN 197, which was obtained from Baştaş Cement factory, was utilized as the main binder. The strength gain mechanism of the reactive magnesia cements are mainly related with the chemical composition of the binder, so two effective different mineral admixtures on changing the composition mostly, were used namely as F-type fly ash and ground granulated blast furnace slag. These were obtained from Sugözü Thermal Power Plant and İsdemir (İskenderun Demir Çelik A.Ş.), respectively. The chemical composition, density and fineness of each mineral admixture as determined by the related standards are also presented in Table 3.1 (ASTM C 188, 2009; ASTM C 204, 2018). To give an idea about their crystal structure, their X-ray diffractograms shown in Figure 3.1 are also obtained.

The mortars were produced using fine aggregates whose gradation curve can be seen in Figure 3.2. From Figure 3.3 showing the XRD profile of the sand used, it can be concluded that the main crystal structure is calcite with a minor impurity of quartz. Its oven-dried specific gravity was measured 2.64.

Table 3.1. The physical properties and oxide composition of the magnesite and raw materials.

| | | **Magnesite** | **Portland Cement** | **Ground Granulated Blast Furnace Slag** | **Fly Ash** |
|---|---|---|---|---|---|
| Chemical Compositions | $CO_2$ (%) | 49.54 | 4.78 | - | - |
| | CaO (%) | 0.87 | 60.11 | 38.2 | 3.74 |
| | MgO (%) | 43.31 | 1.76 | 5.73 | 1.38 |
| | $SiO_2$ (%) | 0.72 | 18.87 | 37.8 | 55.6 |
| | $Fe_2O_3$ (%) | 0.49 | 2.73 | 0.834 | 9.12 |
| | $Al_2O_3$ (%) | 0.068 | 4.02 | 12.9 | 23.1 |
| | $SO_3$ (%) | 0.034 | 5.74 | 1.28 | 0.515 |
| | MnO (%) | - | - | 1.16 | 0.09 |
| Physical Properties | Fineness ($cm^2/g$) | 4200 | 3950 | 4800 | 2850 |
| | Density ($g/cm^3$) | 2.95 | 3.07 | 2.85 | 2.24 |

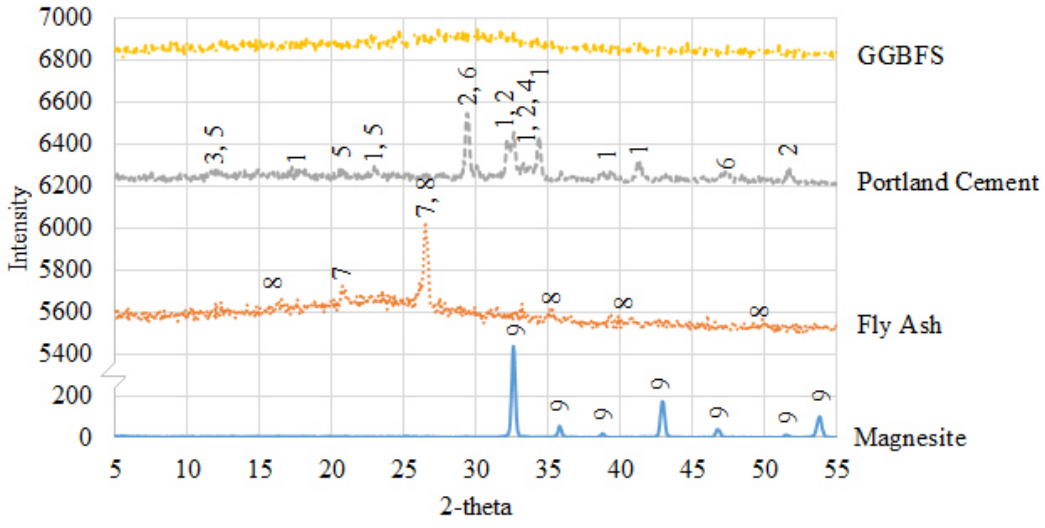


Figure 3.1. The XRD profiles of the raw materials used in the study (1: $C_2S$, 2: $C_3S$, 3: $C_3A$, 4: $C_4AF$, 5: Gypsum, 6: Calcite, 7: Quartz, 8: Mullite, 9: Magnesite).

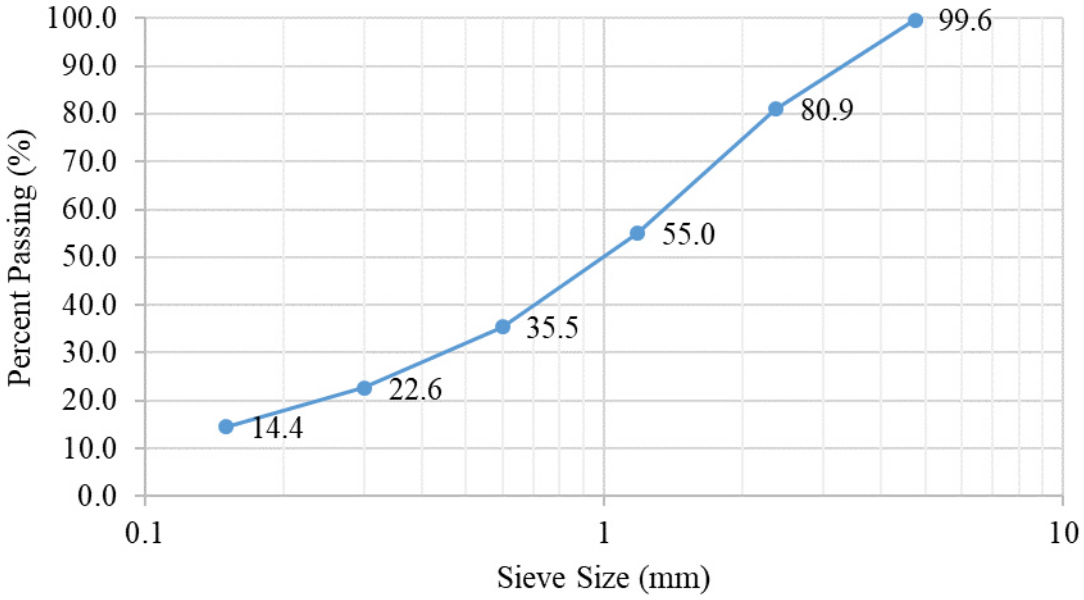


Figure 3.2. Gradation curve of the sand used.

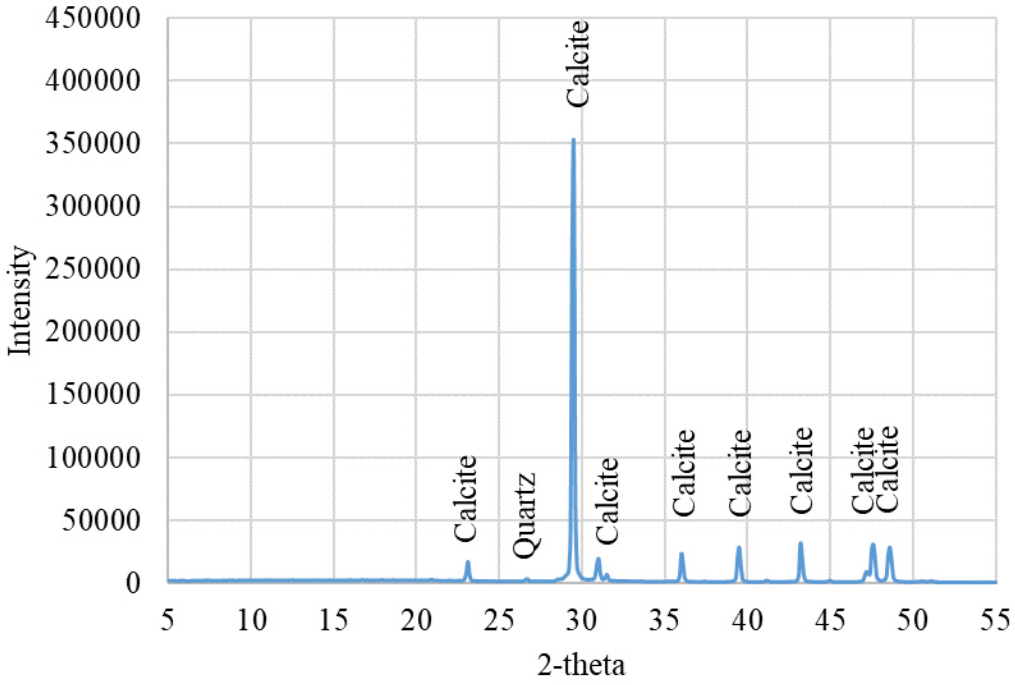


Figure 3.3. The XRD profile of the sand.

### 3.3. Carbonation Chamber

To perform the accelerated carbonation curing to the samples, a carbonation chamber, in which the carbon dioxide concentration, temperature and humidity can be controlled, was designed and built. This chamber monitors the above-mentioned conditions by modifying the internal environment of the chamber.

One of the main requirements is an isolated system, which should not be affected from the outside conditions. To overcome this problem, the body of an old refrigerator was used improving its insulation. The main parts of the chamber, schematically, and the flow chart of the carbonation chamber are shown in Figure 3.4 and 3.5, respectively.

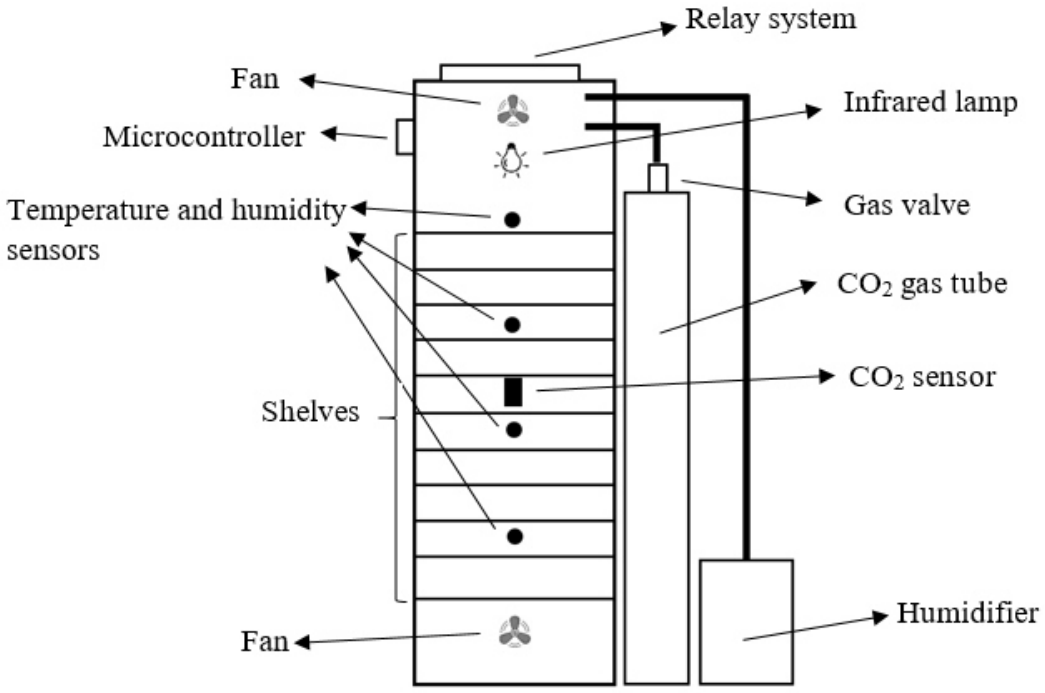


Figure 3.4. Main parts of the carbonation chamber.

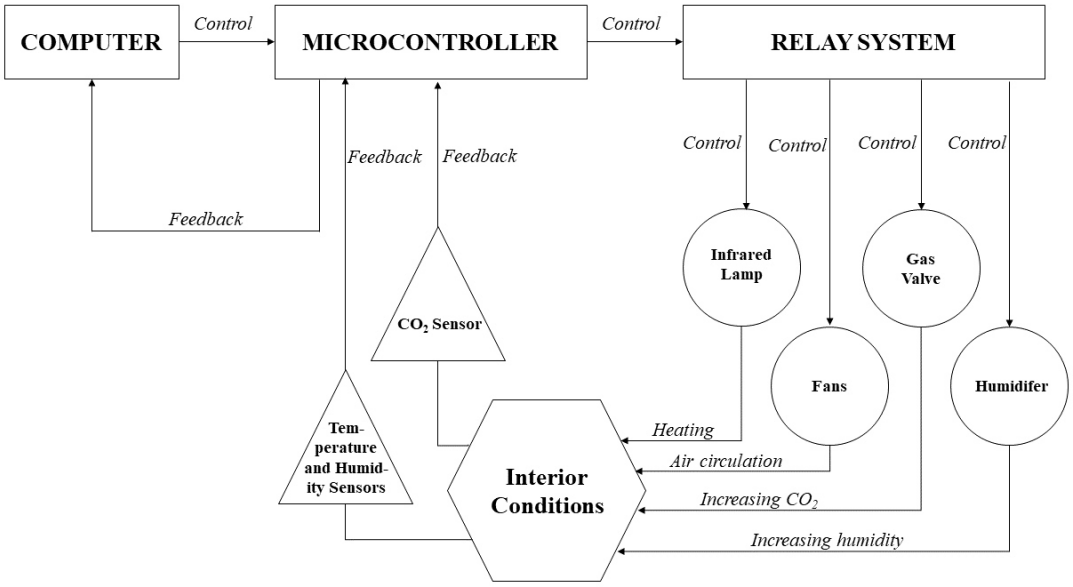


Figure 3.5. Flow chart of the carbonation chamber.

The carbonation chamber, which can be seen in Figure 3.6, has five main components; computer, microcontroller, relay system, devices and sensors.

- The microcontroller, utilized in the chamber, determines the environmental conditions using the sensors and controls the relay system. As the microcontroller, Arduino Mega 2560, which can be controlled by a computer software, is operated. According to the data from the sensors and the required conditions for the environment, it activates the relay system.
- A computer was used to monitor the humidity and carbon dioxide concentration of the curing conditions and control the microcontroller.
- The relay system consists of a relay controlling four different channels and a 220-V socket for each channel. According to the directions given by the microcontroller, the relay turns on or turns off the sockets of each device.
- The devices, connected to the sockets, modifies the environment. An infrared lamp, a humidifier, a gas valve (connecting to carbon dioxide gas tube) and

two fans are used to increase the interior temperature, humidity, carbon dioxide concentration and provide air circulation, respectively.

- To get an accurate result, four humidity and temperature sensors in different places of chamber are placed. A carbon dioxide sensor used is fixed at the middle of the chamber. The specifications of the sensors are given in Table 3.2. The working principles are given in Appendix A.

Figure 3.6. The carbonation chamber.

Table 3.2. The specifications of the sensors used.

| | **ExplorIR® - W100% $CO_2$ Sensor** | **DHT 11 Humidity and Temperature Sensor** |
|---|---|---|
| **Measurement Range** | 0 – 100 % $CO_2$ | 20 – 95 % RH<br>0 – 50 ºC |
| **Accuracy** | 70 ppm | 5 % RH<br>1 ºC |
| **Resolution** | 100 ppm | 1 % RH<br>1 ºC |
| **Sampling Period** | 500 ms | 1000 ms |

## 3.4. Experimental Procedures

The experimental procedure done in this study is generally summarized in Figure 3.7. While the procedures, methods and test conducted until the production of reactive magnesia is called 'preliminary experiments', the 'main experiments' are the tests done with reactive magnesia produced.

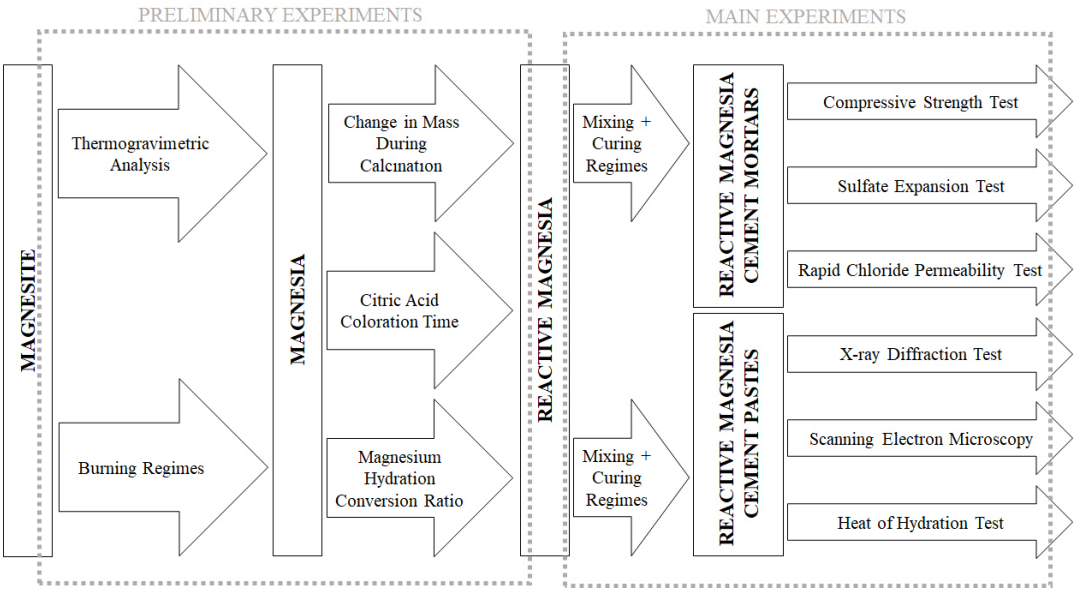


Figure 3.7. The experimental procedure conducted.

### 3.4.1. Preliminary Experiments

Before starting the main experimental work, a preliminary study was carried out to obtain the optimum calcination conditions necessary to get the most reactive magnesia. The main parameters affecting the reactivity of magnesia are the calcination temperature and exposure time in the furnace (Mo et al., 2010). In order to evaluate the effects of different burning regimes thermogravimetric analyses (TGA), measuring the amount of mass loss after calcination, citric acid coloration time, and magnesia hydration conversion ratio were considered.

**Thermogravimetric analyses (TGA):** To detect the temperatures at which the magnesite started to calcine, the materials were exposed to thermogravimetric analyses by using Perkin Elmer Pyris 1 TGA Instrument located at the METU Central Lab. The temperature of the oven-dried sample was risen from 35 ºC to 1050 ºC at air environment and for each temperature increment, five mass measurements were taken.

**Burning regimes:** The type of magnesia used in the study should be light burned so that the hydration/carbonation of magnesia can occur at a comparable or similar time as that of portland cement fraction. In order to determine the most reactive magnesia, the burning regimes for different temperatures and durations were performed to the magnesite samples at a small scale. The burning regimes, shown in Table 3.3, consist of two main parameters, the burning temperature and exposure times. The burning temperatures were in a range of between 500 and 800 ºC with 100 ºC intervals. The exposure times changed from 60 to 180 minutes. In total, 20 different regimes (4 different burning temperatures and 5 different exposure times) were applied to specimens. To get a uniform temperature distribution over the magnesite sample, and correspondingly, a more homogeneous magnesia, the rate of the interior temperature increase was kept constant at about 100 ºC/hour. The obtained magnesia was let to cool down in the oven.

Table 3.3. The main parameters used in burning regime applied to the magnesite specimens.

| Burning Temperature (°C) | Exposure Time (min) |
|---|---|
| 500 | 60 |
| 600 | 90 |
| 700 | 120 |
| 800 | 150 |
| | 180 |

**Change in mass during calcination:** After drying of samples at 105 ºC, the difference between the initial mass ($m_0$) and the final mass ($m_f$) after burning is calculated. Since in the production of reactive magnesia, the carbon dioxide has to be removed from the magnesite, the change in mass can give an indication of the reactivity of the magnesia obtained. The higher change in mass refers to the higher possibility of producing reactive magnesia. However, this measurement is not able to give an idea about the degree of crystallinity of the resulting magnesia which is another important factor affecting the reactivity. For this test, the initial mass is selected 40 grams and the change in mass was calculated by Eqn. 3.1.

$$\text{Change in mass } (\%) = \frac{m_0 - m_f}{m_0} \qquad \text{Eqn. 3.1}$$

**Citric acid coloration time:** The reactivity of the calcined magnesia can be determined by the coloration time of the reaction of the sample with citric acid. The less coloration time indicates higher reactivity of the magnesia obtained (Mo et al., 2010; Zhu et al., 2013).

In the method, 1 g of calcined magnesia sample was mixed with 200 ml 0.0175 M citric acid solution containing phenolphthalein indicator with a constant speed of 600 rpm at 40°C. At the initial stages of the reaction, due to the acidic environment, phenolphthalein could not change the color of solution. The color of the solution was

white due to the color of the powder added to the solution (Figure 3.8, left). As time passes, the reaction results in magnesium citrate and water, and the color changes from white to pink, due to the alkaline environment (Figure 3.8, right). The coloration time was measured as the time duration between the start of mixing and the conversion of the color from white to pink. For this test, the samples obtained from calcination tests were used. After 30 minutes (1800 seconds), for the samples not showing color change, the experiment was terminated.


Figure 3.8. The colors of citric acid solution containing calcined magnesia sample with phenolphthalein indicator at the beginning (left) and at the end (right) of the reaction.

**Magnesia Hydration Conversion Ratio:** This method is based on the reaction between water and the reactive magnesia sample, that produces magnesium hydroxide. According to this method, using the molar masses of water and magnesia (magnesium oxide), the X ratio can be calculated as depicted in Eqn. 3.2 and 3.3 (Zhu et al., 2013).

$$MgO + H_2O \rightarrow Mg(OH)_2 \quad \text{Eqn. 3.2}$$

$$X\,(\%) = \frac{40.30(w_0 - w_1)}{18.02 w_0} \cdot 100 \quad \text{Eqn. 3.3}$$

where, $w_0$ and $w_1$ are the initial and final masses, respectively.

Eqn. 3.3 is valid for magnesium oxide samples of high purity. For the impurities present in the samples, a correction factor should be proposed.

$$X_{corrected}\,(\%) = X\,(\%) \cdot \frac{w_0}{w_{MgO}} = X\,(\%) \cdot \frac{1}{\text{Mass ratio of MgO in calcined sample}} \quad \text{Eqn. 3.4}$$

According to $X_{corrected}$ ratio, $w_{MgO}$ indicates the total mass of magnesia in calcined sample. Using the results of the calcination tests applied to the specimens, the magnesia content can be determined.

During the test, 2 g of calcined magnesia samples were mixed with 100 mL of distilled water for 1 day at 20°C. The solution containing the insoluble residues were vacuum filtered from a filter paper whose mass was recorded initially. The filter and the residues were dried for 1 hour and the final mass of the paper with residues was recorded. Using Eqn. 3.4, the $X_{corrected}$ (%) was calculated.

**Water content:** Since the reaction between reactive magnesia and water is very rapid, in experiments, unless otherwise stated, the water content was modified according to the reaction kinetics. In the chemical analysis shown in Table 3.1, it can be seen that about 43 % and 50 % of magnesite is magnesia and carbon dioxide, respectively. If the total oxide composition is normalized to 100 %, the content of magnesia and carbon dioxide will be 45 % and 52 %, respectively. Assuming that during calcination process, all the carbon dioxide is removed, the percentage of

magnesia in the calcined magnesite (reactive magnesia) will become 95 %. In mortars, the reaction between magnesia and $H_2O$ occurs according to Eqn. 3.2.

It can be calculated that 1 gram of magnesia is reacted with 0.45 (=18.02/40.30 [molar masses of water and magnesia, respectively]) gram of water to form brucite. Because the amount of magnesia in reactive magnesia is 95 %, 1 gram of reactive magnesia will react with 0.43 (=0.45*95 %) gram of water. So, considering also the water requirement for the workability of the reactive magnesia cements, the water requirement was made according to the Eqn. 3.5.

$$W = 0.484 * (C + M + S + F) + 0.43 * M \quad \text{Eqn. 3.5}$$

In this equation, C, M, S, F refer to the content of the portland cement, reactive magnesia, ground granulated blast furnace slag and fly ash, respectively. The coefficient of 0.484 is selected based on the water/cement ratio proposed in ASTM C 109 for ordinary portland cement (ASTM C 109, 2016). The validation of Eqn. 3.5. with respect to the consistency of the reactive magnesia-incorporated cements is given in Appendix B.

**Initial Specimen Castings:** To determine the appropriate curing procedure and water requirement for the main experiments, several sets of specimens were cast and cured under different curing regimes. The optimum water requirement and curing regime were determined by performing compressive strength tests on cubic specimens.

### 3.4.2. Main Experiments

After determining the burning regime in which the most reactive magnesia was produced, the reactive magnesia-incorporated cements were produced using portland

cement, ground granulated blast furnace slag and fly ash. The water requirement is calculated as shown in Eqn. 3.5.

**Mixing Procedure:** The mixing procedure followed was similar to that mentioned in ASTM C 305 (ASTM C 305, 2014). For the mortar preparation, after all the powder materials were put in the mixing bowl, water was added to the mixture. The mixer was started at slow speed and the cement paste was mixed for 30 seconds. In the next two minute-duration, the sand is added slowly. The speed of the mixer was increased and the mixing at medium speed was continued for 30 seconds. Then, the mixer was turned off and the mortar collecting on the surfaces of the bowl, was moved to the center and after 90 seconds, the mixer was started at slow speed. The mixing process was done after 60 seconds.

**Compressive Strength Test:** The compressive strength was determined according to ASTM C 109 (ASTM C 109, 2016). 5 cm-cubic molds were used to cast the specimens and 1 day after casting, they were removed from molds. For each determination of strength test, 3 cubic specimens were used and if the strength of one specimen was not in the range of 8.7 % of the average, it was discarded. The loading rate was adjusted 1.5 kN/s. The statistical analysis was performed with SPSS software, utilizing ANOVA analysis with 95 % confidence.

**Sulfate Expansion Test:** The mortar bars with the dimensions of 28.5 cm x 2.5 cm x 2.5 cm were prepared. 1 day after casting, they were removed from the molds and their curing was continued for 1 week. At the end of the curing, they were immersed in solution containing 50 g sodium sulfate per liter of the solution as stated in ASTM C 1012 (ASTM C 1012, 2015). Using the pins placed on the ends of the bars and a comparator, the lengths of the bars had been determined for more than 2 months. Up to 3 weeks, the measurements were taken every week. In next weeks, the length change was determined for every 2 weeks. This solution was replaced in every 2 weeks.

**Rapid Chloride Permeability Test:** The test was performed according to ASTM C 1202 (ASTM C 1202, 2017). For the test, after 28 days from the casting, the

cylindrical mortar specimens were divided to obtain two slices with 5 cm-depth. The conditioning process recommended was applied to the slices and they were exposed to the sodium chloride and sodium hydroxide solutions in test cells prepared according to the related standard. After applying 60-V potential to the system, for each 30 minutes, the total charge passing through the slice was recorded.

**X-ray Diffraction Test:** The XRD profiles of the raw materials and samples were achieved by the BTX III Benchtop XRD Analyzer Materials of Construction Laboratory in METU. The sample in powder form was investigated in the range of 5-55 2-theta degrees. The identification of the XRD peaks in the pattern was done manually. To remove the water, but not to lose the possible carbonation / hydration products, the specimens were dried in 60 ºC before any XRD test.

**Heat of Hydration Test:** The heat evolved from the cement pastes were investigated through 2 days. The test procedure was done according to the Method B explained in ASTM C 1702 (ASTM C 1702, 2017). For reference sample, 23.5 grams of sand was used. The amount of each ingredient of specimens was prepared so that the heat capacities of the sample and reference were made equal. The heat capacities for each ingredient were obtained from the related standard except that of the reactive magnesia, which was approximately taken as 0.9 J/g.K.

**Scanning Electron Microscopy:** To investigate the structure of the hydration/carbonation products of the reactive magnesia cement paste samples, QUANTA 400F Field Emission SEM having the resolution of 1.2 nm, in the Central Laboratory at METU was used. To remove the moisture, but not to lose the possible carbonation / hydration products, the specimens were dried in 60 ºC.

# CHAPTER 4

# RESULTS AND DISCUSSION

## 4.1. Preliminary Experiments

### 4.1.1. Determining the Burning Regime

To produce the reactive magnesia, the magnesite should be calcined at such a temperature that should not be too high not to decrease the reactivity or not too low not to be able to calcine it. Therefore, thermogravimetric analysis was performed to the sample taken from the magnesite which would be used in the further experiments.

According to the TGA, performed to the magnesite sample and the results of which are shown in Figure 4.1, the sample lost approximately half of its weight at temperatures of about 600 ºC. Since before the experiment, the specimen was dried at 105 ºC in the furnace, all of the mass loss should be resulted from the removal of the carbon dioxide present in the carbonates. The total mass loss is a little bit higher than 50 % and this result coincides with the amount of the carbon dioxide content given by the chemical analysis in Table 3.1.

In the light of the thermogravimetric analysis results, different burning regimes, the details of which were given in Table 3.3, were performed on the magnesite samples and the reactivities of resulting magnesia were determined with several methods like the citric acid reactivity or magnesia hydration conversion ratio. The specimens burned are named according to their burning regimes and the former and latter numbers in the designations of the magnesia obtained represent the burning temperatures in °C and exposure time in minutes, respectively. So, for example,

M800-180 represents the oven-dried magnesia sample obtained by burning at 800 °C for 180 minutes.

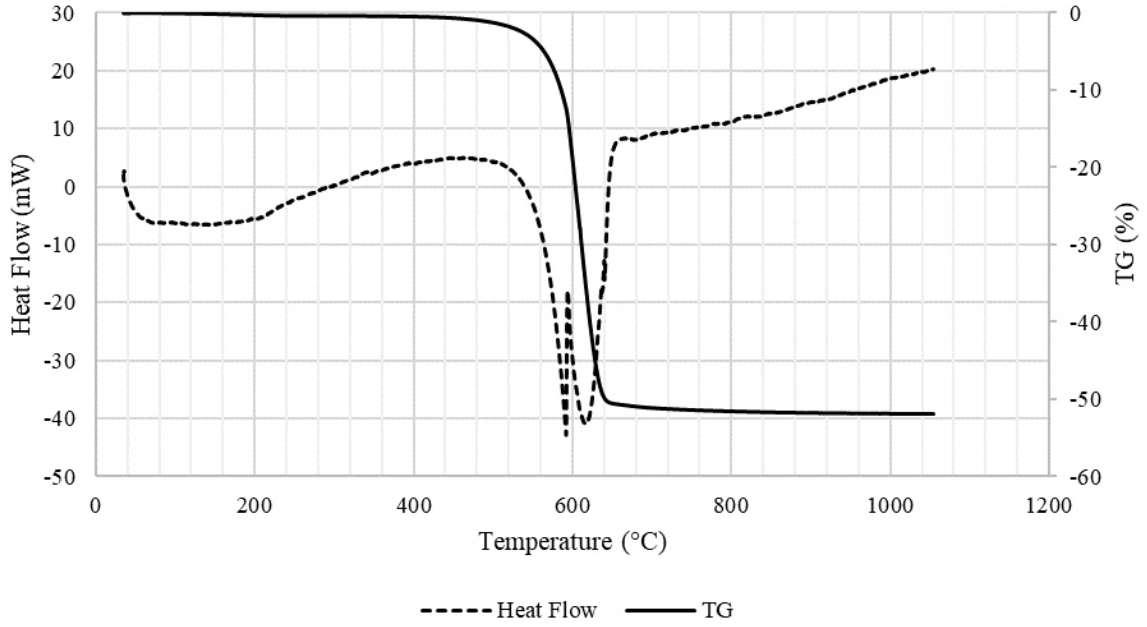


Figure 4.1. The thermogravimetric analysis of magnesite.

The results of the preliminary experiments performed to determine the reactivity of magnesia are shown in Table 4.1.

Table 4.1. Reactivity of magnesia as determined from the preliminary experiments.

| | Burning Regime | | Test Results | | |
|---|---|---|---|---|---|
| **Name of Magnesia** | **Burning Temperature (°C)** | **Exposure Time (min)** | **Mass change during calcination (%)** | **Citric acid coloration time (s)** | **Magnesia Hydration Conversion Ratio (%)** |
| **M500-60** | 500 | 60 | 9.20 | > 1800 | 10.32 |
| **M500-90** | 500 | 90 | 3.97 | > 1800 | -3.97 |
| **M500-120** | 500 | 120 | 4.33 | > 1800 | -6.18 |
| **M500-150** | 500 | 150 | 6.39 | > 1800 | 3.38 |
| **M500-180** | 500 | 180 | 10.58 | > 1800 | 0.92 |
| **M600-60** | 600 | 60 | 31.68 | 154 | 52.57 |
| **M600-90** | 600 | 90 | 49.31 | 40 | 87.96 |
| **M600-120** | 600 | 120 | 51.15 | 26 | 83.25 |
| **M600-150** | 600 | 150 | 49.91 | 32 | 94.03 |
| **M600-180** | 600 | 180 | 37.68 | 90 | 62.11 |
| **M700-60** | 700 | 60 | 50.06 | 30 | 79.05 |
| **M700-90** | 700 | 90 | 49.94 | 31 | 75.75 |
| **M700-120** | 700 | 120 | 50.11 | 29 | 84.24 |
| **M700-150** | 700 | 150 | 50.35 | 33 | 82.69 |
| **M700-180** | 700 | 180 | 50.41 | 34 | 77.59 |
| **M800-60** | 800 | 60 | 50.42 | 31 | 72.07 |
| **M800-90** | 800 | 90 | 50.42 | 28 | 73.48 |
| **M800-120** | 800 | 120 | 50.51 | 32 | 66.06 |
| **M800-150** | 800 | 150 | 50.94 | 33 | 75.25 |
| **M800-180** | 800 | 180 | 50.95 | 32 | 63.32 |

The burning temperature of 500 ºC resulted in the smallest mass loss for all burning periods, indicating that calcination was not complete. At and beyond 600 ºC, mass loss greatly increased as shown in Figure 4.2. For temperatures above 500 ºC, the mass loss is about 50 %, meaning that all the carbon dioxide is removed since it is shown that nearly half of the magnesite, by mass, is carbon dioxide in chemical oxide results.

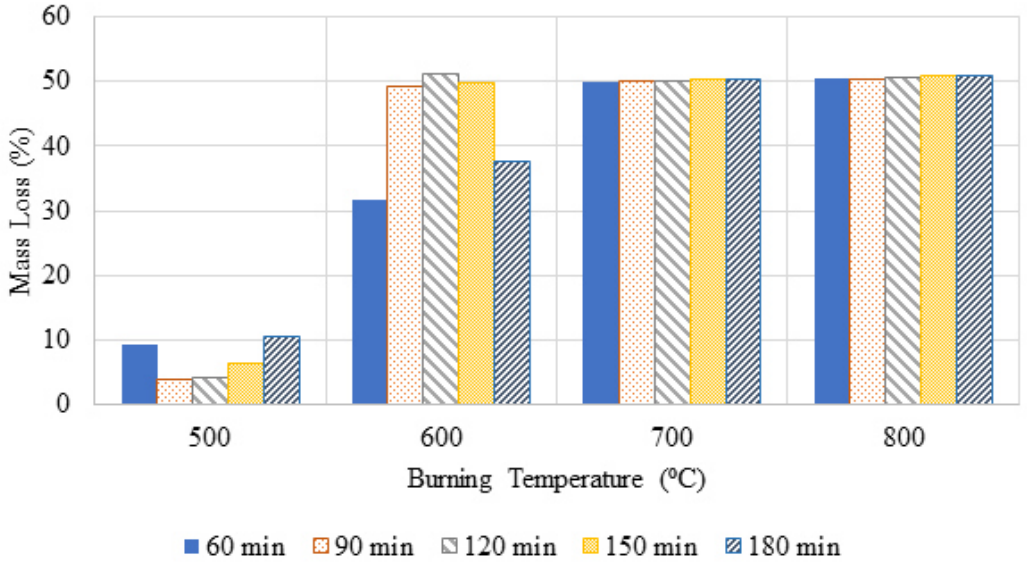


Figure 4.2. Mass losses in magnesite samples at different burning temperatures and durations.

The citric acid coloration time was measured to be around 30 s for the specimens burnt at 700 and 800 ºC. The shortest coloration time (26 s) was obtained for the specimen burnt at 600 ºC for 120 min as shown in Figure 4.3. The coloration time test results for the specimens burnt at 500 ºC were all beyond 1800 s, at which the test was stopped. Therefore, they are not shown in Figure 4.3.

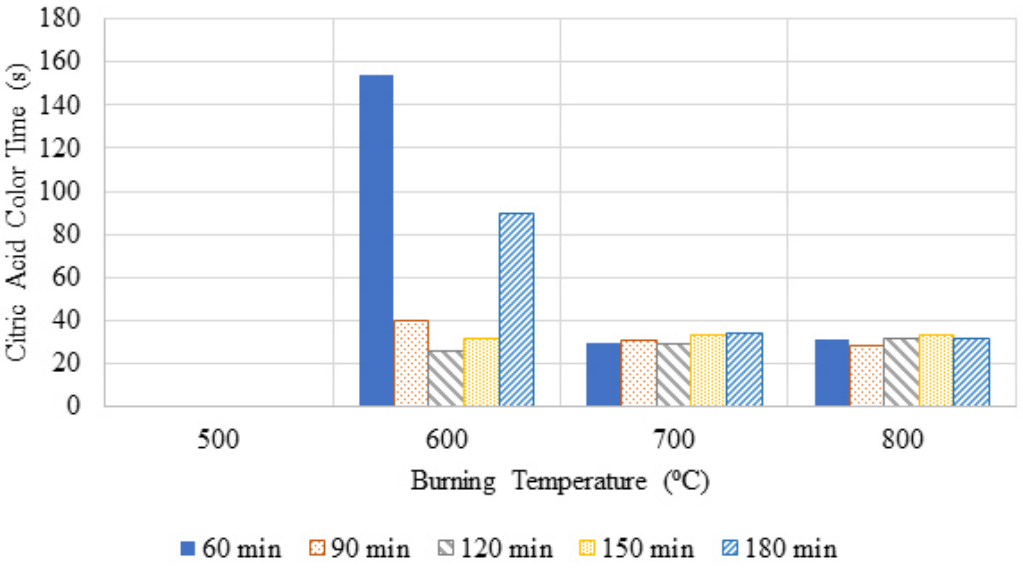


Figure 4.3. Citric acid coloration times of magnesia samples obtained at different burning temperatures and durations.

The corrected magnesia hydration conversion ratios ($X_{corr}$) were calculated by using the equations given in Eqn. 3.4 and plotted as Figure 4.4. It can be seen that highest conversion ratios are obtained in the samples burnt at 600 ºC for 90-150 min. There occurs a reduction in conversion ratios at and above 700 ºC burning temperatures. Similar to the coloration time test, the conversion ratio results for 500 ºC burning temperature were not meaningful and therefore discarded.

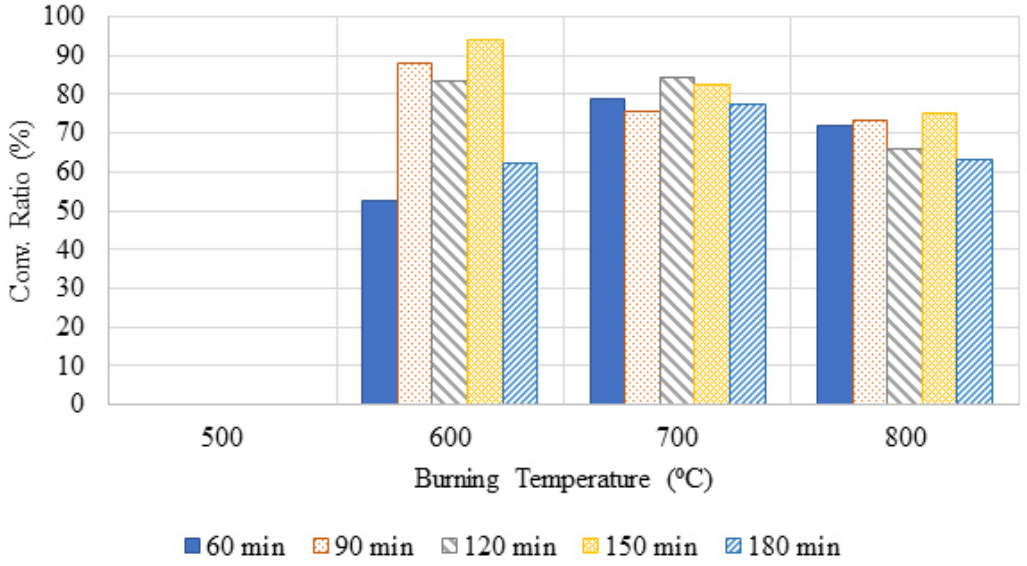


Figure 4.4. Corrected magnesia hydration conversion ratios of magnesia samples obtained at different burning temperatures and durations.

Considering the results obtained from these three preliminary tests, optimal burning temperature and time were 600 ºC and 120 minutes, respectively. Thus, M600-120 magnesia was decided to be used in the main experimental study.

### 4.1.2. Initial Castings

In order to determine the suitable curing conditions to be used in the main experimental part, initially two preceding test series were considered with several different curing conditions.

**1st Initial Casting:** In order to determine the effect of the carbon dioxide concentration of the curing environment, four different mortar specimen series were exposed to three carbon dioxide environments. To observe the effect of magnesia incorporation on low early strengths of pozzolanic cements, in all mortars, fly ash was used as an admixture. The fly ash content was arranged 30 % of total amount of

the fly ash and portland cement. The detailed mix proportions of the mortars are shown in Table 4.2. The reactive magnesia, M600-120 was added to the mixture at 0, 5, 10 and 15 % of total amount of fly ash and portland cement. The water content was kept constant with respect to total amount of portland cement and fly ash. Three different curing regimes were applied to all series of specimens and the compressive strengths were determined at 1, 2 and 3 days of age. While in the first curing regime, the specimens were continuously exposed to ambient conditions for 3 days (low level of carbon dioxide curing) (0.04 % carbon dioxide, 90 % RH, 25 °C) and denoted as '-', the second regime included 3-day medium level of carbon dioxide curing (20 % carbon dioxide, 90 % RH, 25 °C) and denoted as '+'. The last regime, the high level of carbon dioxide curing (denoted as '++') (50 % carbon dioxide, 90 % RH, 25 °C) was continued for 1 day, then the specimens were moved to the ambient curing conditions until the time of test. The first curing regime was basically moist curing since carbon dioxide concentration is very low. Therefore, strength gain within the first three days was due to the hydration process. In the second curing regime, carbonation and hydration processes were simultaneous. The last curing regime was chosen to carbonate the magnesium hydroxide in the early age (one day) as well as hydration of the cement at 90 % RH and then continued hydration in the following two days.

Table 4.2. The mix design of the mortars in 1st initial casting (by weight).

| **Cement Mortars** | **Portland Cement (%)** | **Fly Ash (%)** | **Reactive Magnesia (%)** | **Sand (%)** | **Water (%)** |
|---|---|---|---|---|---|
| **IC1-CF** | 16.43 | 7.04 | 0.00 | 64.29 | 12.24 |
| **IC1-5CF** | 16.24 | 6.96 | 1.16 | 63.54 | 12.10 |
| **IC1-10CF** | 16.05 | 6.88 | 2.29 | 62.81 | 11.96 |
| **IC1-15CF** | 15.87 | 6.80 | 3.40 | 62.10 | 11.83 |

The compressive strength results are shown in Table 4.3. The results show that carbonation affects the early strength even if the cement does not contain any

reactive magnesia. This can be deducted from the different strength results of the cement mortar 'IC1-CF' between different curing conditions. In such a case, calcium hydroxide produced upon the hydration of portland cement carbonates to form $CaCO_3$ which is harder and stronger than $Ca(OH)_2$. The results of first curing regime (low carbon dioxide) show that the presence of reactive magnesia decreases the strength. However, comparing the results of second curing regime (medium carbon dioxide) with those of ambient curing, it was observed that the strength decrease due to magnesia incorporation was compensated and except for 10% magnesia-incorporated specimen at 1 day, all strength results were equal or higher. For curing regime 3 (high carbon dioxide in the first day), higher strengths were obtained for the first day at all three levels of magnesia incorporation but in 2 and 3 days, lower strengths were obtained. Relative strengths of magnesia-incorporated mortars with respect to those of the mortars without magnesia are shown in Figure 4.5.

Table 4.3. The compressive strength results of 1st initial casting.

| | **Compressive strength (MPa) at** | | |
|---|---|---|---|
| **Cement Mortars** | **1st day** | **2nd day** | **3rd day** |
| **IC1-CF++** | 11.44 | 15.85 | 18.36 |
| **IC1-CF+** | 12.31 | 17.19 | 20.83 |
| **IC1-CF-** | 6.11 | 14.13 | 17.29 |
| **IC1-5CF++** | 7.36 | 12.85 | 16.72 |
| **IC1-5CF+** | 7.61 | 14.12 | 17.76 |
| **IC1-5CF-** | 4.21 | 10.73 | 15.08 |
| **IC1-10CF++** | 6.91 | 11.96 | 15.08 |
| **IC1-10CF+** | 7.59 | 16.25 | 19.20 |
| **IC1-10CF-** | 4.65 | 10.72 | 15.35 |
| **IC1-15CF++** | 8.81 | 12.65 | 15.28 |
| **IC1-15CF+** | 6.55 | 15.78 | 18.61 |
| **IC1-15CF-** | 4.25 | 10.40 | 14.44 |

A comparison of Figure 4.5 (b) and 4.5 (c) shows that although third curing regime results in higher strengths in the first day, there occurs a reduction afterwards. The

reason for that can be the insufficient time duration for the reactive magnesia carbonation and/or the carbonation of the C-S-H gel at high carbon dioxide concentration, The latter may lead to the reduction in mechanical performance (Šavija & Luković, 2016). Therefore, the second curing regime with 20 % carbon dioxide concentration was decided to be used in the main experimental study.

**2nd Initial Casting:** The aim of this casting was to understand the difference between the effect of the water and air curing in a 50 % carbon dioxide environment on the strength. In this scope, mortars containing high amount of reactive magnesia were prepared and immediately after casting into molds, they were moved to the 50 % carbon dioxide environment. The mix design is given in Table 4.4. The water content was calculated according to Eqn. 3.5. After determining the 1-day strengths, each half of the remaining specimens was kept in water and air in the 50 % carbon dioxide environment for 2 days and for each day, the compressive strength of the mortars was also determined.

Table 4.4. The mix design of the mortars in 2nd initial casting (by weight).

| Cement Mortars | Portland Cement (%) | Fly Ash (%) | Reactive Magnesia (%) | Sand (%) | Water (%) |
|---|---|---|---|---|---|
| **IC2-50CM** | 11.26 | 0 | 11.26 | 61.70 | 15.78 |
| **IC2-50CMF** | 7.88 | 3.38 | 11.26 | 61.70 | 15.78 |

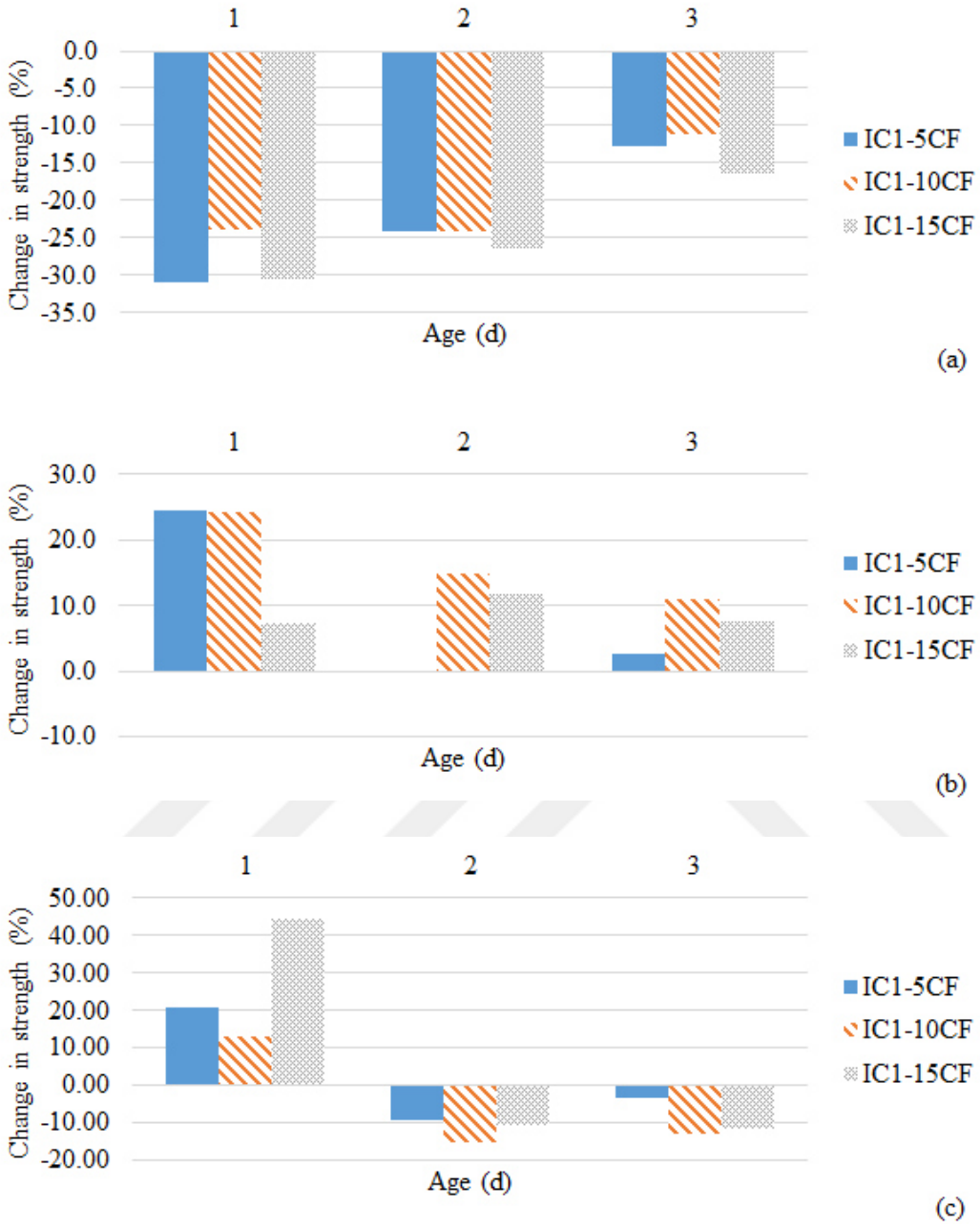


Figure 4.5. Change in strengths of magnesia-incorporated mortars of 1st initial casting cured at (a) first curing regime, (b) second curing regime, and (c) third curing regime, with respect to the strengths of non-magnesia mortars cured at ambient conditions (first curing regime).

The results are given in Table 4.5. It is very clear that the performances of the specimens cured in air in 50 % carbon dioxide environment are better than these cured in water and the presence of the fly ash obviously decreases the strength in early ages.

Table 4.5. The compressive strength results of the mortars in 2nd initial experiments.

| | **Compressive strength (MPa) at** | | |
|---|---|---|---|
| **Cement Mortars** | **1st day** | **2nd day** | **3rd day** |
| **IC2-50CM water-cured** | 1.9 | 3.4 | 4.6 |
| **IC2-50CM air-cured** | 1.9 | 3.9 | 6.9 |
| **IC2-50CMF water-cured** | 1.0 | 1.2 | 2.5 |
| **IC2-50CMF air-cured** | 1.0 | 2.2 | 3.4 |

These two initial experiments show that the most effective curing regime among the regimes applied is the air curing at 20 % carbon dioxide environment for two days in terms of strength gain. In addition to these, it is very clear that the presence of reactive magnesia in cements can have a positive effect on the strength gain of the specimens stored in relatively high carbon dioxide environment in air for 2 days, due possibly to the carbonation of the reactive magnesia present in cements.

## 4.2. Main Experiments

In the light of the initial experiments, to investigate the performances in both short and long term of the reactive magnesia cements, two main castings were planned. Besides the ambient curing conditions, in the tests for the determination of long term performance of reactive magnesia cements, the other curing regime was determined to be 20 % carbon dioxide in air. But, the curing regimes of short term performance of reactive magnesia cements, were ambient conditions, 20 % and 50 % carbon dioxide for a two day-period.

### 4.2.1. Long Term Performance of Reactive Magnesia Cements (1st Main Casting)

The aim of this casting was to determine the mechanical and physical performances of the mortars containing reactive magnesia especially in the long term. Two different curing regimes, including ambient and medium level of carbon dioxide levels were applied to the specimens. These, marked with the signs '+' and '-', were exposed to the medium level (20 % carbon dioxide) and the ambient level (0.04 % carbon dioxide [ambient carbon dioxide]) carbon dioxide curing, respectively, and the curing regimes were continued until the testing day. For both environments, the curing temperature and the relative humidity were kept constant at 25 °C and 90 %, respectively. The weight percentages of the reactive magnesia cement ingredients are given in Table 4.6. The water contents of the cement mortars were adjusted according to the reactive magnesia and powder content as stated in Eqn. 3.5. As a mineral admixture, fly ash whose weight percentage was kept constant at 30 % of the total amount of portland cement and fly ash, was used. The reactive magnesia (M600-120) was added to the cement as a replacement material, the amount of which was arranged as 15, 30, 50 and 100 % of the total powder content. In labelling the cement mortars, the number represents the replacement percent of the reactive magnesia. While, the letter 'C' is the abbreviation of the portland cement, the letters 'F' and 'M' indicate the presence of the fly ash and reactive magnesia (M600-120), respectively.

The compressive strengths of the mortars at 3rd, 7th, 28th, 90th and 360th days were determined in the scope of this casting. In addition to compressive strength, rapid chloride permeability and the sulfate resistance for 1 month were also determined.

Table 4.6. The mix design of the mortars in 1st main casting (by weight).

| Cement Mortars | Portland Cement (%) | Fly Ash (%) | Reactive Magnesia (%) | Sand (%) | Water (%) |
|---|---|---|---|---|---|
| **C** | 23.68 | 0.00 | 0.00 | 64.87 | 11.46 |
| **CF** | 16.57 | 7.10 | 0.00 | 64.87 | 11.46 |
| **15CM** | 19.82 | 0.00 | 3.50 | 63.88 | 12.80 |
| **15CMF** | 13.87 | 5.95 | 3.50 | 63.88 | 12.80 |
| **30CM** | 16.08 | 0.00 | 6.89 | 62.93 | 14.10 |
| **30CMF** | 11.25 | 4.82 | 6.89 | 62.93 | 14.10 |
| **50CM** | 11.26 | 0.00 | 11.26 | 61.70 | 15.78 |
| **50CMF** | 7.88 | 3.38 | 11.26 | 61.70 | 15.78 |
| **100CM** | 0.00 | 0.00 | 21.47 | 58.83 | 19.70 |

**Compressive strength:**

The compressive strength results are tabulated in Table 4.7 As expected, the compressive strengths of almost all specimens for both curing regimes, are increasing with time. The results clearly show that, the continuous 20 % carbon dioxide curing had a positive impact on compressive strength, since the specimens marked with the sign '+' have higher compressive strength than these with the sign '-' due to the carbonation of the cement matrix and/or reactive magnesia. Besides the relatively high strength of the carbonation products, they can fill the pores, increasing the overall strength.

Table 4.7. The compressive strength results of 1st main casting (the coefficient of variances in percent are shown in parenthesis [the values shown with asterisk could not be obtained due to the limited number of specimens]).

| Cement Mortars | Compressive strength (MPa) at | | | | |
|---|---|---|---|---|---|
| | 3rd day | 7th day | 28th day | 90th day | 360th day |
| **C+** | 37.0 (16.4) | 46.9 (8.6) | 49.8 (8.1) | 62.9 (9.6) | 64.5 (7.7) |
| **C-** | 35.3 (13.3) | 40.0 (8.2) | 46.6 (19.8) | 54.7 (14.6) | 60.5 (*) |
| **15CM+** | 25.3 (9.0) | 29.3 (4.8) | 38.2 (8.6) | 52.1 (8.7) | 59.6 (14.5) |
| **15CM-** | 21.8 (2.9) | 27.3 (4.8) | 31.4 (10.0) | 44.3 (3.6) | 35.1 (8.0) |
| **30CM+** | 14.8 (6.9) | 19.7 (3.6) | 28.6 (6.9) | 49.6 (8.7) | 60.7 (7.1) |
| **30CM-** | 12.9 (2.2) | 16.6 (3.5) | 21.7 (4.3) | 29.2 (7.3) | 27.7 (14.6) |
| **50CM+** | 5.8 (5.7) | 13.0 (7.8) | 27.8 (12.9) | 45.8 (3.6) | 55.2 (10.6) |
| **50CM-** | 5.4 (10.8) | 7.5 (2.8) | 11.9 (4.4) | 18.0 (8.0) | 15.8 (8.4) |
| **100CM+** | 1.4 (27.9) | 3.6 (12.3) | 11.3 (25.5) | 18.3 (17.7) | 31.0 (2.8) |
| **100CM-** | 0.9 (13.7) | 1.4 (6.1) | 1.5 (9.7) | 2.5 (7.7) | 3.7 (9.1) |
| **CF+** | 25.0 (5.2) | 32.1 (7.3) | 42.3 (11.7) | 50.5 (5.2) | 56.0 (19.0) |
| **CF-** | 24.4 (4.3) | 31.2 (1.4) | 38.9 (14.9) | 45.5 (*) | 47.4 (3.7) |
| **15CMF+** | 15.1 (5.8) | 20.3 (4.6) | 31.3 (6.5) | 49.1 (6.9) | 55.1 (3.7) |
| **15CMF-** | 13.6 (6.4) | 17.3 (4.0) | 26.4 (10.3) | 36.8 (4.4) | 36.7 (5.4) |
| **30CMF+** | 7.6 (1.5) | 12.5 (16.2) | 23.2 (15.6) | 42.5 (2.8) | 45.7 (18.0) |
| **30CMF-** | 6.2 (6.4) | 10.4 (5.5) | 16.1 (8.0) | 22.4 (5.7) | 27.2 (2.3) |
| **50CMF+** | 3.2 (2.6) | 5.4 (13.4) | 17.1 (8.9) | 29.3 (10.0) | 35.1 (16.5) |
| **50CMF-** | 2.6 (4.7) | 4.1 (5.2) | 9.4 (7.1) | 10.9 (3.6) | 12.5 (2.5) |

When the strength results were investigated statistically, as can be seen from Table 4.8, the design variables were selected as the presence of fly ash (2 factors), age (5 factors), curing conditions (2 factors) and the amount of reactive magnesia (5 factors). The F- and P-values indicate that the most important parameter is the amount of magnesia among the others. In addition, the table shows the importance of the effect of the curing conditions and age of the mortars on the strength.

Table 4.8. ANOVA analysis for 1st main casting.

| | Mean (MPa) | Standard Deviation (MPa) | Variables (ordered) | Df | F | P-value |
|---|---|---|---|---|---|---|
| **Compressive Strength** | 27.01 | 17.82 | Amount of reactive magnesia | 4 | 52.06 | < 0.001 |
| | | | Curing conditions | 1 | 27.854 | < 0.001 |
| | | | Age | 4 | 27.227 | < 0.001 |
| | | | Presence of fly ash | 1 | 1.592 | 0.208 |

To understand the reaction of the reactive magnesia better in different curing conditions, the dilution effect resulted from its addition to the cement should be removed and the 'new' results should be compared with those of the control cement mortar (The mortar 'C') (In Appendix C, the discussion of this approach can be followed). Since the amounts of the cement mortar ingredients are known, the strength results without the dilution effect can be calculated using the ratio of total amount of the fly ash and portland cement to the total powder content. The 'new' results calculated ignoring the dilution effect are shown in Table 4.9, except the cement mortar '100CM', the result of which can not be calculated because it has neither the portland cement nor the fly ash. Therefore, the results for '100CM' are shown with "NA", the abbreviation of "Not Applicable". Especially when compared with the control cement mortar exposed to the ambient conditions, it can be said that, the presence of the reactive magnesia is decreasing the results, dramatically. The possible reason for that is the very low binding ability of its hydration products, and obviously, the carbon dioxide level of the environment may not be sufficient for their carbonation (Martin Liska & Al-Tabbaa, 2012). But, in the case of the environment with enough concentration of carbon dioxide for carbonation, the effect of the reactive magnesia amount differs than that in ambient conditions. It can be seen that the effect of the increase in reactive magnesia content differs for the early and late ages. When the results for the cement mortars '15CM+', '30CM+' and '50CM+' are compared with the cement mortar 'C+', the reactive magnesia increase leads to the

decrease in compressive strength for early ages, but for late ages, results in the strength gain. This behavior, which can also be seen in the cements containing fly ash, can be related with the stability of the carbonation product in the medium of the reactive magnesia cement paste. It is also seen that the addition of fly ash decreases the strength of the cement mortars. On the other hand, if it is considered that the amount of the fly ash utilized with respect to the all powder content is 30 % and the dilution effect due to this addition, the strength reduction is not so pronounced.

Table 4.9. The compressive strength results of 1st main casting removing the dilution effect.

| **Cement Mortars** | **Compressive strength (MPa) at** | | | | |
|---|---|---|---|---|---|
| | **3rd day** | **7th day** | **28th day** | **90th day** | **360th day** |
| **C+** | 37.0 | 46.9 | 49.8 | 62.9 | 64.5 |
| **C-** | 35.3 | 40.0 | 46.6 | 54.7 | 60.6 |
| **15CM+** | 29.8 | 34.5 | 45.0 | 61.3 | 70.2 |
| **15CM-** | 25.7 | 32.2 | 37.0 | 52.2 | 41.3 |
| **30CM+** | 21.1 | 28.2 | 40.8 | 70.9 | 86.7 |
| **30CM-** | 18.4 | 23.7 | 31.0 | 41.7 | 39.6 |
| **50CM+** | 11.6 | 26.0 | 55.5 | 91.6 | 110.5 |
| **50CM-** | 10.7 | 15.1 | 23.9 | 36.0 | 31.5 |
| **100CM+** | NA | NA | NA | NA | NA |
| **100CM-** | NA | NA | NA | NA | NA |
| **CF+** | 25.0 | 32.1 | 42.3 | 50.6 | 56.0 |
| **CF-** | 25.3 | 31.3 | 38.9 | 49.4 | 44.4 |
| **15CMF+** | 17.8 | 23.8 | 36.8 | 57.8 | 64.9 |
| **15CMF-** | 16.0 | 20.3 | 31.0 | 43.3 | 43.2 |
| **30CMF+** | 10.8 | 17.8 | 33.1 | 60.8 | 65.3 |
| **30CMF-** | 8.8 | 14.9 | 23.0 | 31.9 | 38.9 |
| **50CMF+** | 6.4 | 10.9 | 34.2 | 58.7 | 70.2 |
| **50CMF-** | 5.2 | 8.3 | 18.8 | 21.9 | 24.9 |

To observe the effect of carbon dioxide curing, for the cements, the carbonation contribution (the strength gain due to the carbonation) should be considered. The carbonation contribution, which is shown for all the cement mortars in Table 4.10,

can be calculated as the percentage of the increase in compressive strength due to the carbonation to the strength of the specimen cured in ambient environment for the same day. From the table, it is clear that the increase in strength due to the carbonation of the reactive magnesia is higher than that of the portland cement because the carbonation contribution of the cement mortar 'C' is very lower than that of the cement mortar '100CM'. In spite of its lack of the portland cement fraction, all the increase in strength for the cement mortar '100CM' is only due to the carbonation of the reactive magnesia since its hydration products have low binding ability with respect to these of the portland cement (Martin Liska & Al-Tabbaa, 2012). The behaviors of the cement mortars having the same amount of reactive magnesia, like the cement mortars '15CM' – '15CMF' or 'C' – 'CF', are very different, indicating, the presence of fly ash affects the carbonation of the cements. Generally, the carbonation contribution of the cement mortars having fly ash is lower than the cement mortars having none. This can be due to the consumption of alkalis ($Ca(OH)_2$ and/or $Mg(OH)_2$) by the pozzolanic reaction, reducing the amount of the products which may experience carbonation.

Table 4.10. The carbonation contribution for the cement mortars.

| **Cement Mortars** | **Increase in compressive strength (%) at** | | | | |
|---|---|---|---|---|---|
| | **3rd day** | **7th day** | **28th day** | **90th day** | **360th day** |
| **C** | 4.64 | 17.16 | 6.78 | 14.89 | 6.66 |
| **15CM** | 16.13 | 7.28 | 21.57 | 17.46 | 69.74 |
| **30CM** | 14.85 | 18.81 | 31.63 | 69.91 | 118.98 |
| **50CM** | 7.64 | 72.78 | 132.38 | 154.64 | 250.29 |
| **100CM** | 47.87 | 161.76 | 655.70 | 639.11 | 739.84 |
| **CF** | -1.11 | 2.75 | 8.82 | 2.29 | 25.95 |
| **15CMF** | 11.02 | 17.37 | 18.57 | 33.41 | 50.20 |
| **30CMF** | 23.25 | 19.48 | 44.18 | 90.29 | 68.19 |
| **50CMF** | 21.37 | 31.96 | 82.22 | 168.04 | 181.56 |

**Rapid chloride permeameter test:**

At 28th day, the rapid chloride permeability tests were performed to the slice mortar specimens obtained from the cylinder-shaped mortars. The results for the charge passing through the slices are shown in Table 4.11. Since the strength of the cement mortar '100CM-' was very low, the slice could not be obtained from the cylinder specimens and for this mix the test, could not be performed. But, especially for the cement mortars having higher amount of the reactive magnesia, cured in ambient conditions, the temperatures of the solutions were measured higher than 95 °C by a thermal camera. This points out a possible reaction between the reactive magnesia and/or its hydration / carbonation products and the solutions used to perform the test. The tests for these specimens, the results of which, are marked with the sign '*' in Table 4.10, were finalized immediately and their results were estimated using extrapolation considering their existing performance. According to the results, the curing has a great impact on the permeability of the cement mortars. During the carbon dioxide curing, because the carbonation products fill the pores, the permeability decreases. In a similar way, the pozzolan addition reduces the permeability due to the pozzolanic reaction and filler effect.

Table 4.11. The charge passing through the slices.

| Cement Mortars | Charge (Coulombs) | Cement Mortars | Charge (Coulombs) |
|---|---|---|---|
| **C+** | 6512 | **30CMF+** | 12976 |
| **C-** | 9997 | **30CMF-** | 17890 |
| **CF+** | 2857 | **50CM+** | 17717* |
| **CF-** | 6619 | **50CM-** | 17316* |
| **15CM+** | 12814* | **50CMF+** | 5281 |
| **15CM-** | 17875* | **50CMF-** | 8176 |
| **15CMF+** | 6169* | **100CM+** | 16321* |
| **15CMF-** | 14504* | **100CM-** | NA |
| **30CM+** | 12843 | | |
| **30CM-** | 20628 | | |

**Expansion in sulfate solution:**

The length changes of the mortar bars exposed to the sulfate solution had been determined for 9 weeks and the results of the mortars, except that of 100CM- whose bars were damaged while they were removed from the molds due to their low strength, are shown in Table 4.12. For typical portland cement mortar bars, the sulfate ions in solution penetrate into the bars and they react with the calcium hydroxide and AFm in hydrated portland cement paste to form gypsum and ettringite (Erdoğan, 2010). Since their volume is higher than their reactants, the length of the bar increases. At the end of the $9^{th}$ week, it is seen that generally, the length change has a positive sign, in other words, the length of the bars is increasing as expected, since all the mortars, have a certain amount of portland cement, except the cement mortar '100CM'. The difference between the results of the mortars exposed to the carbon dioxide curing and those exposed to ambient carbon dioxide is very clear. The specimens cured in ambient conditions with higher amount of reactive magnesia show higher change in length due to the formation of the hydration products of reactive magnesia. On the other hand, if the curing conditions are changed, their performance is improved. Since the carbonation products reduces the permeability of the bars, the effect of the sulfate ions becomes lower reducing the amount of possible sulfate – calcium hydroxide reactions. In addition, the calcium hydroxide, one of the materials which can be reacted with the sulfate ions, is consumed by the carbonation to form calcium carbonates before the sulfate expansion test. It is clear that the presence of fly ash reduces the length change in all cases due to its filler effect. Also, the pozzolanic reaction affects the bar length decreasing the amount of the alkalis existed in pore solution. But, the behavior of 100CM+ is very different. The 100CM+ shows the decrease first, and then the increase. This can be due to the stability of its hydration/carbonation products in sulfate solution.

Table 4.12. The length change results against sulfate attack.

| Cement Mortars | Length change (%) in | | | | | | |
|---|---|---|---|---|---|---|---|
| | 0th week | 1st week | 2nd week | 3rd week | 5th week | 7th week | 9th week |
| C+ | 0.000 | -0.004 | 0.003 | 0.005 | 0.011 | 0.005 | 0.007 |
| C- | 0.000 | -0.001 | 0.003 | 0.003 | 0.008 | 0.001 | 0.003 |
| 15CM+ | 0.000 | 0.001 | 0.008 | 0.009 | 0.010 | 0.016 | 0.020 |
| 15CM- | 0.000 | 0.004 | 0.009 | 0.015 | 0.018 | 0.031 | 0.036 |
| 30CM+ | 0.000 | 0.011 | 0.013 | 0.017 | 0.024 | 0.021 | 0.031 |
| 30CM- | 0.000 | 0.020 | 0.032 | 0.041 | 0.058 | 0.067 | 0.075 |
| 50CM+ | 0.000 | 0.004 | 0.005 | 0.005 | 0.011 | 0.013 | 0.017 |
| 50CM- | 0.000 | 0.025 | 0.039 | 0.047 | 0.072 | 0.088 | 0.100 |
| 100CM+ | 0.000 | -0.011 | -0.013 | -0.011 | -0.007 | -0.004 | -0.003 |
| 100CM- | NA | NA | NA | NA | NA | NA | NA |
| CF+ | 0.000 | 0.004 | 0.002 | 0.006 | 0.007 | 0.009 | 0.001 |
| CF- | 0.000 | -0.001 | 0.000 | 0.005 | 0.005 | 0.007 | 0.011 |
| 15CMF+ | 0.000 | 0.001 | 0.001 | 0.005 | 0.008 | 0.011 | 0.016 |
| 15CMF- | 0.000 | 0.000 | 0.006 | 0.013 | 0.019 | 0.025 | 0.030 |
| 30CMF+ | 0.000 | -0.001 | 0.002 | 0.011 | -0.006 | 0.010 | 0.016 |
| 30CMF- | 0.000 | 0.008 | 0.020 | 0.036 | 0.032 | 0.054 | 0.068 |
| 50CMF+ | 0.000 | 0.004 | 0.004 | 0.017 | 0.004 | 0.008 | 0.007 |
| 50CMF- | 0.000 | 0.029 | 0.046 | 0.067 | 0.077 | 0.095 | 0.104 |

### 4.2.2. Short Term Performance of Reactive Magnesia Cements (2nd Main Casting)

To find out the effect of higher carbon dioxide concentration in short term and the effects of different supplementary cementitious composites, 9 different mortars were prepared. Each mortar specimen was cured in ambient (0.04 %), medium (20 %) and high level (50 %) of carbon dioxide concentration and in the naming of the specimens cured in these environments were marked with the signs '-', '+' and '++', respectively. The relative humidity and temperature were kept constant at 90 % and 25 °C, respectively, but unlike the 1st main casting, the curing was continued for only 2 days. For the cements containing fly ash and ground granulated blast furnace slag, its amount was kept constant at 30 % of the portland cement fraction and for all cements, the reactive magnesia content was 15 and 30 % with respect to the total

powder content apart from the reactive magnesia as the addition. The water amount was calculated according to Eqn. 3.5. The mix design of the mortars is shown in Table 4.13. In naming, the number shows the amount of reactive magnesia in cement. The letters 'S' and 'F' are representing the presence of the ground granulated blast furnace slag and fly ash, respectively. The letter 'A' at the end of the naming represents that the reactive magnesia is added to the mixture as an addition and 'C' represents the control cement having no amount of the reactive magnesia.

Table 4.13. The mix design of the mortars in 2nd main casting (by weight).

| Cement Mortars | Portland Cement (%) | Ground Granulated Blast Furnace Slag (%) | Fly Ash (%) | Reactive Magnesia (%) | Sand (%) | Water (%) |
|---|---|---|---|---|---|---|
| **C-A** | 23.67 | 0.00 | 0.00 | 0.00 | 64.88 | 11.45 |
| **CS-A** | 18.20 | 5.47 | 0.00 | 0.00 | 64.88 | 11.45 |
| **CF-A** | 18.20 | 0.00 | 5.47 | 0.00 | 64.88 | 11.45 |
| **15CM-A** | 20.31 | 0.00 | 0.00 | 3.05 | 64.02 | 12.62 |
| **15CMS-A** | 15.62 | 4.68 | 0.00 | 3.05 | 64.02 | 12.62 |
| **15CMF-A** | 15.62 | 0.00 | 4.68 | 3.05 | 64.02 | 12.62 |
| **30CM-A** | 17.78 | 0.00 | 0.00 | 5.34 | 63.38 | 13.50 |
| **30CMS-A** | 13.68 | 4.10 | 0.00 | 5.34 | 63.38 | 13.50 |
| **30CMF-A** | 13.68 | 0.00 | 4.10 | 5.34 | 63.38 | 13.50 |

Besides their 1st, 3rd, 7th and 28th day-compressive strength, the changes in length of the specimens exposed to the sodium sulfate solution were also measured.

**Compressive strength:**

The compressive strength results are shown in Table 4.14. The results clearly show that the curing regime has an effect on the strength of the mortars depending on the carbon dioxide concentration. The 20 % carbon dioxide curing increases the strength, but a strength reduction is observed when the concentration is increased to 50 % due possibly to the carbonation of the C-S-H gel. As it can lead to the production of

calcium carbonates, reducing the porosity and correspondingly, increasing the strength, it can also decrease the amount of C-S-H gel which is the main hydration product responsible of the strength development in cement matrix.

Table 4.14. The compressive strength results of 2nd main casting (the coefficient of variances in percent are shown in parenthesis [the values shown with asterisk could not be obtained due to the limited number of specimens]).

| **Cement Mortars** | **Compressive strength (MPa) at** | | | |
|---|---|---|---|---|
| | **1st day** | **3rd day** | **7th day** | **28th day** |
| **C-A++** | 15.3 (2.1) | 25.8 (7.5) | 30.5 (5.5) | 39.3 (4.4) |
| **C-A+** | 14.8 (4.2) | 24.0 (2.6) | 31.5 (4.8) | 34.5 (1.5) |
| **C-A-** | 7.4 (5.8) | 23.1 (1.2) | 29.5 (5.0) | 35.0 (6.1) |
| **CS-A++** | 13.2 (3.7) | 23.2 (4.5) | 27.9 (6.1) | 39.0 (3.5) |
| **CS-A+** | 14.9 (6.9) | 25.8 (1.9) | 33.2 (5.7) | 38.3 (2.5) |
| **CS-A-** | 12.7 (3.3) | 26.1 (2.6) | 31.1 (3.5) | 43.8 (1.0) |
| **CF-A++** | 10.7 (1.9) | 20.7 (3.9) | 24.6 (4.2) | 31.0 (5.7) |
| **CF-A+** | 17.6 (1.5) | 26.7 (3.3) | 29.9 (1.9) | 33.9 (5.4) |
| **CF-A-** | 16.1 (7.5) | 26.1 (5.5) | 29.5 (4.0) | 40.1 (11.4) |
| **15CM-A++** | 3.8 (5.8) | 11.3 (5.8) | 15.5 (6.3) | 22.4 (0.8) |
| **15CM-A+** | 9.6 (6.7) | 19.7 (3.9) | 22.7 (8.2) | 24.3 (2.4) |
| **15CM-A-** | 5.9 (5.6) | 15.7 (6.3) | 21.4 (2.0) | 25.0 (2.7) |
| **15CMS-A++** | 2.9 (4.9) | 9.8 (6.8) | 16.7 (3.4) | 22.5 (5.7) |
| **15CMS-A+** | 4.3 (5.3) | 11.8 (5.9) | 18.2 (3.5) | 24.6 (4.1) |
| **15CMS-A-** | 4.0 (4.6) | 11.7 (2.1) | 18.5 (2.2) | 27.5 (5.1) |
| **15CMF-A++** | 3.2 (*) | 8.0 (0.4) | 13.4 (7.1) | 17.5 (2.0) |
| **15CMF-A+** | 7.9 (6.7) | 15.2 (2.6) | 19.0 (2.4) | 21.6 (4.6) |
| **15CMF-A-** | 5.9 (5.3) | 13.9 (5.5) | 18.2 (1.4) | 24.6 (2.3) |
| **30CM-A++** | 1.6 (6.9) | 6.1 (6.5) | 8.8 (1.9) | 14.3 (6.4) |
| **30CM-A+** | 6.9 (1.3) | 14.1 (6.3) | 16.1 (4.7) | 22.9 (4.6) |
| **30CM-A-** | 5.8 (4.6) | 13.6 (6.4) | 16.3 (4.3) | 19.9 (6.8) |
| **30CMS-A++** | 1.6 (7.7) | 5.8 (5.7) | 9.3 (7.7) | 16.9 (4.6) |
| **30CMS-A+** | 3.1 (5.1) | 8.8 (4.7) | 14.5 (6.6) | 19.5 (4.9) |
| **30CMS-A-** | 2.6 (7.5) | 8.1 (1.1) | 14.6 (1.3) | 19.0 (1.6) |
| **30CMF-A++** | 1.7 (2.9) | 4.1 (2.0) | 7.9 (7.7) | 12.0 (4.5) |
| **30CMF-A+** | 3.8 (5.3) | 9.3 (0.8) | 13.1 (0.7) | 17.1 (4.8) |
| **30CMF-A-** | 3.0 (5.2) | 8.8 (3.6) | 13.3 (1.7) | 17.1 (4.0) |

The statistics for the strength results were studied to determine the importance of the parameters. The results can be seen from Table 4.15. The design variables were selected as the presence of fly ash (2 factors), the presence of slag (2 factors), age (4 factors), curing conditions (2 factors) and the amount of reactive magnesia (3 factors). It can be concluded that the most important parameters for the strength are the amount of magnesia and the age.

Table 4.15. ANOVA analysis for 2nd main casting.

| | **Mean (MPa)** | **Standard Deviation (MPa)** | **Variables (ordered)** | **Df** | **F** | **P-value** |
|---|---|---|---|---|---|---|
| **Compressive Strength** | 16.94 | 9.97 | Amount of reactive magnesia | 2 | 107.41 | < 0.001 |
| | | | Age | 3 | 77.60 | < 0.001 |
| | | | Curing conditions | 2 | 3.58 | 0.029 |
| | | | Presence of fly ash | 1 | 1.82 | 0.179 |
| | | | Presence of slag | 1 | 0.14 | 0.709 |

To understand clearly the effect of the reactive magnesia amount, its percentage in all cement content and the dilution effect due to its presence should be considered. Table 4.16 shows the compressive strength results removing the dilution effect due to the addition of the reactive magnesia to the cement. It is very obvious that the addition of the reactive magnesia to the system has a detrimental effect on the compressive strength. Almost all the strength results of the cement mortars having an amount of the reactive magnesia is lower than the corresponding control cement mortar results. In addition, when considering all the results, it is determined that the addition of the mineral additions has different effects on the strength. When ground granulated blast furnace slag is used, the strength values are generally decreasing in early ages, but later, increasing. The reason for that is the relatively low reactivity of

the slag. As the rate of the reactions due to the slag are low, the strengths obtained at early ages from the reactive magnesia cement mortars containing slag give lower results as well.

Table 4.16. The compressive strength results of 2nd main casting removing the dilution effect.

| Cement Mortars | Compressive strength (MPa) at | | | |
|---|---|---|---|---|
| | 1st day | 3rd day | 7th day | 28th day |
| **C-A++** | 15.3 | 25.8 | 30.5 | 39.3 |
| **C-A+** | 14.8 | 24.0 | 31.5 | 34.5 |
| **C-A-** | 7.4 | 23.1 | 29.5 | 35.0 |
| **CS-A++** | 13.2 | 23.2 | 27.9 | 39.0 |
| **CS-A+** | 14.9 | 25.8 | 33.2 | 38.3 |
| **CS-A-** | 12.7 | 26.1 | 31.1 | 43.8 |
| **CF-A++** | 10.7 | 20.7 | 24.6 | 31.0 |
| **CF-A+** | 17.6 | 26.7 | 29.9 | 33.9 |
| **CF-A-** | 16.1 | 26.1 | 29.5 | 40.1 |
| **15CM-A++** | 4.3 | 13.0 | 17.8 | 25.7 |
| **15CM-A+** | 11.0 | 22.7 | 26.1 | 27.9 |
| **15CM-A-** | 6.8 | 18.1 | 24.6 | 28.8 |
| **15CMS-A++** | 3.4 | 11.2 | 19.2 | 25.9 |
| **15CMS-A+** | 5.0 | 13.6 | 21.0 | 28.3 |
| **15CMS-A-** | 4.6 | 13.5 | 21.3 | 31.6 |
| **15CMF-A++** | 3.7 | 9.2 | 15.5 | 20.1 |
| **15CMF-A+** | 9.1 | 17.5 | 21.9 | 24.9 |
| **15CMF-A-** | 6.7 | 16.0 | 20.9 | 28.2 |
| **30CM-A++** | 2.0 | 7.9 | 11.5 | 18.6 |
| **30CM-A+** | 8.9 | 18.4 | 21.0 | 29.7 |
| **30CM-A-** | 7.5 | 17.7 | 21.2 | 25.8 |
| **30CMS-A++** | 2.0 | 7.5 | 12.1 | 22.0 |
| **30CMS-A+** | 4.0 | 11.5 | 18.9 | 25.3 |
| **30CMS-A-** | 3.4 | 10.5 | 19.0 | 24.7 |
| **30CMF-A++** | 2.3 | 5.4 | 10.3 | 15.6 |
| **30CMF-A+** | 4.9 | 12.1 | 17.0 | 22.2 |
| **30CMF-A-** | 3.9 | 11.5 | 17.3 | 22.3 |

**Expansion in sulfate solution:**

Table 4.17 shows the length change of the mortars exposed to sulfate attack for 9 weeks. It is very obvious that the carbon dioxide concentration of the curing environment has a significant effect on the sulfate resistance. The higher the concentration is, the lower the change in length is. While the addition of fly ash reduces the length change, the effect of the presence of slag becomes insignificant independently from the curing conditions. The reactive magnesia addition has a great impact on the resistance of the mortar against sulfate attack. This can be due to a possible reaction between the hydration / carbonation product of reactive magnesia and the solution used.

## 4.3. Microstructural Characterization of Hydration Products

### 4.3.1. XRD Profiles of Reactive Magnesia Cements

To identify hydration / carbonation products of the reactive magnesia cement pastes when subjected to different carbon dioxide concentrations, their X-ray diffraction profiles were obtained. In the scope of these tests, seven different reactive magnesia pastes, five of which were selected from the cement samples used in 2$^{nd}$ main casting. The XRD profiles of the other two cements (100CM-A and 50CM-A) were also determined for comparison purposes. The mix designs of the pastes are given in Table 4.18. In the pastes, the water content was determined according to Eqn. 3.5.

Table 4.17. The length change results against sulfate attack.

| Cement Mortars | Length change (%) in | | | | | | |
|---|---|---|---|---|---|---|---|
| | 0th week | 1st week | 2nd week | 3rd week | 5th week | 7th week | 9th week |
| **C-A++** | 0.000 | 0.000 | 0.000 | 0.003 | 0.001 | 0.005 | 0.011 |
| **C-A+** | 0.000 | -0.002 | 0.001 | 0.000 | 0.008 | 0.014 | 0.013 |
| **C-A-** | 0.000 | -0.003 | -0.002 | 0.001 | 0.007 | 0.011 | 0.017 |
| **CS-A++** | 0.000 | 0.000 | 0.003 | -0.001 | 0.009 | 0.014 | 0.006 |
| **CS-A+** | 0.000 | 0.003 | 0.005 | 0.007 | 0.016 | 0.020 | 0.021 |
| **CS-A-** | 0.000 | 0.001 | 0.002 | 0.002 | 0.008 | 0.014 | 0.016 |
| **CF-A++** | 0.000 | -0.003 | 0.003 | 0.005 | 0.004 | 0.010 | 0.011 |
| **CF-A+** | 0.000 | -0.002 | 0.005 | 0.000 | 0.007 | 0.009 | 0.016 |
| **CF-A-** | 0.000 | 0.000 | 0.005 | -0.001 | 0.005 | 0.011 | 0.010 |
| **15M-A++** | 0.000 | 0.000 | 0.013 | 0.011 | 0.013 | 0.014 | 0.016 |
| **15M-A+** | 0.000 | 0.005 | 0.010 | 0.011 | 0.018 | 0.024 | 0.027 |
| **15M-A-** | 0.000 | 0.008 | 0.015 | 0.014 | 0.028 | 0.031 | 0.039 |
| **15MS-A++** | 0.000 | -0.004 | -0.003 | 0.001 | 0.004 | 0.011 | 0.011 |
| **15MS-A+** | 0.000 | 0.003 | 0.008 | 0.011 | 0.019 | 0.023 | 0.025 |
| **15MS-A-** | 0.000 | 0.006 | 0.010 | 0.018 | 0.027 | 0.034 | 0.038 |
| **15MF-A++** | 0.000 | -0.003 | -0.004 | 0.003 | 0.008 | 0.012 | 0.013 |
| **15MF-A+** | 0.000 | 0.005 | 0.006 | 0.017 | 0.017 | 0.025 | 0.028 |
| **15MF-A-** | 0.000 | 0.002 | 0.010 | 0.017 | 0.020 | 0.026 | 0.034 |
| **30M-A++** | 0.000 | 0.004 | 0.008 | 0.008 | 0.008 | 0.017 | 0.022 |
| **30M-A+** | 0.000 | 0.007 | 0.006 | 0.006 | 0.016 | 0.019 | 0.030 |
| **30M-A-** | 0.000 | 0.010 | 0.015 | 0.018 | 0.029 | 0.037 | 0.050 |
| **30MS-A++** | 0.000 | 0.004 | 0.004 | 0.003 | 0.003 | 0.011 | 0.023 |
| **30MS-A+** | 0.000 | 0.005 | 0.011 | 0.015 | 0.024 | 0.028 | 0.034 |
| **30MS-A-** | 0.000 | 0.010 | 0.016 | 0.025 | 0.039 | 0.045 | 0.054 |
| **30MF-A++** | 0.000 | 0.014 | 0.010 | 0.013 | 0.022 | 0.022 | 0.035 |
| **30MF-A+** | 0.000 | 0.012 | 0.016 | 0.018 | 0.026 | 0.034 | 0.042 |
| **30MF-A-** | 0.000 | 0.024 | 0.026 | 0.034 | 0.042 | 0.049 | 0.060 |

Table 4.18. The mix design of the cement pastes used (by weight).

| Cement Pastes | Portland Cement (%) | Ground Granulated Blast Furnace Slag (%) | Fly Ash (%) | Reactive Magnesia (%) | Water (%) |
|---|---|---|---|---|---|
| **C-A** χ | 67.39 | 0.00 | 0.00 | 0.00 | 32.61 |
| **100CM-A** χ | 0.00 | 0.00 | 0.00 | 52.15 | 47.85 |
| **50CM-A** χ | 40.93 | 0.00 | 0.00 | 20.48 | 38.59 |
| **CF-A** | 51.84 | 0.00 | 15.55 | 0.00 | 32.61 |
| **30CMF-A** | 37.34 | 0.00 | 11.20 | 14.58 | 36.88 |
| **CS-A** | 51.84 | 15.55 | 0.00 | 0.00 | 32.61 |
| **30CMS-A** | 37.34 | 11.20 | 0.00 | 14.58 | 36.88 |

The specimens were cured with three different curing regimes, each of which was labelled with the curing codes, I, II and III. In the curing regime coded with I and III, the specimens were cured in ambient and carbon dioxide environments, respectively. The 'ambient' environments represent the condition with 0.04 % carbon dioxide concentration, 25 ºC temperature and 90 % RH. In carbon dioxide environments, the carbon dioxide concentration is 20 %, other factors are same as in the 'ambient' conditions. During these two curing regimes, the conditions did not change, however, the regime coded with II included the carbon dioxide environment with just 2 day-period following the casting day. After two days, the specimens were subjected to ambient conditions.

To determine their XRD profiles, the specimens were ground until all their particles were able to pass through the No.100 sieve and their diffractogram were obtained at $2^{nd}$, $7^{th}$ and $28^{th}$ day. To determine the hydration / carbonation products for long term, the cement samples marked with the sign 'χ' and cured according to the curing codes I and III, were also examined via XRD device after 360 days. Up to this day, these samples were stored in ambient conditions, following the regular curing conditions.

The naming in the results is done with this notation: 'Cement name'_'curing code'_'day after casting'. For example, '50CM-A_III_28d' represents the XRD

result taken at 28$^{th}$ day after the casting of the sample ‘50CM-A’ cured in carbon dioxide environment for 28 days. The results are shown in Figures 4.6 – 4.12. The identified minerals are indicated on the top of the related XRD peak in figures.

As seen from the XRD results of the cement paste ‘C-A’ in Figure 4.6, for especially early ages, the main observed hydration product is ettringite. As well as the ettringite, portlandite, which is produced as a by-product of portland cement hydration, is also recognized due to the portland cement fraction. For the specimens cured in the environments with high carbon dioxide concentrations, it can be realized that the calcite was formed due to the carbonation of the portlandite and ettringite. The slight consumption of the portlandite and ettringite and the increase in calcite content because of the carbonation between the 3$^{rd}$ and 28$^{th}$ day can also be seen from the figures. In addition, the increase in the calcite amount can be due to the possible carbonation of the C-S-H gel, which can be hardly recognized in its XRD pattern because of its poorly crystalline structure. For the cement paste ‘C-A’ cured with higher carbon dioxide concentration at early ages, the ettringite formation is not found possibly due to the excess carbonation. As shown in the graph of the cement paste ‘C-A_II', there is almost no effect on the crystal structure of the curing conditions change in one month.

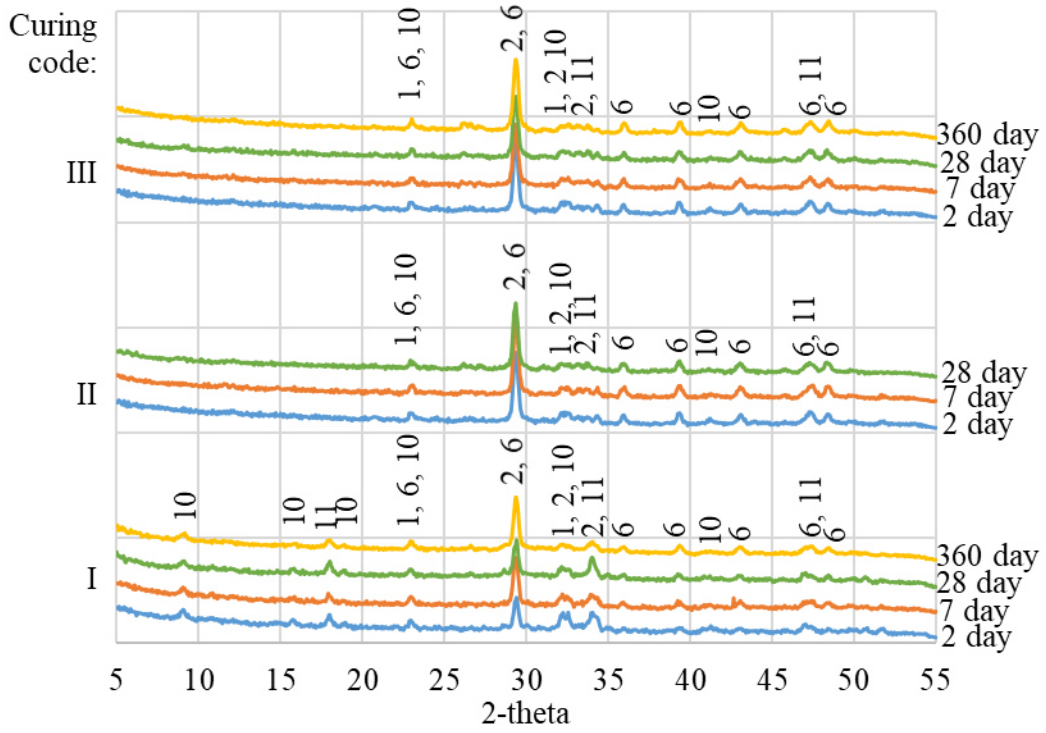


Figure 4.6. XRD profiles of the portland cement ('C-A') subjected to various environmental exposures at various ages (1: $C_2S$, 2: $C_3S$, 6: Calcite, 10: Ettringite, 11: Portlandite).

Figure 4.7 shows the XRD patterns of the '100CM-A' cement samples. The cement paste '100CM-A_I' produces brucite as the main hydration product in ambient conditions. In its XRD profile, the unreacted magnesia particles, which are periclase, can also be recognized. Because the reactive magnesia used in cements has small amount of lime, the peak of the calcite, the carbonation product of the lime, can be identified, too. For ambient conditions, the magnesium carbonate detected is magnesite and from its very low intensity, it can be concluded that the carbon dioxide concentration was not sufficient to produce significant amount of magnesium carbonates for the reactive magnesia for early ages. For the cement paste '100CM-A_I', since the peaks shown with the sign 'X' corresponding lower than 10 2-theta degrees, are not classified in the databases used and the magnesite, as the raw

material, used for the reactive magnesia production, has lower impurity amount, the presence of these peaks points out an unidentified magnesium hydrate / carbonate formed at late ages. From 28 days to 360 days after the casting, the change in 2-theta degrees and the intensity for the relevant peaks indicates the instability of this product. In this cement paste, at 360$^{th}$ day, hydromagnesite can also be recognized. The figure of the cement paste '100CM-A_III' shows that the main carbonation product is the nesquehonite (To clarify the product clearly, the cement paste '100CM-A_III_360d' was also investigated through thermogravimetric analyses as given in Appendix D). As the '100CM-A_III_2d' shows the presence of the nesquehonite clearly, in the XRD profile of the same specimen in later ages, it is seen that its peaks disappear. When '100CM-A_III_360d' is examined, it is realized that the nesquehonite peaks are appearing, again. The reason for that can be related with the stability of the nesquehonite against high pH (Tanaka et al., 2019). At the very beginning, the reactive magnesia is reacting with water, yielding $Mg^{+2}$ and $(OH)^{-}$ ions. The brucite precipitated is reacting with the carbon dioxide dissolved in water and the concentration of $(OH)^{-}$ ions is not high enough to increase the pH of the pore solution significantly and prevent the nesquehonite formation. However, as time passes, due to the dissolution of the brucite, the pH of the environment becomes too high to form the nesquehonite, therefore its XRD peaks are dissappering. The fact that other XRD peaks are not seen in the results '100CM-A_III_7d' and '100CM-A_III_28d', can point out the formation of an amorphous phase of magnesium carbonate or the conversion to the brucite (Rausis, et al., 2020). The '100CM-A_III_360d' shows the presence of the nesquehonite due possibly to the conversion of this amorph phase to the nesquehonite, when the pH becomes low enough because of the carbonation in spite of the ambient conditions. The same situation can also be seen in the cement paste '100CM-A_II'. The slight decrease in the nesquehonite's peak intensity can be recognized between 2$^{nd}$ and 7$^{th}$ day. The increase in the intensity of the brucite peak refers the possible conversion of the magnesium carbonates to it and the continuing hydration of the reactive magnesia. Although between 7$^{th}$ and 28$^{th}$ days, there is no carbon dioxide curing for the

specimen ‘100CM-A_II’, the ‘100CM-A_II_28d’ shows the presence of the nesquehonite.

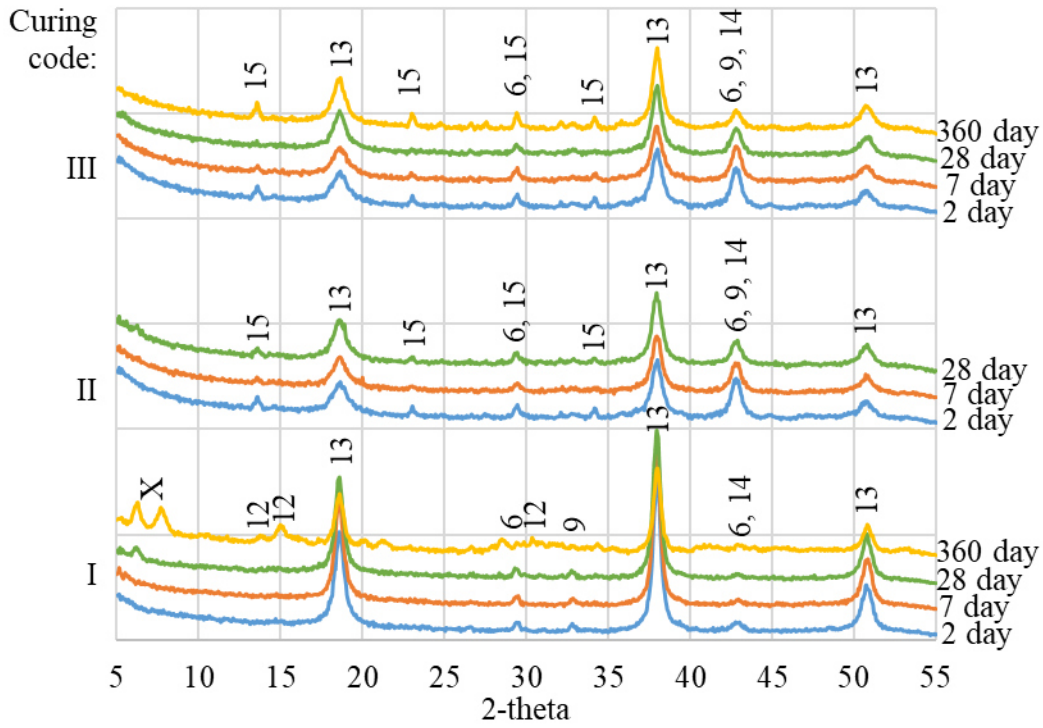


Figure 4.7. XRD profiles of the reactive magnesia cement containing no portland cement (100CM-A) subjected to various environmental exposures at various ages (1: $C_2S$, 2: $C_3S$, 6: Calcite, 9: Magnesite, 12: Hydromagnesite, 13: Brucite, 14: Periclase, 15: Nesquehonite).

In addition to the peaks observed in the result of the cement paste ‘C-A’, the brucite and periclase can also exist due to the presence of the reactive magnesia for the ‘50CM-A’ samples cured in ambient conditions and it is not possible to detect the XRD peaks of any magnesium carbonates indicated in literature with the graph shown in Figure 4.8. However, to analyze the XRD results of the cement pastes ‘50CM’ cured in carbon dioxide environment like ‘50CM-A_II’ or ‘50CM-A_III’ is

not too straightforward due to the overlaps of the main XRD peaks of the magnesium carbonates with those of the products of portland cement fraction. When compared the main XRD peaks of the ettringite and magnesite, it is clearly seen that the main peak of the magnesite found at about 33.5 2-theta degrees is overlapped with one of the peaks of the ettringite. It is also seen that in even for the cement paste '50CM-A_I', the ettringite is not recognized because of the absence of its main peak at 9 2-theta degrees. In other studies, the similar behavior of ettringite is also observed in other studies and the possible explanation for that behavior is suggested to be an interaction between the brucite and ettringite (Li, et al., 2020; Bhattacharja and Miller, 2005). Therefore, the peak found at about 33.5 2-theta degrees can be due to the presence of the magnesite only. Since the structural alteration is not observed when the curing regime is changed ('50CM-A_II'), this magnesite can be said to be stable. The reason why the nesquehonite is not determined in the '50CM-A' and this conversion occurs can be its lower stability. Though the stability of the nesquehonite is reported to be a debatable issue, the main factors affecting its stability can be said to be pH, temperature and carbon dioxide concentration (Unluer and Al-Tabbaa, 2013). Due to the higher amount of portland cement fraction in '50CM-A' than '100CM-A', the pH of its system is higher than the '100CM-A' preventing the formation of the nesquehonite (Note that the pH of the brucite-rich environment is lower than that of typical portland cement paste [Jin et al., 2013; Liska and Al-Tabbaa, 2012]). Both the $Ca^{2+}$ and $Mg^{2+}$ ions in the cement pastes can change the reaction kinetics and carbonation products (Rausis et al., 2020).

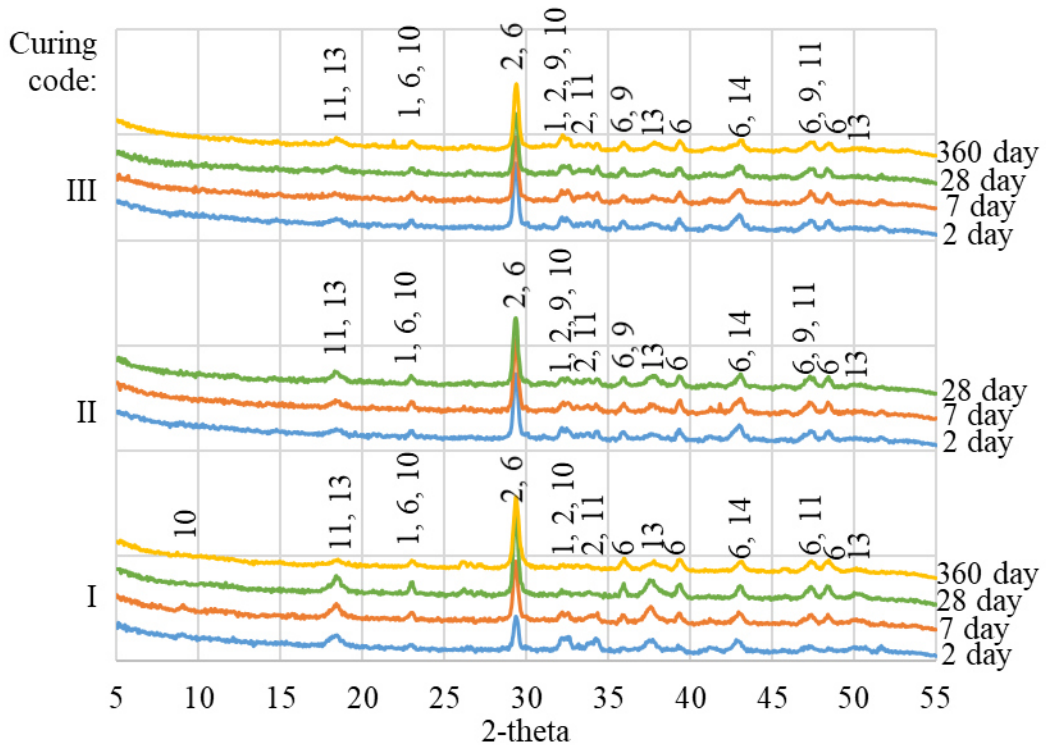


Figure 4.8. XRD profiles of the portland cement ('50CM-A') containing reactive magnesia subjected to various environmental exposures at various ages (1: $C_2S$, 2: $C_3S$, 6: Calcite, 9: Magnesite, 10: Ettringite, 11: Portlandite, 13: Brucite, 14: Periclase).

Figure 4.9 shows the XRDs of the control samples containing fly ash ('CF-A') in different curing conditions. The peak around 26.5 2-theta degrees belongs to the quartz which is present in the fly ash. The decrease in the intensities of the portlandite peaks refer to the pozzolanic activity of the fly ash addition to the cement system for the cement paste 'CF-A_I'. This behavior is very obvious when 'CF-A_I_7d' and 'CF-A_I_28d' are compared. Similarly, the relatively lower intensity of the calcite peak realized in especially early ages than that of the corresponding the samples points out the presence of small amount of the portlandite. In the XRD of the cement paste 'CF-A_III', there seems no portlandite peak, probably all the portlandite carbonates and produces calcite, resulting higher calcite peaks than that of the

cement paste ‘CF-A_I’. It can be concluded that the addition of the fly ash to the portland cement system does not have a clear effect on the carbonation process. The ‘CF-A_II’ shows that the change in curing condition seems no effect on the crystal structure of the cement paste ‘CF-A’.

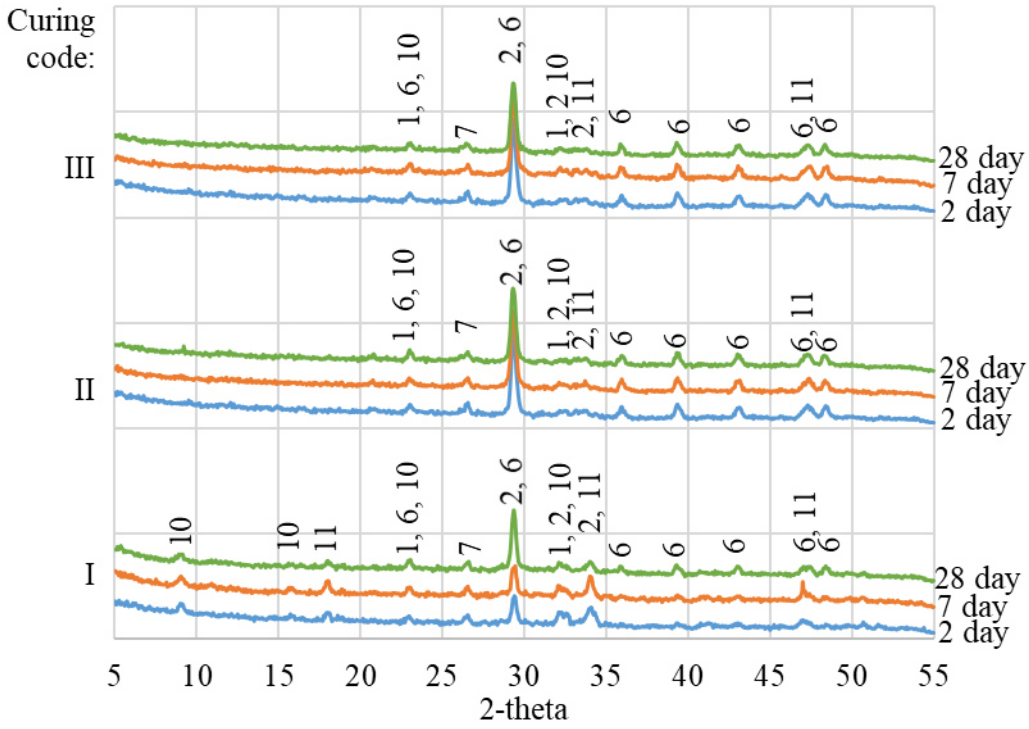


Figure 4.9. XRD profiles of the portland cement (‘CF-A’) containing fly ash subjected to various environmental exposures at various ages (1: $C_2S$, 2: $C_3S$, 6: Calcite, 7: Quartz, 10: Ettringite, 11: Portlandite).

The X-ray diffraction patterns of ‘30CMF-A’ cements are shown in Figure 4.10. When compared with the cement paste ‘CF-A_I’, ‘30CMF-A_I’ shows lower ettringite peaks due to the reaction between the ettringite and brucite (Bhattacharja and Miller, 2005). The increase of the peak in the intensity at 32.5 2-theta degrees in

cement paste '30CMF-A_III', with respect to that in 'CF-A_III', refers to the presence of the magnesite, whose main peak occurs at that location.

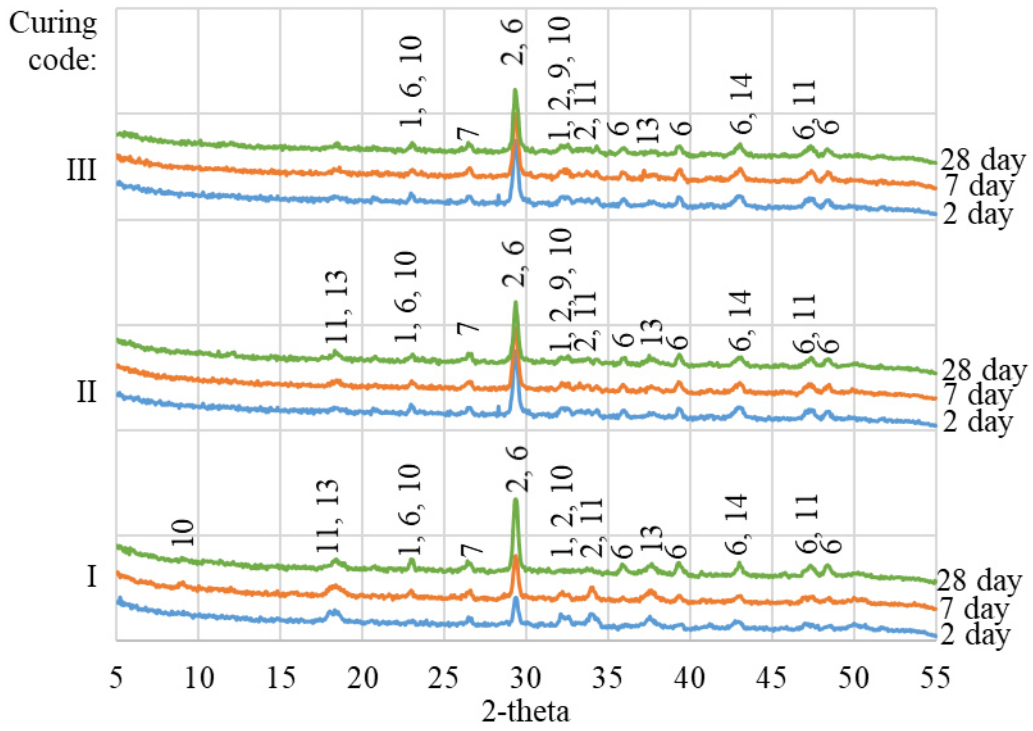


Figure 4.10. XRD profiles of the portland cement ('30CMF-A') containing fly ash and reactive magnesia subjected to various environmental exposures at various ages (1: $C_2S$, 2: $C_3S$, 6: Calcite, 7: Quartz, 10: Ettringite, 11: Portlandite, 13: Brucite, 14: Periclase).

Figures 4.11 shows the XRD results of 'CS-A' cements. Generally, the results are very similar to these obtained for 'CF-A' cements, except the absence of the 'Quartz' peak at 26.5 2-theta degrees. While the slag added to the system is in amorph form, no crystal structures are seen due to the addition. When compared the main peak of the calcite peak of the 'CS-A_III' at about 29.5 2-theta degrees with the 'C-A_III', it is realized that the effect of the presence of the slag differs with respect to time. In

early ages, the intensity of the calcite peak is lower for ‘C-A_III’ than ‘CS-A_III’, indicating the carbonation rate for the calcite formation becomes lower. Due to the dilution effect and slow hydration characteristics of slag, the calcium hydroxide content in early ages is lower. On the other hand, for 28 days, the intensities of the both cement paste is similar. The change of the curing environment can be suggested to have no effect on the carbonation / hydration products from the cement paste ‘CS-A_II’.

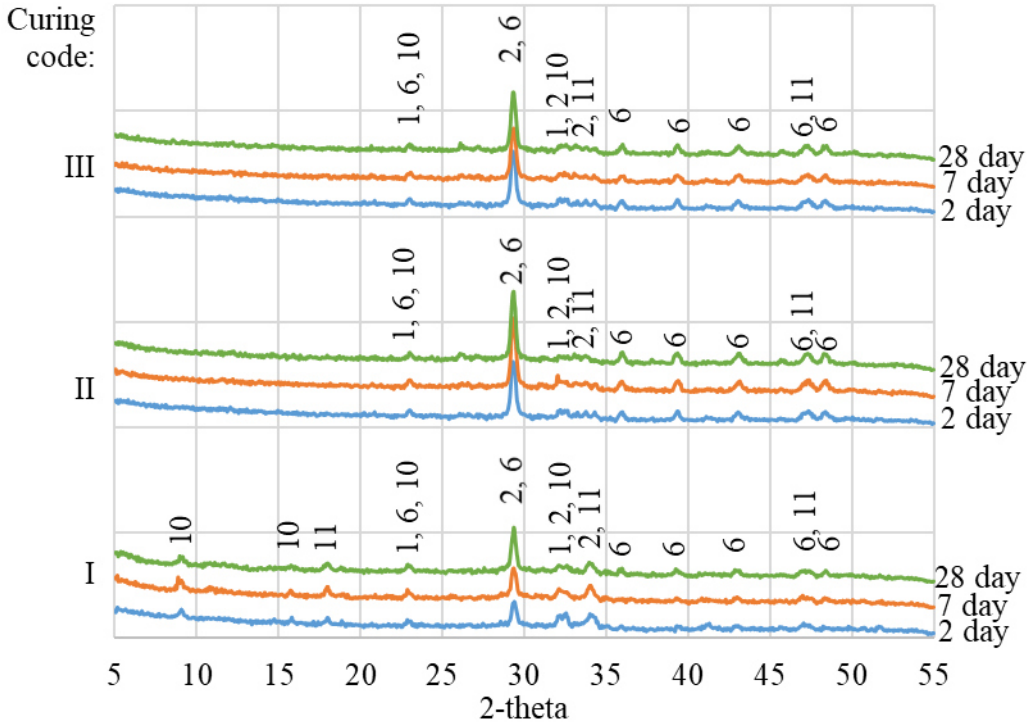


Figure 4.11. XRD profiles of the portland cement (‘CS-A’) containing slag subjected to various environmental exposures at various ages (1: $C_2S$, 2: $C_3S$, 6: Calcite, 10: Ettringite, 11: Portlandite).

The XRD patterns are revealed in Figure 4.12 for ‘30CMS-A’. The patterns are similar to the ones for ‘30CMF-A’ cements. It can be concluded that the addition of

fly ash has no or insignificant effect on the crystal structure of the reactive magnesia cement paste. It is found that the XRD patterns of '50CM-A' and '30CMF-A' are very similar. Figure 4.12 shows that the change in curing environment has no effect on the XRD results.

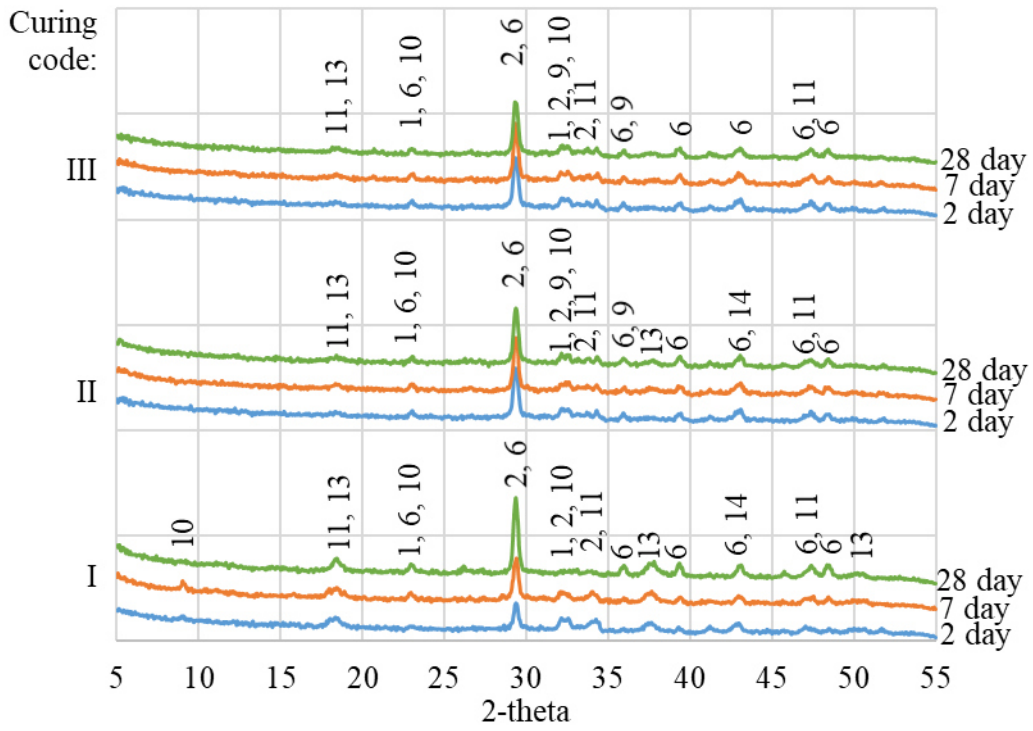


Figure 4.12. XRD profiles of the portland cement ('30CMS-A') containing slag and reactive magnesia subjected to various environmental exposures at various ages (1: $C_2S$, 2: $C_3S$, 6: Calcite, 9: Magnesia, 10: Ettringite, 11: Portlandite, 13: Brucite, 14: Periclase).

### 4.3.2. Hydration / Carbonation Products against Various Chemical Agents

The XRD profiles of the paste samples containing just water and reactive magnesia were taken to determine their durability against the chemicals used in rapid chloride permeability test and the tests considering the length change against the sulfate attack. In the scope of this test, the cement paste '100CM' was prepared with the water content adjusted according to the Eqn. 3.5. The material was cured in the ambient (0.04 % carbon dioxide, 25 ºC, 90 % RH) and medium (20 % carbon dioxide, 25 ºC, 90 % RH) level of carbon dioxide environment for 7 days. The specimens cured in medium level of carbon dioxide environment are marked with the sign '+'. After curing, the small specimens taken from the same cement paste were exposed to the solutions for 3 days. The concentrations of the chemicals, which are shown in Table 4.19, were arranged according to the solutions used in the durability tests.

Table 4.19. The concentrations of the solutions which the specimens were exposed to.

| **Solution** | **Concentration** |
|---|---|
| Distilled water | - |
| NaCl | % 3 |
| NaOH | 0.3 N |
| $Na_2SO_4$ | 50 g/L |

Characterization of the hydration / carbonation products, before and after the exposure of the cement pastes to these solutions were performed via XRD analysis. For comparison, the specimen, exposed to no chemical agent, was also examined. The Figure 4.13 shows the regime and the notation during the test. For example, after the specimen '100CM- (NaCl)' was cured in ambient conditions for 7 days, was exposed to NaCl solution for 3 days. To determine its XRD profile at $14^{th}$ day, it was dried at 60 ºC for 4 days.

| | Time | | | | |
|---|---|---|---|---|---|
| | $0^{th}$ day (Casting day) | $3^{rd}$ day | $7^{th}$ day | $10^{th}$ day | $14^{th}$ day |
| Specimen | | | | | |
| 100CM-(7d) | Cured in ambient conditions | Dried in 60 ºC | | | |
| 100CM-(14d) | Cured in ambient conditions | | | | Dried in 60 ºC |
| 100CM-(water) | Cured in ambient conditions | | | Be exposed to distilled water | Dried in 60 ºC |
| 100CM-(NaCl) | Cured in ambient conditions | | | Be exposed to NaCl solution | Dried in 60 ºC |
| 100CM-(NaOH) | Cured in ambient conditions | | | Be exposed to NaOH solution | Dried in 60 ºC |
| 100CM-($Na_2SO_4$) | Cured in ambient conditions | | | Be exposed to $Na_2SO_4$ solution | Dried in 60 ºC |
| 100CM+(7d) | Cured in medium level of carbon dioxide | Dried in 60 ºC | | | |
| 100CM+(14d) | Cured in medium level of carbon dioxide | | | Cured in ambient conditions | Dried in 60 ºC |
| 100CM+(water) | Cured in medium level of carbon dioxide | | | Be exposed to distilled water | Dried in 60 ºC |
| 100CM+(NaCl) | Cured in medium level of carbon dioxide | | | Be exposed to NaCl solution | Dried in 60 ºC |
| 100CM+(NaOH) | Cured in medium level of carbon dioxide | | | Be exposed to NaOH solution | Dried in 60 ºC |
| 100CM+($Na_2SO_4$) | Cured in medium level of carbon dioxide | | | Be exposed to $Na_2SO_4$ solution | Dried in 60 ºC |

Figure 4.13. The regimes applied to the specimens.

The XRD results are shown in Figures 4.14 and 4.15. When the results of the cement pastes '100CM-' are considered, it is clear that the hydration product of the reactive magnesia is the brucite. As a carbonation product, a little amount of magnesite is determined. It is also found that the chemical agents used have no effect on these products as well as the distilled water. The results of the cement paste cured in medium level of carbon dioxide environment show that the main carbonation product is the nesquehonite. The NaCl solution has no effect on the presence of the nesquehonite, but it is very clear that the solutions of $Na_2SO_4$ and NaOH dissolve the structure of the nesquehonite. However, it can be seen from the intensity difference of the nesquehonite that the effect of the former is lower than the latter.

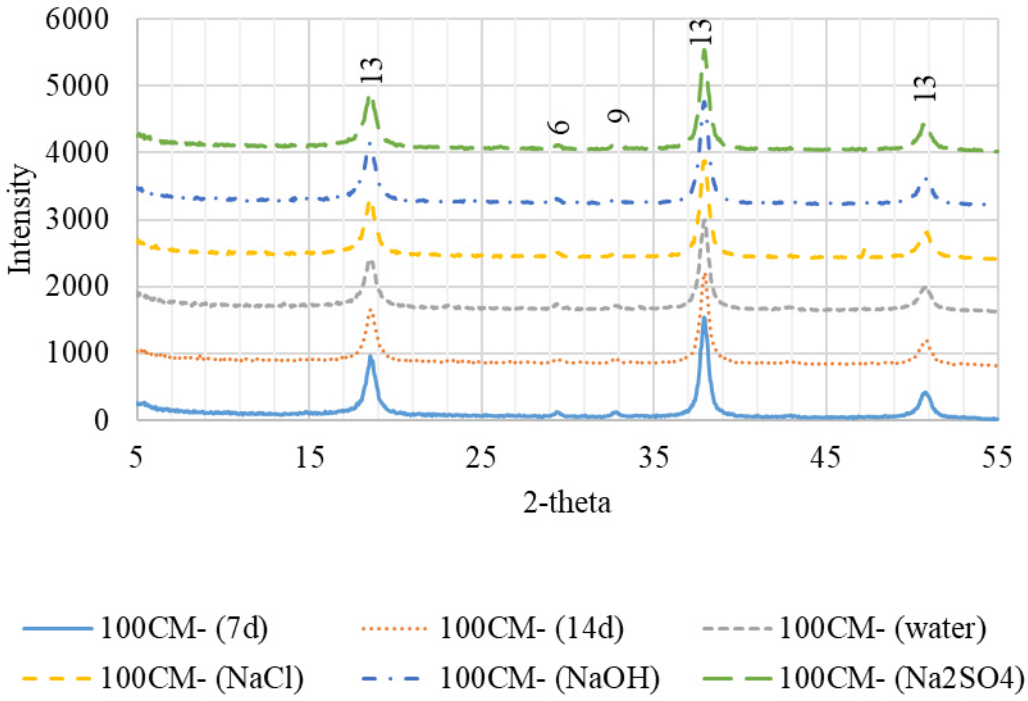


Figure 4.14. XRD results of the specimens subjected to ambient environment (6: Calcite, 9: Magnesite, 13: Brucite).

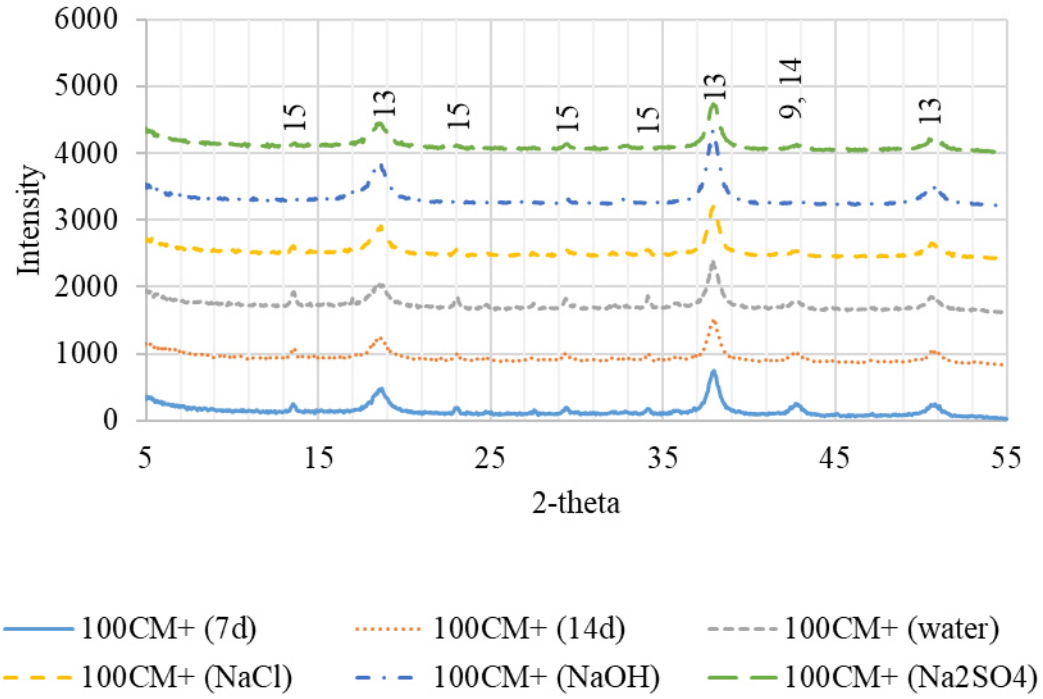


Figure 4.15. XRD results of the specimens subjected to carbon dioxide environment (9: Magnesite, 13: Brucite, 14: Magnesite, 15: Nesquehonite).

### 4.3.3. Microstructural Characterization through SEM

The pastes containing either only reactive magnesia or only portland cement were investigated via scanning electron microscopy to determine their microstructure. The samples were prepared according to Table 4.20. The water content was arranged according to the Eqn. 3.5. While one set of the specimens was kept in atmospheric conditions (0.04 % carbon dioxide), the other set was exposed to medium level of carbon dioxide (20 % carbon dioxide). For both regimes, the relative humidity and temperature were kept same and constant. The curing was continued for one year.

Table 4.20. The mix design of the cement pastes (by weight).

| Cement Pastes | Portland Cement (g) | Reactive Magnesia (g) | Water (g) |
|---|---|---|---|
| C | 6.79 | 0 | 3.26 |
| 100CM | 2.50 | 2.50 | 3.48 |

The SEM images of the cement pastes ‘C’ in atmospheric condition and medium level of carbon dioxide environment are shown in Figures 4.16 and 4.17, respectively. As expected, the specimen in atmospheric condition shows the hydration products like C-S-H gels, ettringite and portlandite. On the other hand, as seen in Figure 4.17, the specimen exposed to carbon dioxide, the products can not be seen due to the carbonation products collected on other hydration products.

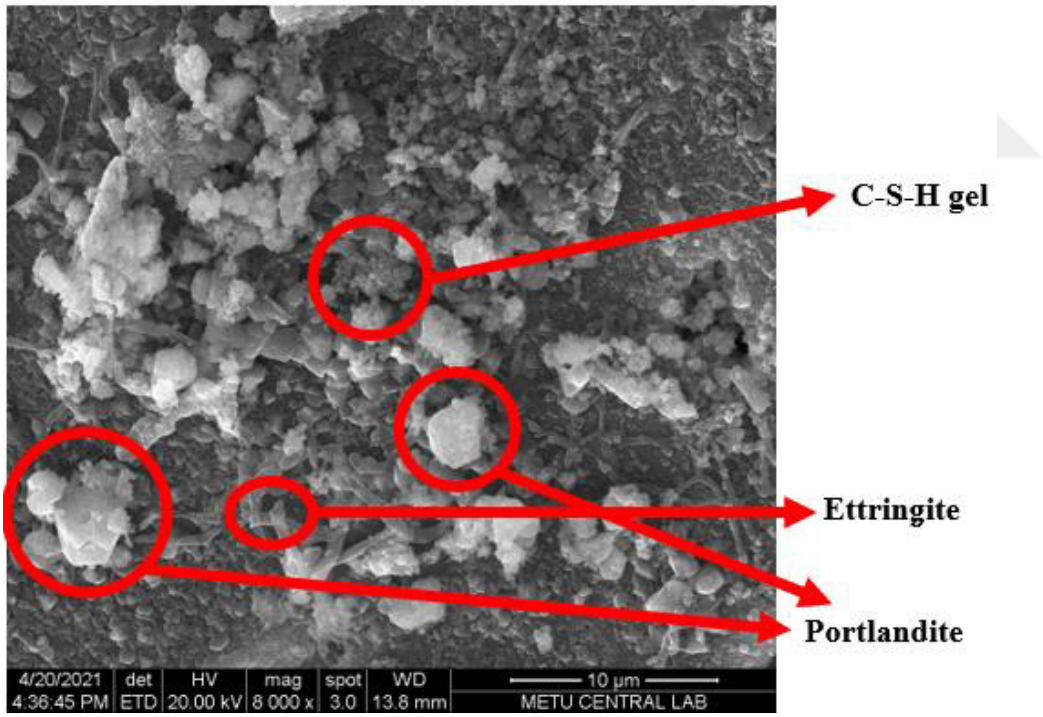


Figure 4.16. SEM image of the cement paste ‘C’ in atmospheric conditions for one year.

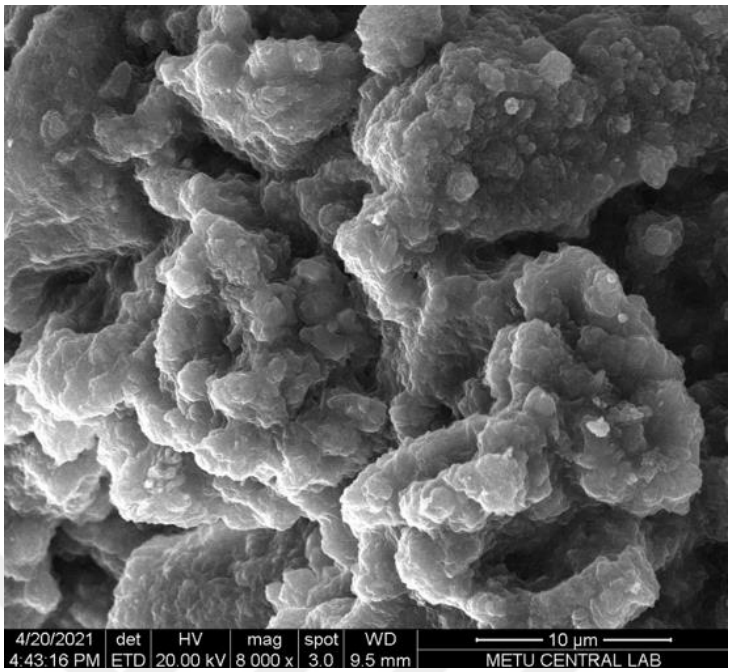


Figure 4.17. SEM image of the cement paste ‘C’ in the medium level of carbon dioxide environment for one year.

The images with different scales taken from the cement paste ‘100CM’ cured in atmospheric conditions are shown in Figures 4.18 and 4.19. Figure 4.18, which has lower magnification rate shows that the cement paste ‘100CM’ cured in the atmospheric conditions has its hydration product, probably brucite (Walling & Provis, 2016). But, Figure 4.19 taken with higher magnification rate reveals that these products are covered with rosette-like crystals similar to hydromagnesite (Dung & Unluer, 2016). Figure 4.20 shows the SEM image taken for the same sample, but cured in the medium level of carbon dioxide environment. It is seen that the cement paste has long and thin crystals in one direction.

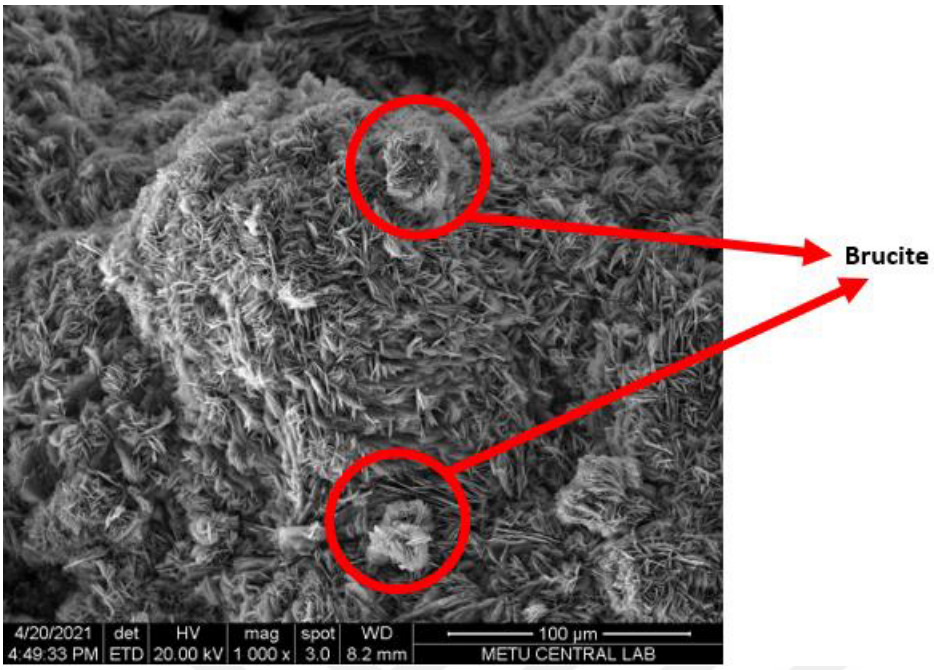


Figure 4.18. SEM image of the cement paste '100CM' in the low level of carbon dioxide environment with lower magnification rate for one year.

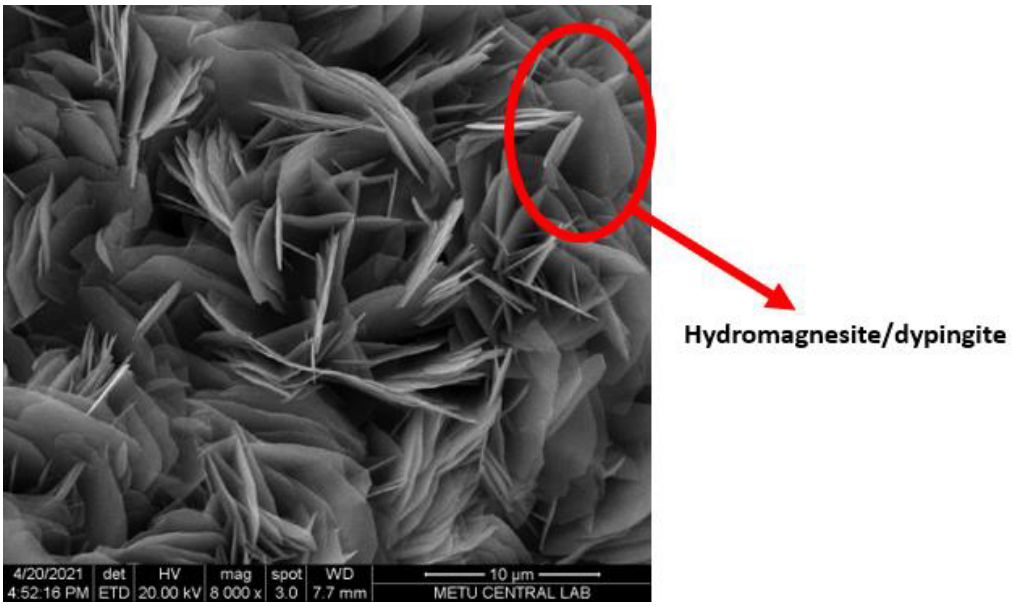


Figure 4.19. SEM image of the cement paste '100CM' in the low level of carbon dioxide environment with higher magnification rate for one year.

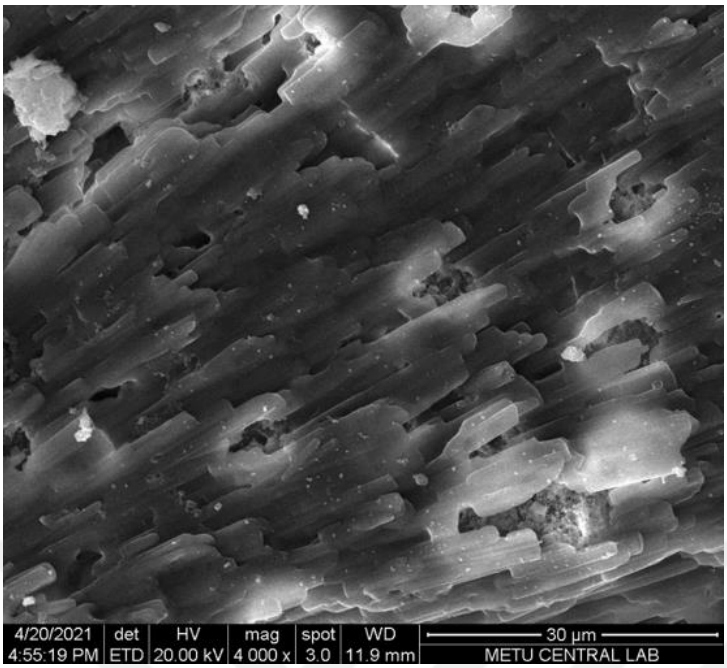


Figure 4.20. SEM image of the cement paste '100CM' in the medium level of carbon dioxide environment with higher magnification rate for one year.

## 4.4. Verification of the Possible Reaction between Reactive Magnesia and Portland Cement

To find out the possible reaction between the portland cement and the reactive magnesia, the heats of hydration of the reactive magnesia cements were examined. As well as the portland cement and the reactive magnesia individually, the 50CM cement was also tested by the isothermal calorimeter for comparison purposes. The cement paste samples were prepared according to the mix design stated in Table 4.21. The water content was arranged according to the Eqn. 3.5.

Table 4.21. The mix design of the cement pastes (by weight).

| Cement Pastes | Portland Cement (g) | Reactive Magnesia (g) | Water (g) |
|---|---|---|---|
| C | 6.79 | 0 | 3.26 |
| 100CM | 2.50 | 2.50 | 3.48 |
| 50CM | 0 | 3.97 | 3.61 |

The tests for each cement paste are repeated at least twice. The normalized results according to the total powder content are shown in Figure 4.21. It is very obvious that the heat of hydration of the cement paste '100CM' is very higher than the cement paste 'C'. The result marked with '50CM-Measured' shows the results obtained from the calorimeter, but the result '50CM-Calculated' is based on the weighted average of the results of the test pastes '100CM' and 'C'. If there is no reaction between the reactive magnesia and the portland cement, the curves of the '50CM-Calculated' and '50CM-Measured' should coincide with each other. But this is not the case, the results obtained from the calorimeter are lower than those from the calculation, indicating the presence of the possible interaction between the portland cement and reactive magnesia fractions. Due to this, the reaction kinetics of the reactive magnesia are reduced by those of the portland cement.

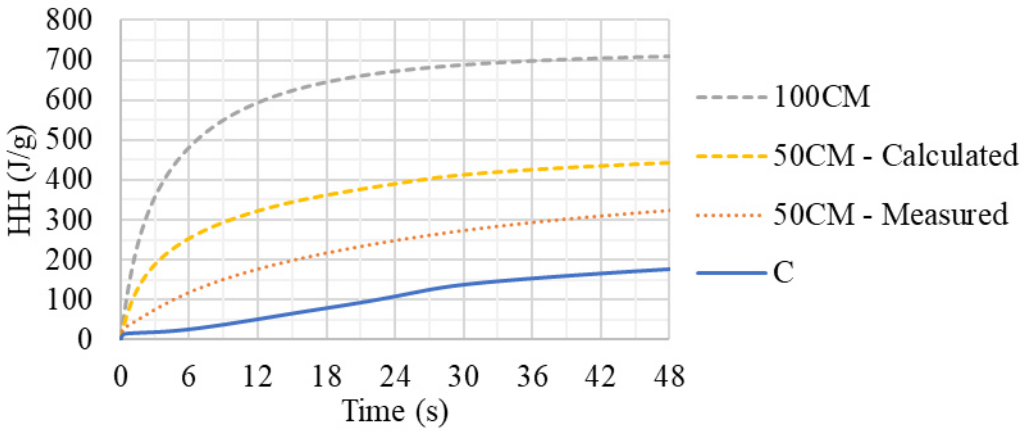


Figure 4.21. The heat evolution curves of the cement samples.

## 4.5. General Discussions

Considering all the results obtained from the experiments, these conclusions can be reached.

The preliminary experiments show that to obtain the reactive magnesia, the burning temperature and the exposure time of the raw material, magnesite are important parameters. In this study, the optimum temperature and exposure time to attain the most reactive magnesia are found to be 600 ºC and 120 minutes, respectively.

It is found that the air curing results in more carbonation for a reactive magnesia cements than the water curing. This can be due to the excess conversion of the periclase to the brucite in water since the binding ability of it is reported to be lower. In addition, the volume of it is higher than that of the periclase, indicating that it can create the internal stresses and reduce the mechanical performance.

To increase the carbon dioxide concentration increases the strength up to a certain point because of the carbonation which leads to the carbonation products with their relatively high strength, filling the pores. After this point, it affects the mechanical properties negatively, due to the excess carbonation of the C-S-H gel, the main hydration product for the portland cement fraction, responsible for the strength development. The results of the 1$^{st}$ initial and 2$^{nd}$ main casting show this fact very clearly, the results taken from the 20 % carbon dioxide environment are higher than that of 50%.

It is very obvious that the presence of reactive magnesia leads to the decrease in mechanical performance in ambient curing conditions when the XRD results are considered. The main hydration/carbonation products due to the reactive magnesia are the brucite and for late ages, hydromagnesite as well as unidentified materials, which probably belong to a hydration or carbonation product of the periclase. So, it can be deducted that the strength of the reactive magnesia hydrates is lower.

The most of the compressive strength results of the specimens cured in higher carbon dioxide environment are higher than these in ambient conditions. This situation becomes very clear when removing the dilution effect. When the results for the cement mortars '15CM+', '30CM+' and '50CM+' are compared with the cement mortar 'C+' removing the dilution effect, the reactive magnesia increase leads to the decrease in compressive strength for early ages, but for late ages, results in the strength gain. For the cement paste '100CM', the XRD shows the presence of the nesquehonite and its strength is significantly higher. But, the XRD results show the peaks of the magnesite in reactive magnesia cements in the presence of an amount of portland cement fraction instead of these of the nesquehonite, which can point out the stability problem of the nesquehonite against the high pH of the system. (This situation is also seen in the 2$^{nd}$ XRD tests, the nesquehonite is destroyed by the high pH of the NaOH solution.) The pH of the brucite-rich environment is lower than the portlandite-rich one, and the solubility of the brucite is lower, so at the very beginning, the pH of this medium is not high enough to dissolve the nesquehonite (Al-Tabbaa, 2013; Jin et al., 2013; Martin Liska & Al-Tabbaa, 2012). The nesquehonite can be formed, but the increasing pH of the pore solution over time can convert the nesquehonite to an amorph phase, which can not be detected by the XRD tests (Tanaka, et al., 2019). But, while the continuous carbonation of the system is decreasing the pH and a carbonation product, magnesite formed from the possible conversion of this carbonation product, becomes stable. This explains the effect of the reactive magnesia on the compressive strength. Similarly, the nesquehonite formed in XRD result of the cement paste '100CM' becomes invisible, but this phenomenon is much slower due to the slower reaction rate of the brucite. In addition, the product formed after the pH reduction is the nesquehonite, not the magnesite because of the inexplicable chemical problem called "magnesite problem", indicating the difficulties to produce magnesite at ambient pressures and temperatures (Xu et al., 2013). In spite of this behavior of magnesium carbonates formed in nesquehonite and magnesite, the strength gain resulted from these is very

much higher than that from the carbonation of portland cement paste fraction. This can be seen very clearly when the carbonation contribution is considered.

The statistical analysis show that, for mechanical properties, the importance of the curing conditions and the content of the reactive magnesia in cements is higher than other parameters such as the presence of fly ash and ground granulated blast furnace slag.

It was determined that the changes in length of the specimens showing better performance in rapid chloride permeability test, were smaller due to the lower permeability of these mortars, for especially the cement mortars ‘C+’, ‘C-’, ‘CF+’ and ‘CF-’. But, this was not correct for the specimens having higher amount of reactive magnesia. While the performance of the cement mortar ‘50CMF-’ in rapid chloride permeability test was relatively better compared to others, its change in length in sulfate solution was very higher than the others. This can be related with the possible reaction between the reactive magnesia and the sulfate ions in solution.

The required time for the conversion of the reactive magnesia to the magnesium carbonates, completely, was found to be higher in comparison with that for the portland cement components. The intensities belonging to the magnesite, which is the carbonation product of the reactive magnesia, is very lower than those of the calcite, especially in the cement paste ‘50CM-A_III’. The carbonation tendency of the lime, even C-S-H gels and the ettringite is higher than the reactive magnesia. On the other hand, when considered the carbonation contributions of ‘C’ and ‘100CM’, it shows the strength gain due to the carbonation of brucite is very much higher than that due to the hydration products of portland cement.

The XRD results clearly reveal that even for late ages, some of brucite can not be carbonated completely for medium level of carbon dioxide concentration. This can be due to the lower permeable barrier formed by magnesium carbonates on the surface. This formation can prevent further carbon dioxide diffusion to the inside of the paste.

The effect of the mineral admixtures to the reactive magnesia cements differs with respect to the type of the admixture used. In case of fly ash, the carbonation contributions are always lower than their control counterparts. Since this is a low lime fly ash, it reduces the amount of alkalis (CH and/or MH), consuming in pozzolanic reactions. Since they could have been carbonated, the pozzolanic reactions taking place, reduces the effect of carbon dioxide curing. On the other hand, due to its filler effect, it reduces the permeability. The effect of slag addition differs with its chemical composition and the hydration rate which is very low in comparison with the portland cement. In the experiment where the effect of slag is investigated, the carbon dioxide curing has been continued only for 2 days. Because of the lower hydration rate of slag and the decrease in portland cement fraction for slag-containing reactive magnesia cements, the lime concentration in pore solution this time duration is not sufficient for an efficient carbonation, so the strength gain due to the carbonation is quite low. After the specimens are moved to the ambient curing conditions, their strength starts increasing with time due not to the carbonation but the hydraulic binding property of slag.

From the XRD results for the specimens exposed to chemical agents, it is very clear that $Na_2SO_4$ and NaOH solutions have similar effect on the stability of the nesquehonite. The molarity of the NaOH solution is about 0.3 M, so the pH of that solution is $14 + \log 0.3 = 13.48$. The structure of the nesquehonite can be destroyed by the harsh environment caused by the NaOH solution. For this reason, the reactive magnesia cement mortars exposed to the rapid chloride permeability tests show exaggerative temperatures, but it is seen that the effect of it can be reduced by adding fly ash to the system. The similar but extenuated effect can also be observed in $Na_2SO_4$ solution. The pH of 5 % of this solution can be reached 9.0, where the environment can also be destructive of the nesquehonite (Butts et al., 2013). This can explain the strange behavior of '100CM+' in sulfate attack tests. In first weeks, the medium created by $Na_2SO_4$ solution destroys the nesquehonite, so the mortar shows the contraction. But, at the same time, the water molecules in solutions react with the

periclase particles, yielding the brucite. Moreover, since the barrier created by the nesquehonite is damaged, it becomes easier for water to penetrate to the specimen.

The interaction between the brucite and ettringite is also recognized in the XRD results of all reactive magnesia cements containing an amount of portland cement. In the presence of the brucite, the ettringite peaks are disappearing due to the interaction between them (Bhattacharja & Miller, 2005).

It is also concluded that the permeability of the cement mortar containing any amount of the reactive magnesia can not be determined by rapid chloride permeameter test. During the test, the temperatures of the solutions used reached at higher 95 ºC, indicating a possible reaction between the material and the solutions. The 2$^{nd}$ XRD test shows the reaction between the nesquehonite and NaOH solution, clearly. Therefore, it is not possible to perform the rapid chloride permeameter test to the mortars containing reactive magnesia which results in the formation of the nesquehonite.

It is revealed that the change in curing conditions does not have any significant effect on the crystal structure, indicating that for at least 28 days, the carbonation/hydration products of the reactive magnesia cements are stable against the change in curing conditions.

The calorimeter and XRD results show a reaction between the reactive magnesia and portland cement. For the heat of hydration test, the difference between the results '50CM-Measured' and '50CM-Calculated' shows this fact clearly. The XRD pattern of the cement paste '50CM-A', showing no ettringite proves this reaction. This results contradicts the findings of the earlier studies (Al-Tabbaa, 2013; M. Liska & Al-Tabbaa, 2009).

The images taken with scanning electron microscopy and the XRD tests show the microstructure of the pastes 'C' and '100CM'. It is clear that the carbon dioxide concentration of the curing environment has an effect on the microstructure. For the cement paste 'C' cured in 20 % carbon dioxide environment, the carbonation

products collected on hydration products are calcite according to XRD results. The rosette-like crystals seen on the SEM image of ‘100CM’ are seemed to be hydromagnesite. The small size and the shape of the crystals explain the lower strength results obtained for these samples. According to the XRD results, the fibrous structure identified in the cement paste ‘100CM’ cured in 20 % carbon dioxide environment belongs to nesquehonite, which is responsible for the higher mechanical performance.

# CHAPTER 5

# CONCLUSION AND RECOMMENDATIONS

## 5.1. Conclusion

The following conclusions were drawn as a result of the experimental program conducted:

- For the naturally-obtained magnesite used in this study, the most reactive magnesia was produced with the burning temperature of 600 ºC and the exposure time of 120 minutes.
- In ambient conditions, the carbonation rate of reactive magnesia was lower, therefore, its strength contribution was almost zero. On the contrary, since its presence resulted in the reduction of the portland cement amount, relatively, the strength decreased.
- Higher concentrations of carbon dioxide in the curing environment enhanced the mechanical and physical properties of the cement-based materials, however, its use in excessive amounts can result in a strength reduction due to the destruction of the hydration products.
- The pozzolanic activities reduced the effect of carbon dioxide curing because they led to the reduction of alkalinity of the pore solution.
- The strength contribution of reactive magnesia due to the carbonation was higher than that of portland cement fraction.
- The main carbonation product of reactive magnesia was nesquehonite in the case of a higher concentration of carbon dioxide in the curing environment. With its fibrous structure, it contributed the overall strength of the

cementitious system. However, its stability against a higher pH of the medium and sulfates was low, so the long term performance of reactive magnesia-incorporated cements shows some fluctuations in strength results.

- The statistical analysis of the compressive strength tests showed that, the importance of the curing conditions and the content of the reactive magnesia in cements is higher than other parameters such as the presence of fly ash and ground granulated blast furnace slag.
- For the cement composite including only reactive magnesia, the main carbonation product is the nesquehonite. The magnesite can not be produced because of the so-called 'magnesite problem'.
- The hydration and carbonation reactions of reactive magnesia and portland cement affected each other.

## 5.2. Recommendations

For future studies, the following recommendations can be useful:

- In this study, the calcination temperature and exposure time was found specifically for the magnesite sample used. In order to consider other parameters affecting the reactivity, like the impurities present in magnesite or the alterations of the crystal structure, several types of magnesite samples obtained from different parts of the world can be used.
- The reaction between water and reactive magnesia resulted in rapid heating of the mix, and correspondingly higher water consumption due to the evaporation. Therefore, the water content used in the mixes was normalized according to the chemical reaction in this study. To decrease heat release, the possible use of chemical admixtures can be considered.
- The continuous carbon dioxide curing was determined to be the best curing regime to carbonate the samples in this study. However, other curing regimes like the fluctuating curing regime, where the carbon dioxide level is increased

to a point and after that, decreasing to the atmospheric curing conditions at a certain time period, can be investigated.

- To examine the microstructure of the reactive magnesia-incorporated cements deeply, besides the techniques utilized in this study, other methods, like visualizing via optical microscope or determination of hydration heat in the environment rich in carbon dioxide can be considered.
- It was found that the presence of reactive magnesia prevented the formation of ettringite, which was one of the main hydration products of ordinary portland cement. To overcome this problem, instead of portland cement, a modified portland cement, whose $C_3A$ content is lower than a typical ordinary portland cement, can be used.
- One of the challenges faced with was the inability of the inner parts of the reactive magnesia cement mortars to carbonate sufficiently due to the inability of carbon dioxide to penetrate in. To carbonate these parts, a new mix design can be employed. For example, the amount of the fine parts of the mix can be decreased, therefore the porosity and correspondingly, permeability of the sample can be increased.
- Theoretically, the carbonation process leads to the increase in mass due to the absorption of carbon dioxide by the samples. The mass increase of the samples can give an idea about the possible maximum carbonation capability of the samples.

# REFERENCES


AirTest. (2012). *COZIR-W (5%, 20%, 60%, 100% CO2) Ultra Low Power CO2 Sensor For OEM Applications*. https://www.airtest.com/support/datasheet/COZIR-W.pdf

Al-Tabbaa, A. (2013). Reactive magnesia cement. In *Eco-Efficient Concrete* (pp. 523–543). Elsevier. https://doi.org/10.1533/9780857098993.4.523

Ashraf, W. (2016). Carbonation of cement-based materials: Challenges and opportunities. *Construction and Building Materials*, *120*, 558–570. https://doi.org/10.1016/j.conbuildmat.2016.05.080

ASTM C 1012. (2015). *C 1012 - 15 Standard Test Method for Length Change of Hydraulic-Cement Mortars Exposed to a Sulfate Solution*. https://doi.org/10.1520/C1012_C1012M-15

ASTM C 109. (2016). *C 109/C109M - 16a Standard Test Method for Compressive Strength of Hydraulic Cement Mortars (Using 2-in. or [50-mm] Cube Specimens)*. https://doi.org/10.1520/C0109_C0109M-16A

ASTM C 1202. (2017). *C 1202 - 17 Standard Test Method for Electrical Indication of Concrete's Ability to Resist Chloride Ion Penetration*. https://doi.org/10.1520/C1202-17

ASTM C 1437. (2020). *Standard Test Method for Flow of Hydraulic Cement Mortar*. https://doi.org/10.1520/C1437- 20

ASTM C 150. (2020). *C150/C150M − 20 Standard Specification for Portland Cement*. https://doi.org/10.1520/C0150_C0150M-20

ASTM C 151. (2018). *C151/C151M-18 Standard Test Method for Autoclave Expansion of Hydraulic Cement*. https://doi.org/10.1520/C0151_C0151M-18

ASTM C 1702. (2017). *C 1702 - Standard Test Method for Measurement of Heat of Hydration of Hydraulic Cementitious Materials Using Isothermal Conduction Calorimetry*. https://doi.org/10.1520/C1702-17

ASTM C 188. (2009). *C 188 - 09 Standard Test Method for Density of Hydraulic Cement*. https://doi.org/10.1520/C0188-09

ASTM C 204. (2018). *C 204 - 18 Standard Test Methods for Fineness of Hydraulic Cement by Air-Permeability Apparatus*. https://doi.org/10.1520/C0204-18

ASTM C 305. (2014). *C 305-14 Standard Practice for Mechanical Mixing of Hydraulic Cement Pastes and Mortars of Plastic Consistency*. https://doi.org/10.1520/C0305-14

Bhattacharja, S., & Miller, F. M. (2005). *Expansion in Mortar Bars Subjected to Accelerated Curing RD132*.

Birchal, V. S. ., Rocha, S. D. ., & Ciminelli, V. S. . (2000). The effect of magnesite calcination conditions on magnesia hydration. *Minerals Engineering*, *13*(14–15), 1629–1633. https://doi.org/10.1016/S0892-6875(00)00146-1

Butts, D., Bush, D. R., & Updated by Staff. (2013). Sodium Sulfates and Sulfides. In *Kirk-Othmer Encyclopedia of Chemical Technology*. John Wiley & Sons, Inc. https://doi.org/10.1002/0471238961.1915040902212020.a01.pub3

Canterford, J. H., Tsambourakis, G., & Lambert, B. (1984). Some observations on the properties of dypingite, Mg5(CO3)4(OH)2 5H2O, and related minerals. In *Mineralogical Magazine* (Vol. 48, Issue September, pp. 437–442).

Chatterji, S. (1995). Mechanism of expansion of concrete due to the presence of dead-burnt CaO and MgO. In *Cement and Concrete Research* (Vol. 25, Issue 1, pp. 51–56). https://doi.org/10.1016/0008-8846(94)00111-B

Chen, X., Zhao, W., & Li, P. (2013). Elements enrichment characteristics in interfacial transition zone of MgO concrete. In *Wuhan University Journal of Natural Sciences* (Vol. 18, Issue 1, pp. 88–92). https://doi.org/10.1007/s11859-

013-0898-8

De Silva, P., Bucea, L., Moorehead, D. R., & Sirivivatnanon, V. (2006). Carbonate binders: Reaction kinetics, strength and microstructure. In *Cement and Concrete Composites* (Vol. 28, Issue 7, pp. 613–620). https://doi.org/10.1016/j.cemconcomp.2006.03.004

De Silva, P., Bucea, L., & Sirivivatnanon, V. (2009). Chemical, microstructural and strength development of calcium and magnesium carbonate binders. In *Cement and Concrete Research* (Vol. 39, Issue 5, pp. 460–465). https://doi.org/10.1016/j.cemconres.2009.02.003

Demir, F., Dönmez, B., Okur, H., & Sevim, F. (2003). Calcination kinetic of magnesite from thermogravimetric data. In *Chemical Engineering Research and Design* (Vol. 81, Issue 6, pp. 618–622). https://doi.org/10.1205/026387603322150462

Dung, N. T., & Unluer, C. (2016). Improving the performance of reactive MgO cement-based concrete mixes. In *Construction and Building Materials* (Vol. 126, pp. 747–758). https://doi.org/10.1016/j.conbuildmat.2016.09.090

Dung, N. T., & Unluer, C. (2017a). Carbonated MgO concrete with improved performance: The influence of temperature and hydration agent on hydration, carbonation and strength gain. In *Cement and Concrete Composites* (Vol. 82, pp. 152–164). https://doi.org/10.1016/j.cemconcomp.2017.06.006

Dung, N. T., & Unluer, C. (2017b). Influence of nucleation seeding on the performance of carbonated MgO formulations. In *Cement and Concrete Composites* (Vol. 83, pp. 1–9). https://doi.org/10.1016/j.cemconcomp.2017.07.005

Dung, N. T., & Unluer, C. (2018). Development of MgO concrete with enhanced hydration and carbonation mechanisms. *Cement and Concrete Research*, *103*, 160–169. https://doi.org/10.1016/j.cemconres.2017.10.011

Electronics|Projects|Focus. (n.d.). *DHT11 Sensor and Its Working*. https://www.elprocus.com/a-brief-on-dht11-sensor/

Erdoğan, T. Y. (2010). *Beton*. ODTÜ Geliştirme Vakfı Yayıncılık ve İletişim A.Ş.

Fernández Bertos, M., Simons, S. J. R., Hills, C. D., & Carey, P. J. (2004). A review of accelerated carbonation technology in the treatment of cement-based materials and sequestration of CO2. In *Journal of Hazardous Materials* (Vol. 112, Issue 3, pp. 193–205). https://doi.org/10.1016/j.jhazmat.2004.04.019

Ferrini, V., De Vito, C., & Mignardi, S. (2009). Synthesis of nesquehonite by reaction of gaseous CO2 with Mg chloride solution: Its potential role in the sequestration of carbon dioxide. *Journal of Hazardous Materials*, *168*(2–3), 832–837. https://doi.org/10.1016/j.jhazmat.2009.02.103

Fricker, K. J., & Park, A.-H. A. (2013). Effect of H2O on Mg(OH)2 carbonation pathways for combined CO2 capture and storage. *Chemical Engineering Science*, *100*, 332–341. https://doi.org/10.1016/j.ces.2012.12.027

Gaze, M. E., & Smith, M. A. (1978). Fly Ash and Granulated Blast-Furnace Slag As "Stabilisers" of Portland Cements With Added Periclase. In *J Appl Chem Biotechnol* (Vol. 28, Issue 11, pp. 687–698). https://doi.org/10.1002/jctb.5700281101

Harrison, A. J. W. (2003). New cements based on the addition of reactive magnesia to Portland cement with or without added pozzolan. In *Proc., CIA Conf.: Concrete in the ...* (pp. 1–11). http://moleconomics.org/files/conferencepapers/NewCementsBasedontheAdditionofReactiveMagnesiatoPCCIAConcreteintheThirdMilleniumBrisbane170704.pdf

Harrison, A. J. W. (2008). *Reactive Magnesium Oxide Cements* (Patent No. US 7347896 B2).

Harrison, A. L., Mavromatis, V., Oelkers, E. H., & Bénézeth, P. (2019). Solubility of the hydrated Mg-carbonates nesquehonite and dypingite from 5 to 35 °C:

Implications for CO 2 storage and the relative stability of Mg-carbonates. In *Chemical Geology* (Vol. 504, pp. 123–135). https://doi.org/10.1016/j.chemgeo.2018.11.003

Hopkinson, L., Rutt, K., & Cressey, G. (2008). The Transformation of Nesquehonite to Hydromagnesite in the System CaO-MgO-H 2 O-CO 2 : An Experimental Spectroscopic Study. *The Journal of Geology*, *116*(4), 387–400. https://doi.org/10.1086/588834

Jauffret, G., Morrison, J., & Glasser, F. P. (2015). On the thermal decomposition of nesquehonite. In *Journal of Thermal Analysis and Calorimetry* (Vol. 122, Issue 2, pp. 601–609). https://doi.org/10.1007/s10973-015-4756-0

Jin, F., Abdollahzadeh, A., & Al-Tabbaa, A. (2013). Effect of different MgO on the hydration of MgO-activated granulated ground blastfurnace slag paste. In *Sustainable Construction Materials and Technologies* (Vols. 2013-Augus).

Joint Research Centre. (2013). *BAT document for the production of Cement*.

Kabir, H., & Hooton, R. D. (2020). Evaluating soundness of concrete containing shrinkage-compensating MgO admixtures. *Construction and Building Materials*, *253*, 119141. https://doi.org/10.1016/j.conbuildmat.2020.119141

Langmuir, D. (1965). Stability of Carbonates in the System MgO-CO 2 -H 2 O. *The Journal of Geology*, *73*(5), 730–754. https://doi.org/10.1086/627113

Liska, M., & Al-Tabbaa, A. (2009). Ultra-green construction: reactive magnesia masonry products. *Proceedings of the Institution of Civil Engineers - Waste and Resource Management*, *162*(4), 185–196. https://doi.org/10.1680/warm.2009.162.4.185

Liska, M., Vandeperre, L. J., & Al-Tabbaa, A. (2008). Influence of carbonation on the properties of reactive magnesia cement-based pressed masonry units. In *Advances in Cement Research* (Vol. 20, Issue 2, pp. 53–64). https://doi.org/10.1680/adcr.2008.20.2.53

Liska, Martin, & Al-Tabbaa, A. (2012). Performance of magnesia cements in porous blocks in acid and magnesium environments. In *Advances in Cement Research* (Vol. 24, Issue 4, pp. 221–232). https://doi.org/10.1680/adcr.11.00011

Liu, Z., Tang, M., & Cui, X. (1998). Expansion of Cement Containing Crystalline Magnesia with and Without Fly Ash and Slag. In *Cement, Concrete and Aggregates* (Vol. 20, Issue 1, pp. 180–185). https://doi.org/10.1520/cca10452j

Maryška, M., & Bláha, J. (1997). Hydration kinetics of magnesium oxide: Part 3 - Hydration rate of MgO in terms of temperature and time of its firing. In *Ceramics - Silikaty* (Vol. 41, Issue 4, pp. 121–123). https://www.irsm.cas.cz/materialy/cs_content/1997/Maryska_CS_1997_0001.pdf

Mehta, P. K., & Monteiro, P. J. M. (2006). *Concrete: Microstructure, Properties, and Materials* (3rd ed.). McGraw-Hill Company. https://doi.org/10.1036/0071462899

Mo, L., Deng, M., & Tang, M. (2009). Effect of calcination temperature on the microstructure, activity and expansion of Mgo-type expansive additive used in cement-based materials. In *Key Engineering Materials* (Vols. 400–402, pp. 169–174). https://doi.org/10.4028/www.scientific.net/kem.400-402.169

Mo, L., Deng, M., & Tang, M. (2010). Effects of calcination condition on expansion property of MgO-type expansive agent used in cement-based materials. In *Cement and Concrete Research* (Vol. 40, Issue 3, pp. 437–446). https://doi.org/10.1016/j.cemconres.2009.09.025

Mo, L., Deng, M., Tang, M., & Al-Tabbaa, A. (2014). MgO expansive cement and concrete in China: Past, present and future. In *Cement and Concrete Research* (Vol. 57, pp. 1–12). https://doi.org/10.1016/j.cemconres.2013.12.007

Mo, L., & Panesar, D. K. (2012). Effects of accelerated carbonation on the microstructure of Portland cement pastes containing reactive MgO. In *Cement and Concrete Research* (Vol. 42, Issue 6, pp. 769–777).

https://doi.org/10.1016/j.cemconres.2012.02.017

MTA. (1981). *Türkiye Maden Yatakları Haritaları*. https://www.mta.gov.tr/v3.0/bilgi-merkezi/maden-yataklari

Nokken, M. (2010). Expansion of MgO in Cement Pastes Measured by Different Methods. *ACI Materials Journal*, *107*(1). https://doi.org/10.14359/51663469

Qureshi, T., & Al-Tabbaa, A. (2014). The effect of magnesia on the self-healing performance of Portland cement with increased curing time. *The International Conference on Ageing of Materials & Structures*. https://doi.org/10.13140/RG.2.1.4458.4804

Rausis, K., Ćwik, A., & Casanova, I. (2020). Phase evolution during accelerated CO2 mineralization of brucite under concentrated CO2 and simulated flue gas conditions. In *Journal of CO2 Utilization* (Vol. 37, pp. 122–133). https://doi.org/10.1016/j.jcou.2019.12.007

Rheinheimer, V., Unluer, C., Liu, J., Ruan, S., Pan, J., & Monteiro, P. J. M. (2017). XPS study on the stability and transformation of hydrate and carbonate phases within MgO systems. In *Materials* (Vol. 10, Issue 1). https://doi.org/10.3390/ma10010075

Ruan, S., & Unluer, C. (2016). Comparative life cycle assessment of reactive MgO and Portland cement production. In *Journal of Cleaner Production* (Vol. 137, pp. 258–273). https://doi.org/10.1016/j.jclepro.2016.07.071

Ruan, S., & Unluer, C. (2017). Influence of supplementary cementitious materials on the performance and environmental impacts of reactive magnesia cement concrete. In *Journal of Cleaner Production* (Vol. 159, pp. 62–73). https://doi.org/10.1016/j.jclepro.2017.05.044

Šavija, B., & Luković, M. (2016). Carbonation of cement paste: Understanding, challenges, and opportunities. *Construction and Building Materials*, *117*, 285–301. https://doi.org/10.1016/j.conbuildmat.2016.04.138

Shand, M. A. (2006). The Chemistry and Technology of Magnesia. In *The Chemistry and Technology of Magnesia* (pp. 1–266). https://doi.org/10.1002/0471980579

Shen, W., Cao, L., Li, Q., Wen, Z., Wang, J., Liu, Y., Dong, R., Tan, Y., & Chen, R. (2016). Is magnesia cement low carbon? Life cycle carbon footprint comparing with Portland cement. *Journal of Cleaner Production*, *131*, 20–27. https://doi.org/10.1016/j.jclepro.2016.05.082

Smithson, G. L., & Bakhshi, N. N. (1973). Kinetics and Mechanism of Carbonation of Magnesium Oxide Slurries. In *Industrial and Engineering Chemistry Process Design and Development* (Vol. 12, Issue 1, pp. 99–106). https://doi.org/10.1021/i260045a019

Sonat, C., Lim, C. H., Liska, M., & Unluer, C. (2017). Recycling and reuse of reactive MgO cements – A feasibility study. In *Construction and Building Materials* (Vol. 157, pp. 172–181). https://doi.org/10.1016/j.conbuildmat.2017.09.068

Tanaka, J., Kawano, J., Nagai, T., & Teng, H. (2019). Transformation process of amorphous magnesium carbonate in aqueous solution. *Journal of Mineralogical and Petrological Sciences*, *114*(2), 105–109. https://doi.org/10.2465/jmps.181119b

Teir, S., Eloneva, S., Fogelholm, C.-J., & Zevenhoven, R. (2006). Stability of calcium carbonate and magnesium carbonate in rainwater and nitric acid solutions. *Energy Conversion and Management*, *47*(18–19), 3059–3068. https://doi.org/10.1016/j.enconman.2006.03.021

Tokyay, M. (2016). *Cement and Concrete Admixtures*. CRC Press.

TS EN 196-3. (2002). TS EN 196-3 Çimento deney metotları - Bölüm 3: Priz Süresi ve genleşme tayini. *Turkish Standard*, 10.

TS EN 197-1. (2011). EN 197 - 1 Cement - Part 1: Composition, specifications and conformity criteria for common cements. *Turkish Standard*, 39.

Unluer, C., & Al-Tabbaa, A. (2013). Impact of hydrated magnesium carbonate additives on the carbonation of reactive MgO cements. In *Cement and Concrete Research* (Vol. 54, pp. 87–97). https://doi.org/10.1016/j.cemconres.2013.08.009

Unluer, C., & Al-Tabbaa, A. (2014). Enhancing the carbonation of MgO cement porous blocks through improved curing conditions. In *Cement and Concrete Research* (Vol. 59, pp. 55–65). https://doi.org/10.1016/j.cemconres.2014.02.005

Unluer, Cise. (2018). Carbon dioxide sequestration in magnesium-based binders. In *Carbon Dioxide Sequestration in Cementitious Construction Materials* (pp. 129–173). Elsevier. https://doi.org/10.1016/B978-0-08-102444-7.00007-1

Vandeperre, L. J., Liska, M., & Al-Tabbaa, A. (2008). Microstructures of reactive magnesia cement blends. In *Cement and Concrete Composites* (Vol. 30, Issue 8, pp. 706–714). https://doi.org/10.1016/j.cemconcomp.2008.05.002

Walling, S. A., & Provis, J. L. (2016). Magnesia-Based Cements: A Journey of 150 Years, and Cements for the Future? In *Chemical Reviews* (Vol. 116, Issue 7, pp. 4170–4204). https://doi.org/10.1021/acs.chemrev.5b00463

Xu, J., Yan, C., Zhang, F., Konishi, H., Xu, H., & Teng, H. H. (2013). Testing the cation-hydration effect on the crystallization of Ca-Mg-CO 3 systems. In *Proceedings of the National Academy of Sciences of the United States of America* (Vol. 110, Issue 44, pp. 17750–17755). https://doi.org/10.1073/pnas.1307612110

Zhou, Q., & Glasser, F. P. (2000). Kinetics and mechanism of the carbonation of ettringite. *Advances in Cement Research*, *12*(3), 131–136. https://doi.org/10.1680/adcr.2000.12.3.131

Zhu, J., Ye, N., Liu, J., & Yang, J. (2013). Evaluation on Hydration Reactivity of Reactive Magnesium Oxide Prepared by Calcining Magnesite at Lower Temperatures. *Industrial & Engineering Chemistry Research*, *52*(19), 6430–

6437. https://doi.org/10.1021/ie303361u

# APPENDIX A

## WORKING PRINCIPLES OF THE SENSORS

In carbonation chamber, two types of sensors were used to measure the levels of the interior conditions:

- To determine the carbon dioxide level, ExplorIR® - W100% $CO_2$ Sensor produced by the company 'CO2meter' was utilized inside the chamber. A LED emitting the infrared light which can be absorbed only by carbon dioxide gas and a photo detector which can measure the light emitted by the LED were mounted to the sensor. The difference between the levels of the light emitted by the LED and measured by the photo detector gives the carbon dioxide concentration of the air (AirTest, 2012).
- The humidity and temperature levels of the chamber were measured by DHT 11 manufactured by the company 'Aosong (Guangzhou) Electronics Co.,Ltd.'. This sensor includes a humidity sensing element having two electrodes and a moisture holding-medium. The change in the capacitance between the electrodes points out the humidity level. In addition to this, the sensor uses its thermistor also mounted, to measure the temperature levels (Electronics|Projects|Focus, n.d.)

# APPENDIX B

## VALIDATION OF EQN. 3.5 IN WORKABILITY POINT OF VIEW

To determine the necessary water content of reactive magnesia-incorporated cement mortars having similar workability, Eqn. 3.5 was proposed.

3 different mortar mixes, the mix designs of which are given in Table B.1, were prepared. According to ASTM 1437-20, in order to verify that these have similar consistency properties, their flows were determined and the percent flows for these are also given in Table B.1 (ASTM C 1437, 2020). The first two mixtures were prepared by using a constant water/binder ratio of 0.484. As seen from the last column, the mixture that utilizes reactive magnesia did not have any consistency. The third mixture, however, was prepared by using Eqn. 3.5. Since the amount of the flow for the 1st and 3rd mixtures were similar, Eqn. 3.5 was verified.

Table B.1. Mix designs of the mixes (by weight).

| | **Portland Cement (g)** | **Reactive Magnesia (g)** | **Aggregate (g)** | **Water (g)** | **Flow (%)** |
|---|---|---|---|---|---|
| **1st mix** | 500 | 0 | 1375 | 242 | 70 |
| **2nd mix** | 0 | 500 | 1375 | 242 | 0 |
| **3rd mix** | 0 | 500 | 1375 | 457 | 70 |

## APPENDIX C

## STRENGTH REDUCTION DUE TO THE DILUTION EFFECT

The effect of the mineral admixture on the strength properties of the mortar / concrete mixture can be estimated if it is chemically inert and its physically effect is negligible. In such a case, the inert mineral admixture in the mixture will act as a filler material and the strength change will be attributed to the reduction in the cement content, known as the dilution effect.

The relation between cement amount and compressive strength with various air content is given in Figure C.1 (Mehta & Monteiro, 2006). From this graph, it can be easily said that there is a linear relation between cement content and compressive strength for a non-air entrained concrete.

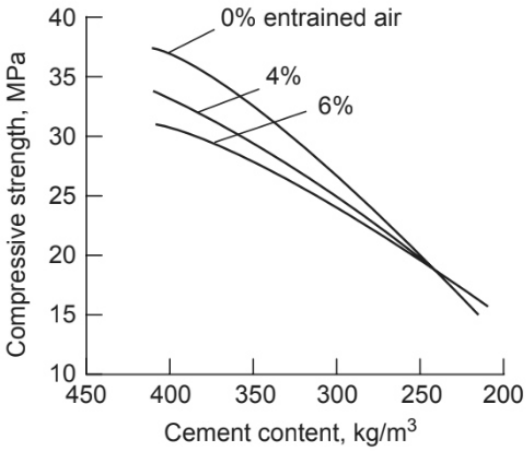


Figure C.1. The relation between cement amount and compressive strength (Mehta & Monteiro, 2006).

If the reactive magnesia studied was completely chemically inert admixture, all the strength change was resulted from the dilution effect due to the addition of the reactive magnesia (From the mix designs of the cement mortars prepared, it can be concluded that the aggregate amount is similar). Therefore, to investigate the effect of reactive magnesia on compressive strength, the strength reduction due to the dilution effect, firstly, should be removed.

# APPENDIX D

## THERMOGRAVIMETRIC ANALYSES OF 100CM-A_III_360d

The specimen was investigated through thermogravimetric analyses to understand its chemical composition as shown in Figure D.1. The specimen exposed to no pre-heating lost its about 10 % of its mass until the temperature of 200 ºC due to possible water loss. There also occurred mass reduction of about 30 % in between 200 and 500 ºC. For higher temperatures, the mass change was not so pronounced. The fact that the temperature range (300 – 500 ºC) of the highest mass change differed than that of the magnesite (~600 ºC) (see Figure 4.1.) used as a raw material, shows that 100CM-A_III_360d has no magnesite. However, the decomposition temperature range of the nesquehonite was reported to be 450º C approximately (Jauffret et al., 2015). This confirms the presence of the nesquehonite in 100CM-A_III_360d.

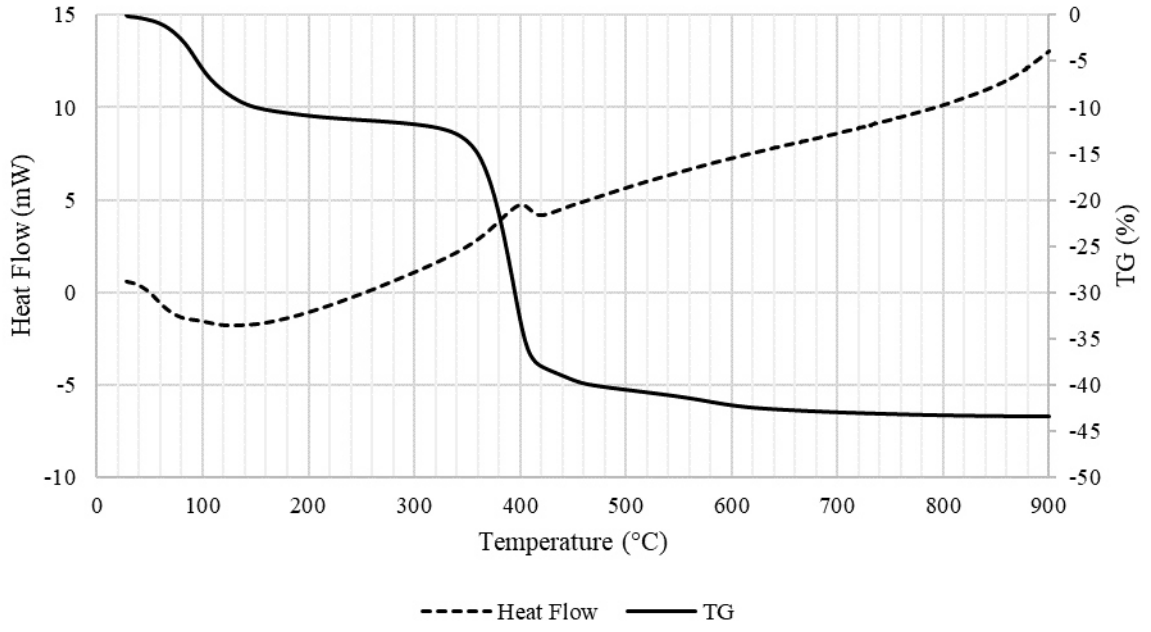


Figure D.1. The thermogravimetric analysis of 100CM-A_III_360d.

## CURRICULUM VITAE

### PERSONAL INFORMATION

Surname, Name: Ardoğa, Mehmet Kemal

### EDUCATION

| Degree | Institution | Year of Graduation |
|---|---|---|
| MS | METU Civil Engineering | 2014 |
| BS | METU Civil Engineering | 2011 |
| High School | İçel Anadolu High School, Mersin | 2006 |

### WORK EXPERIENCE

| Year | Place | Enrollment |
|---|---|---|
| 2012-2021 | METU Civil Engineering Department | Research Assistant |

### FOREIGN LANGUAGES

Advanced English, Basic German

### PUBLICATIONS

1. Ardoğa M. K., Erdoğan S. T. and Tokyay M. " Effect of particle size on early heat evolution of interground natural pozzolan blended cements ", Construction and Building Materials, 206, 210-218 (2019)

2. Ardoğa M. K., Engin D. and Yaman İ. Ö. " Effect of Cubic Specimen Size on the Compressive Strength of Concrete ", Cement and Concrete World, 21, 76-84 (2016)

Astronomy, astrophography, puzzle,